universität wien

MASTERARBEIT/MASTER'S THESIS

Titel der Masterarbeit / Title of the Master's Thesis

„Fully Automated Synthesis of Triazolopeptidomimetics“

verfasst von / submitted by

Barbara Kaudela, BSc

angestrebter akademischer Grad / in partial fulfilment of the requirements for the degree of

Master of Science (MSc)

Wien, 2022 / Vienna, 2022

Studienkennzahl lt. Studienblatt / degree programme code as it appears on the student record sheet:	UA 066 862
Studienrichtung lt. Studienblatt / degree programme as it appears on the student record sheet:	Masterstudium Chemie
Betreut von / Supervisor:	Assoz. Prof. Dr. Thomas Mindt, Privatdoz.

Acknowledgement

First, I want to thank Prof. Dr. Thomas Mindt for giving me the opportunity to complete my master thesis in his research group at the Ludwig Boltzmann Institute for Applied Diagnostics in the facilities of the Department of Inorganic Chemistry at the University of Vienna.

Secondly, I would like to thank Prof. Dr. Markus Mitterhauser for the possibility to join the Ludwig Boltzmann Institute for Applied Diagnostics as well as the Austrian Research Promotion Agency for the financial support (FEMtech Career).

I also want to thank everyone in the research group of Assoc.-Prof. Dr. Thomas L. Mindt for the warm welcome into their team and the nice time and talks during work, in the lunch breaks and in our free time. Special thanks go to Xabi, Irene, Max and Barbara with whom I spent most of my time in Lab 1 and who supported me where they could.

A huge thank you goes to Xabi, who patiently guided me through the practical work and through the preparation of my written thesis. He always supported me with his expertise and taught me a lot in the field of organic chemistry, in the handling of technical devices and in general many laboratory skills.

The biggest thank you belongs to my family and especially to my father Dr. Karl Kaudela for all his love and unconditional support of any kind. I also want to thank my sister Veronika in particular for all her emotional encouragement and her honest heart. Without my family, nothing what I have achieved would have been possible.

I am very thankful for all my friends, all the study and work colleagues I got to know and the beautiful time I had as student. Thank you!

Abstract

Providing high selectivity, effectiveness, structural diversity, biocompatibility and favorable pharmacokinetic properties peptides are of great interest to be used as drugs and vectors for drug delivery.[1,2] These advantages are restrained by their rapid proteolytic degradation and low pharmacological stability posing a limitation for the use of peptides *in vivo*.[3,4]

In order to enhance the metabolic stability of peptides, different stabilization techniques have been developed. Approaches for modifying the peptide sequence involving cyclization, N-methylation, the incorporation of D-amino acids or the strategic replacement of amide bonds by surrogates have been shown to have a positive impact on the peptide stability.[1] However, the biochemical and biophysical properties of the resulting peptidomimetic can often be altered leading to limited bioavailability and loss of receptor affinity.[5]

Bioisosters like 1,2,3-triazoles have shown to be competent peptide bond surrogates. These heterocycles can mimic the properties of *trans*-amide bonds with regard to dipolar moment, hydrogen bonding capability, size, planarity and polarity but are not susceptible to proteolytic degradation.[6,1] The systematic replacement of amide bonds with triazoles has led to the discovery of clinically relevant peptides with enhanced *in vivo* stability. To give a recent example, the study of Grob et al. resulted in the identification of several minigastrin triazolo-peptidomimetics with enhanced stability resulting in higher tumor uptake.[7]

The availability of peptides is given by straight forward, quick and automatable solid phase peptide synthesis (SPPS). Additionally, the emergence and availability of automated peptide synthesizers has increased throughout the last years as they present a convenient, time-saving and reliable alternative compared to the manual approach.[1] So far, the incorporation of triazoles into peptides has not been accomplished in a fully automated fashion. In this thesis the optimization and implementation of a methodology for the fully automated synthesis of triazole bearing peptides is presented. With this protocol, research in the field of peptidomimetics is accelerated and the accessibility for efficient and fast synthesis of triazolopeptidomimetics provided.

Zusammenfassung

Aufgrund ihrer hohen Selektivität, Wirksamkeit, strukturellen Vielfalt, Biokompatibilität und Pharmakokinetik sind Peptide als Wirkstoffe und Vektoren für den Arzneimitteltransport von großem Interesse.[1,2] Die Anwendung von Peptiden *in vivo* wird durch ihren schnellen, proteolytischen Abbau und ihre geringe pharmakologische Stabilität erschwert und limitiert.[3,4]

Um die metabolische Stabilität von Peptiden zu erhöhen wurden verschiedene Ansätze entwickelt. Modifizierungen von Peptiden wie Zyklisierung, N-Methylierung, der Einbau von D-Aminosäuren oder das strategische Ersetzen von Amidbindungen durch Surrogate haben nachweislich positive Auswirkungen auf die Peptidstabilität gezeigt.[1] Jedoch können diese Modifizierungen die biochemischen und biophysikalischen Eigenschaften der resultierenden Peptidderivate verändern, was zu einer begrenzten Bioverfügbarkeit und einem Verlust der Rezeptoraffinität führen kann.[5]

Bioisostere wie 1,2,3-Triazole haben sich als kompetente Peptidbindungssurrogate erwiesen. Diese Heterozyklen können die Eigenschaften von *trans*-Amidbindungen in Bezug auf Dipolmoment, Wasserstoffbrückenbindungsfähigkeit, Größe, Planarität und Polarität nachahmen, sind jedoch nicht anfällig für proteolytischen Abbau.[6,1] Der systematische Ersatz von Amidbindungen durch Triazole hat zur Entdeckung klinisch relevanter Peptide mit erhöhter *in vivo* Stabilität geführt. Ein aktuelles Beispiel ist die Studie von Grob et al., die zur Identifizierung mehrerer Minigastrin-Triazolpeptide mit erhöhter Stabilität und in weiterer Folge zu einer verbesserten Tumoraufnahme geführt hat.[7]

Die Verfügbarkeit von Peptiden ist durch die simple, schnelle und automatisierbare Festphasen-Peptidsynthese (SPPS) gegeben. Darüber hinaus sind in den letzten Jahren immer mehr Geräte für die automatisierte Peptidsynthese aufgekommen, da sie eine bequeme, zeitsparende und zuverlässige Alternative zur manuellen Synthese darstellen.[1] Bislang wurde der Einbau von Triazolen in Peptide noch nicht automatisiert durchgeführt. In dieser Arbeit wird die Optimierung und Implementierung einer Methode für die vollautomatische Synthese von Triazolpeptidomimetika vorgestellt. Mit diesem Protokoll wird die Forschung auf dem Gebiet der Peptidomimetika beschleunigt sowie die Möglichkeiten für eine effiziente und schnelle Synthese von Triazolopeptidomimetika zur Verfügung gestellt.

Content

Abbreviations

AA	amino acid
MeCN	acetonitrile
Bn	benzyle
BOP	(benzotriazole-1-yloxy)tris(dimethylamino)phosphonium hexafluorophosphate
Boc	tertButyloxycarbonyl
CuAAC	Copper(I)-catalyzed Azide-Alkyne Cycloaddition
DCM	dichloromethane
DCC	*N*,*N*′-dicyclohexylcarbodiimide
DIBAL-H	diisobutylaluminum hydride
DIC	diisopropylcarbodiimide
DIPEA	*N*,*N*-diisopropylethylamine
DMSO	dimethyl sulfoxide
DMF	*N*,*N*-dimethylformamide
DMAP	4-dimethylamino pyridine
DOSY	diffusion ordered spectroscopy
EtOAc	ethyl acetate
FA	formic acid
Fmoc	9-fluorenylmethyloxycarbonyl
Fmoc-OSu	9-fluorenylmethylsuccinimidyl carbonate
HF	hydrofluoric acid
HOBt	1-hydroxybenzotriazole
HPLC	high pressure liquid chromatography
ISA.HCl	imidazole-1-sulfonyl azide hydrochloride

LC	liquid chromatography
MeOH	methanol
MTBE	methyltertbutyl ether
MS	mass spectrometry
MW	microwave
$NaBH_4$	sodium borhydride
OXYMA	ethyl cyanohydroxyiminoacetate
Pbf	2,2,4,6,7-pentamethyldihydrobenzofuran-5-sulfonyl
PEG	polyethylene glycole
PG	protecting group
PS	polystyrene
rt	room temperature
SPPS	solid phase peptide synthesis
t_r	retention time
tBu	*tert*-butyl
TBTA	tris[(1-benzyl-1*H*-1,2,3-triazol-4-yl)methyl]amine
THF	tetrahydrofuran
TLC	thin layer chromatography
TFA	trifluoroacetic acid
TIPS	triisopropylsilane
Trt	trityl
Tz	triazole

1. Introduction

1.1. Peptides

Native peptides are biomolecules composed out of 20 different, natural amino acids usually occurring in their L-configuration, with a few rare exceptions.[8] The amino acids are distinguished from one another due to their different sidechain functionalities with variations in size, polarity and electric charge, hence defining the properties and biological role of the peptide. Peptides consist of up to 50 amino acids resulting in an ample variety of different combinations, structures and functionalities. They are involved in a vast number of biochemical and physiological processes acting as intrinsic signaling molecules presenting an opportunity for therapeutic applications by closely mimicking natural pathways.[9,8]

1.2. Peptide Synthesis and Solid Phase Peptide Synthesis

The first known synthesis of a peptide-derivative dates back from the 19th century when Theodor Curtius synthesized benzoylglycylglycine in 1882.[10] However, Emil Fischer developed the first acknowledged steps in the creation of natural substances with the synthesis of the free dipeptide glycylglycine in 1901.[10] He then managed to synthesize an octapeptide consisting out of three different amino acids, but his further progress was restrained due to the lack of appropriate protecting groups. Fifty years later, another milestone in peptide chemistry was set as Vincent du Vigneaud synthesized oxytocin which is still widely used in medicine.[10] With the synthesis of oxytocin, organic protecting groups were introduced in order to ensure specific peptide bond formation.[9] Bruce Merrifield began his studies on solid phase peptide synthesis in 1959 as he experienced that the peptide synthesis in solution is a time consuming and technical demanding process. He reported that the synthesis of a pentapeptide in solution took him 11 months to gain a yield of 7%, displaying the need for a more efficient and rapid methodology.[10] In 1963 Merrifield published his revolutionary approach and with this, the first synthesis of a tetrapeptide on a solid support.[10] On the way to implementing his novel concept, he encountered some limitations. Many synthetic peptide chemists were skeptical as he did not include any isolation, purification or characterization of intermediates, compared to solution peptide synthesis, where these steps are essential.[9]

Solid phase peptide synthesis (SPPS) is the step by step construction of a peptide covalently attached to an insoluble polymer carrier in a single reaction vessel. Thereby, the first amino acid is

coupled to a linker attached to a solid support or resin with its C-terminus. Reactive amino acid sidechains and the N-terminus have to be blocked with protecting groups to overcome side reactions and the formation of byproducts. After each cycle, the temporary N-terminal protecting groups are removed to enable the coupling of the following amino acid. Excess reagents and solvents can be easily removed by washing and filtration steps. To enable the formation of new amide bonds, the carboxy group has to be activated with coupling reagents. The consecutive steps; deprotection, activation and coupling are repeated until the desired peptide is obtained. The final step is to cleave the peptide from the resin and to remove all the temporary and permanent protecting groups.[9] Scheme 1 shows the general synthesis of peptides on solid phase.

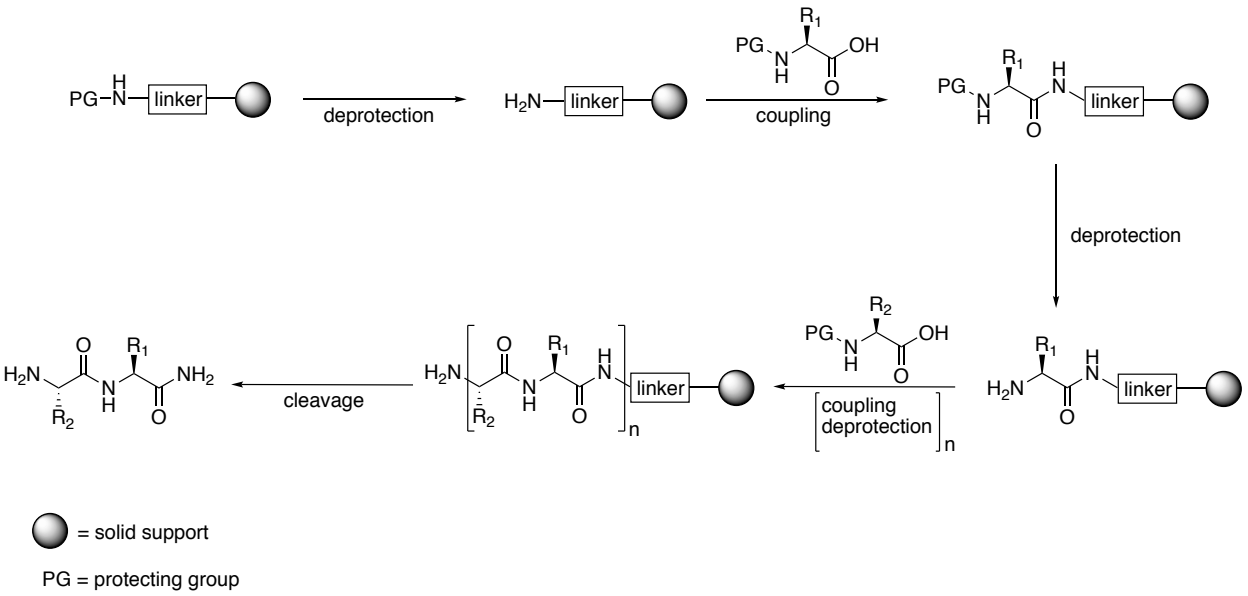

Scheme 1: General procedure of solid phase peptide synthesis with and amide-functionalized linker.

The primary goal of the work of Merrifield and coworkers was to open the path for a simple and rapid method for chemical peptide synthesis. Another objective was the performance of SPPS in a controlled, automated manner offering great advantages for the synthesis of larger polypeptides.[11] Merrifield's first instrument for automated SPPS was described in 1966 and was able to perform all steps for the synthesis automatically. It featured a plumbing system to ensure solution transport, mixing of the reaction components and removal of liquids via filtration. The system contained reservoirs for all chemicals and was equipped with a reaction vessel placed in a reactor block. Nowadays, a variety of modern automated peptide synthesizers is commercially available that fulfil different claims for the preparation of peptides.[12,9]

1.2.1. Fmoc- and Boc-Strategy

For the synthesis of peptides on solid matrices, two approaches have been consolidated; the orthogonal Fmoc (9-fluorenylmethyloxycarbonyl) strategy and the Boc (tert-butyloxycarbonyl) strategy.[9] Merrifield established and optimized the synthesis of peptides following the Boc-strategy between 1960 and 1980. In this strategy, the N^{α}-terminus is temporarily protected with an acid labile Boc functionality, easily cleavable with acids like TFA (trifluoracetic acid). The repetitive TFA treatment of the peptide can harm sensitive peptide bonds and promote acid-catalyzed side reactions. Within the Boc approach, amino acid sidechains are protected by benzyl-based groups that are stable against acids like TFA but labile against strong, corrosive acids like HF (fluoric acid) requiring special reaction vessels. The Boc strategy shows advantages for the synthesis of demanding and base sensitive sequences, also contributing to lower peptide aggregation.[9]

In 1970 Carpino et al. reported the use of Fmoc as an alternative, temporary and base labile protecting group. This led to a novel and different approach for SPPS; the Fmoc strategy.[13] Permanent protecting groups for amino acid sidechains used within the Fmoc-strategy are acid-labile *tBu* (Asp, Glu, Ser, Thr, Tyr), Trt (Asn, Cys, Gln, His), Boc (Lys, Trp) and Pbf (Arg). The Fmoc group can be removed through ß-elimination with piperidine whereas the permanent protecting groups can be cleaved with acids like TFA. The orthogonal Fmoc approach offers great advantages compared to the Boc strategy as it presents a milder method and the selective removal of the protecting groups is possible by applying individual chemical conditions, represented in Figure 1.[9]

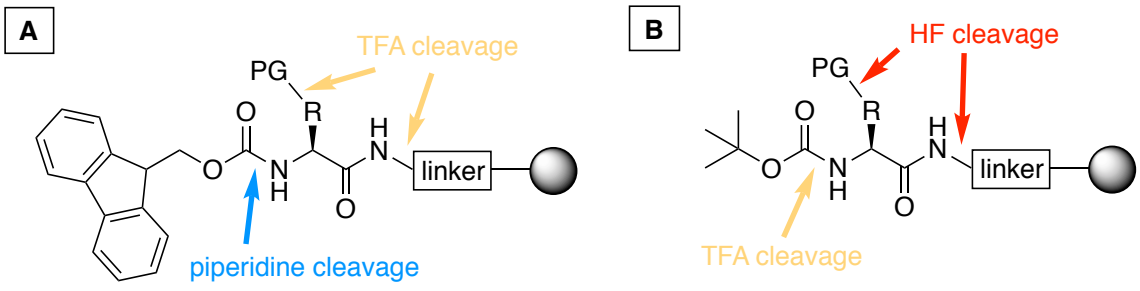

Figure 1: Cleavage conditions for the Fmoc strategy (A) and the Boc strategy (B).

Within both strategies the final step of the synthesis is to cleave the peptide from the resin and to remove the permanent protecting groups. The peptide cleavage off the resin is carried out with TFA for the Fmoc- and with HF for the Boc-strategy.[9] The removal of permanent protecting groups with TFA involves the formation of reactive cations that can further react with TFA to form

alkylating agents. These cleavage-products have tendency to react with nucleophilic functionalities (*e.g.* hydroxy groups) of the peptide chain resulting in undesired side products and impurities. To scavenge these reactive species, scavengers acting as weak bases are added that are often structures including thiol groups like 1,2-ethanedithiol as well as trialkylsilane derivatives such as triisopropylsilane (TIPS).[14]

1.2.2. Solid Supports

Solid supports used for SPPS are polymeric materials or resins in form of beads available in different sizes (mesh) and various loading capacities. The loading capacity is defined by the equivalents of amino acids in mmol/g that can be attached to the resin. Currently, there is a vast number of commercially available resins, yet three main classes are commonly used. Polystyrene based resins (PS), polyethylene glycol functionalized polystyrene resins (PEG-PS) and pure PEG-based resins.[15,9,13] The resin needs to satisfy various requirements to be suitable for the peptide synthesis and the conditions prevailing in the process. Besides the essential insolubility of the solid support, it has to be chemically and physically resistant as well as mechanically resilient to enable filtration. It is crucial for the solid phase to have good swelling properties to enable the accessibility of the molecules to the interior of the matrix. To ensure rapid diffusion of reagents inside the polymeric matrix and to enable the accommodation the bulky, growing peptide chain, low crosslinking is favorable. In order to bind the first amino acid of the peptide chain to the polymer carrier, a reversible connection (linker) has to be coupled to a functional group of the resin. The linker is typically a short organic structure that defines the C-terminal functionality of the synthetic peptide. It also determines the distance between peptide and resin as well as the loading capacity of the resin. Rink amide moieties are linkers that leave the peptide with an amide group at the C-terminus whereas wang linkers release the peptide with an acid functionality.[9,16] The structure of rink amide and wang resin are shown in Figure 2.

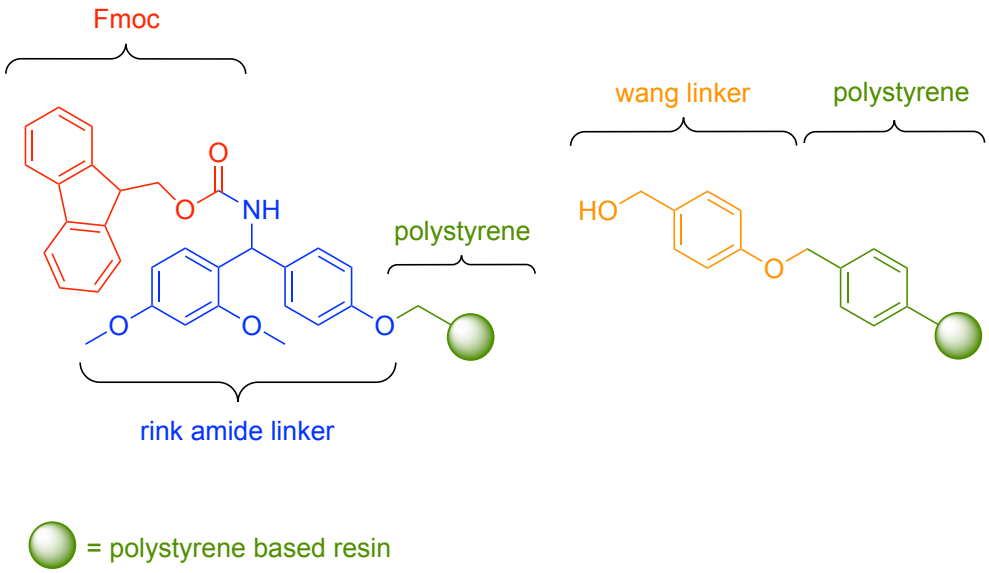

Figure 2: Polystyrene based resin with Fmoc-protected rink amide linker (left) and a polystyrene based resin with wang linker including a hydroxy-functionality (right).

1.2.3. Coupling Reagents

In order to prolong the peptide chain, adjacent amino acids have to be coupled by the formation of amide bonds. Therefore, the carboxy group of the free amino acid has to be transformed into a more electrophilic species to be able to react with the amino group of the resin-coupled amino acid. Today, a wide range of different coupling agents is available. Well established methodology makes use of efficient carbodiimide-based reagents such as DIC (*N,N'*-diisopropylcarbodiimide) and DCC (*N,N'*-dicyclohexylcarbodiimide). Additives such as HOBt and HOAt (1-hydroxybenzotriazole and 1-hydroxy-7-azabenzotriazole) are used with carbodiimide-mediated couplings to suppress racemization. Other common coupling reagents are urinium salts like HATU (N-[(dimethylamino)-1H-1,2,3-triazolo-[4,5-b]pyridin-1-ylmethylene]-N-methylmethanaminium hexafluorophosphate N-oxide), HBTU (2-(1H-benzotriazole-1-yl)-1,1,3,3-tetramethyluronium-hexafluorophosphate), TBTU (N-[(1H-benzotriazol-1-yl)(dimethyl-amino)methylene]-N-methylmethan-aminium tetra-fluoroborate N-oxide) and phosphonium salts such as PyBOP (benzotriazol-1-yloxytri(pyrrolidino)phosphonium hexafluorophosphate). Oxyma is a relatively new additive (2009) for DIC-mediated amide bond formation and presents a safe alternative to the potentially explosive HOBt.[9] Depending on the bulkiness of the amino acids as well as on the synthesized peptide type, proper additives have to be chosen. In general, the

coupling reagents should be stable and safe to handle while enhancing the reactivity of the amino acids as well as reducing the epimerization or keeping it to a minimum.[13,9]

1.3. Peptides in Medicine

Natural and synthetic peptides have been used as biologically active tools over a century to treat numerous diseases.[17] Nowadays, illnesses like cancer, osteoporosis, inflammations, diabetes as well as obesity and cardiovascular diseases can be treated with different peptide drugs.[8] In 2021 more than 80 peptide-based drugs have reached the market and in 2018 more than 600 peptides were in clinical or preclinical trials.[18,19,16] Compared to organic drug molecules, peptides are generally bigger and can cover a larger area on the targeted site. Additionally, they have a more predictable metabolism and are degraded to metabolites that are rarely toxic. Due to their highly specific targeting capacity, peptides act with a low occurrence of side effects. They provide high potency and are suitable for investigating peptide-protein or peptide-receptor interactions, thus offering a big range of possible targets.[18] Moreover, peptides have the ability to efficiently penetrate cells, other than bigger biomolecules like proteins.[20] Their favorable pharmacological properties, fast uptake, rapid tissue penetration and distribution encourage the development of several peptide-based therapeutics.[21,19,1]

Peptides are able to interact with high affinity with medically associated antigens and receptors such as the widely expressed G-protein coupled receptors (GPCRs), natriuretic peptide receptors and cytokine receptors.[22,8] Other targets for peptide drugs are ion channels and extracellular units such as structural proteins and enzymes.[8]

To give a historic example, in 1920 the hormone insulin was isolated and applied for the first time for the treatment of diabetes. This peptide drug acts as essential replacement therapeutic that supplements the endogenous peptide for proper physiological function.[8] In 1962 endogenous oxytocin was introduced into clinic as the first peptide hormone to be biochemically described and synthesized. Oxytocin has a broad spectrum of functions including stress-coping, influencing the autonomic nervous and immune system as well as the support of growth patterns and healing by stimulating the oxytocin receptor.[16,23]

As well as being valuable in the treatment of endocrine diseases, peptides provide remarkable features that are useful for cancer therapy. A fundamental objective for the use of peptides in tumor therapy is the overexpression of certain peptide receptors on tumor cells in contrast to normal

cells. Approved peptide drugs for cancer therapy that are still very successful are Octreotide, Leuprolide and Goserelin for instance.[21,19]

Peptides also serve as delivery systems for different types of therapeutic or diagnostic agents to reach specific targets such as tumor cells, immune cells or signaling pathways.[24,20] Therefore, the active compound is coupled to a peptide acting as vector to selectively carry it to its target site. The reaction of the peptide to a certain physiological environment (*e.g.* pH) at the targeted site results in a controlled and selective release of the active substance by diminishing the exposure to non-targeted tissue.[25,20] Peptides are able to carry and deliver diagnostic or therapeutic units including imaging probes such as fluorescent moieties and radioisotopes.[26,27] Also cytotoxic cargoes like cisplatin, paclitaxel and radionuclides for therapy can be transported to their targets by peptides.[28]

Although peptides have all these beneficial properties, there are some limitations for their use as drugs and delivery moieties in the human body. Major drawbacks of the application of peptide-pharmaceuticals is their lack of stability *in vivo* and their limited oral availability. Naturally occurring or non-modified peptides are usually rapidly degraded in the organism and are more likely to undergo enzymatic cleavage compared to larger biomolecules like proteins or antibodies.[21] While endopeptidases are able to cleave the amide bonds of a peptide, exopeptidases are capable of degrading the peptide from the N- or C-terminus.[21] Mechanistically, hydrolysis of an amide bond occurs through nucleophilic reaction at its carbonyl carbon. Depending on the amino acid located at the active site of the enzyme, nucleophilic amino acids like cysteine and serine react directly whereas residues such as glutamate and aspartate assist water molecules in their nucleophilic reaction.[21]

Within the application of peptides as drugs, their pharmacological instability significantly disrupts their ability to localize to the target tissue, resulting in a loss of drug efficacy. When acting as delivery agents, the short biological half-life of the peptide *in vivo* might not be sufficient enough to deliver adequate amounts of its cargo to the target tissue and can therefore not fulfill its therapeutic purpose.[29] Moreover, the enzymatic cleavage leads to the formation of side products and a non-specific release of the imaging probe or cytotoxic cargo causing unwanted side effects and/or harm to healthy tissue. As a consequence of their low stability, many pharmacologically interesting peptide-based drugs might never see application.[28] Therefore, different modifications that stabilize and prolong the half-life of peptides have shown to be helpful and necessary in order to efficiently employ them as drugs, delivery agents or vectors.[21]

1.4. Peptide Modifications

To prevent enzymatic degradation various modification strategies have been established to generate metabolically stable and thus effective peptides. These strategies include modifications of the peptide backbone like N-methylation, incorporation of D-amino acids, C- or N-terminal modifications, cyclization, PEGylation and the replacement of peptide bonds by bioisosteres.[3,21]

1.4.1. Cyclization and Modification of N- and C-termini

A peptide can be modified through head-to-tail cyclization by the formation of an amide bond between the C- and N-terminus of the sequence, thus blocking the target site from exopeptidases. A clear advantage is that the sidechains that are usually essential for biological activity remain unaltered.[21,29] The structural rigidity derived from peptide cyclization can enhance the metabolic stability and binding properties by locking it into a conformation less prone to enzymatic degradation. On the other hand, it can also result in a loss of activity. To give an example, Marastoni et al. proved that both, the linear and the cyclic form of "peptide T" show high biological activity and that the cyclic peptide is resistant against plasma and brain enzymes.[30] Besides the head-to-tail cyclization also cyclization between amino acid sidechains or cyclization between amino acids and the N- or C-termini of the sequence are possible.[21,29] The half-life of the growth regulatory factor GRF(1-29)-NH_2 was increased from 13 min to more than two hours in porcine plasma, through sidechain to sidechain cyclization as shown in the study of Su et al.[31]

The attachment of certain functional groups to the C- and N termini of a linear peptide also effectively blocks exopeptidase activity, thus increasing the resistance against enzymatic degradation. Capping the C-terminus of a peptide by amidation for instance, eliminates the hydroxy group of the sequence. This may result in reduced solubility as it removes the charge of the C-terminus.[32] The N-terminus can be altered by acetylation or formylation leading to a loss of its charge and decreased solubility.[33] Brinckerhoff et al. managed to significantly improve the plasma stability of the immunogenic peptide MART-I_{27-35} by acetylation and amidation of the N- and C- terminus respectively.[34]

1.4.2. PEGylation

The introduction of PEG chains into the sequence has shown to entail improved pharmacokinetic properties of peptide-based pharmaceuticals.[21] This includes better receptor binding affinity and increased tumor uptake, compared to non-modified analogues. Furthermore, PEGylation enhances drug stability by increasing the size of the drug and generating steric hinderance, thus protecting the molecule from proteolytic degradation.[21] In addition, increased molecule size leads to a decreased kidney uptake and prolonged half-life.[29] Dapp et al. investigated the stability of PEG-modified and unmodified bombesin based radiopharmaceuticals in human serum. They found that after five days *in vitro* only 14% of the unmodified compound was left compared to the PEGylated compound where still 52% was intact in human serum.[21]

1.4.3. Modification and Substitution of Amino Acids

In nature, amino acids generally occur in their L-configuration whereas the incidence of D-amino acids is rare. The conformational difference between the two forms makes peptides constructed out of D-amino acids unrecognizable for many proteins, involving peptidases. Due to the lack of recognition this modification is of high interest in peptide drug design. Unfortunately, the exchange of the L-form to its D-counterpart leads to a different chain orientation and can prevent the peptide from correct target binding as the secondary structure of the peptide can be altered. Therefore, the replacement of labile amino acids is a common strategy to increase the stability of a peptide by keeping the overall peptide conformation intact and closely mimicking its native form. Hong et al. investigated the stability improvement by D-amino acid substitution of the amino acid sequence KKVVFKVKFKK, an antimicrobial peptide that acts on the lipid membrane of pathogens.[35] By replacing the four N- and C-terminal lysine (K) residues with its D-enantiomers, the half-life of the peptide in serum could be increased by 7-fold. Despite the modification the activity for the six test microorganisms remained the same as for the unmodified peptide.[35]

1.4.3.1. Substitution of Amide Bonds with Amide Bond Surrogates

An established way to increase the metabolic stability of peptides with a minimal impact on binding properties is the replacement of amide groups in the backbone with peptide bond surrogates. Some of these peptide bond mimetics are able to mimic amide bond characteristics such as dipolar moment, H-bonding properties and size while not being cleavable by enzymes. The

resulting peptidomimetics resemble native peptides while enhancing their therapeutic and/or diagnostic properties.

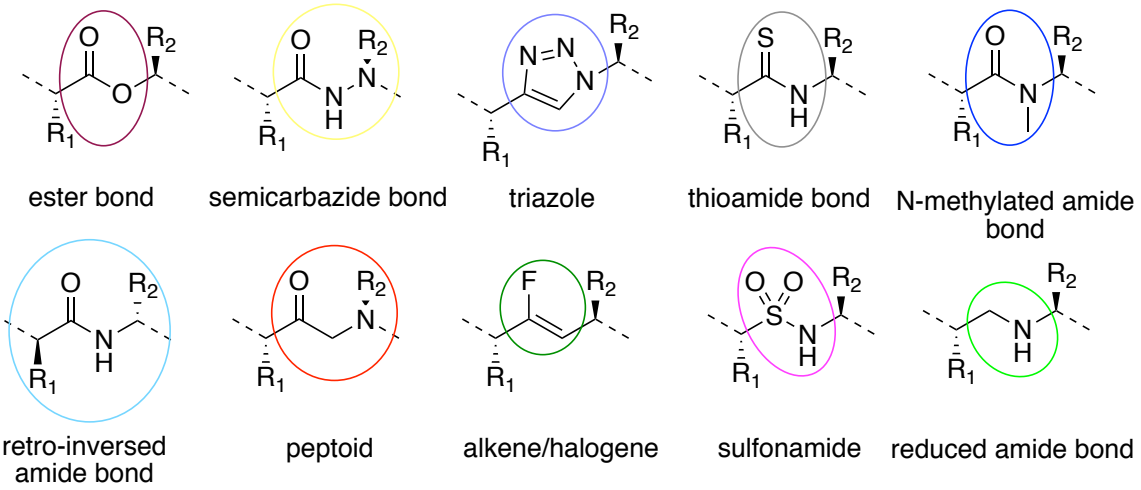

Figure 3: Examples for different amide bond surrogates.

These non-peptidic structural moieties include sulfonamides, esters, semicarbazides, peptoids as well as methylated, reduced and retro inversed amide bonds as depicted in Figure 3. The introduction of heteroatoms like fluorine, sulfur and boron as well as alkenes are examples for potential peptide bond imitators.[1]

Peptidosulfonamides have shown increased stability towards proteases by maintaining biological activity although some crucial properties like the geometry and the hydrogen-bonding characteristics of the amide bond are altered.[21] Compared to the NH of an amide group, the NH moiety of a sulfonamide group is more acidic making the sulfonamide group a better hydrogen bond donor. Regarding the hydrogen bond accepting character, the sulfonamide group provides two possible accepting sites with its two oxygen atoms. Additionally, the sulfonamide moiety is more freely rotatable compared to the relatively rigid peptide bond. De Bont et al. treated peptidosulfonamides derived from the peptide leu-enkephalin with peptidases like pepsin. They found that leu-enkephalin derivatives with sulfonamide groups in different positions were far more stable against pepsin catalyzed hydrolysis than the unmodified analogues.[38]

Another strategy that has been applied to improve the stability of peptides is the N-methylation of amide bonds. The replacement of the NH-hydrogen by a methyl group prevents the modified amide bond from forming potential intra- and intermolecular hydrogen bonds. N-methylation can strongly influence and alter the overall conformation of peptides.[21] This can result in decreased affinity of the peptide for the active site of proteolytic enzymes, thus increasing resistance to

proteases. It has been shown that N-methylation of adjacent amide bonds to the cleavage site can create greater resistance against peptidases than methylation of the peptide bond at the cleavage site itself in some cases.[21] N-methylation can also result in increased membrane permeability and enhanced steric hindrance of the peptide.[21] To give an example, the peptide R1 binds to AMA1, a membrane antigen of a malaria parasite, and further blocks parasite invasion. Harris et al. successfully improved bioactivity, affinity and stability against proteolysis by N-methylation of several residues of the R1 peptide.[36]

Amide bonds can also be modified by reduction which can increase the stability of a peptide *in vitro*.[37] The group of T. P. Davis reduced amide bonds susceptible to enzymatic degradation in the opoid peptide dynorphin A. They showed that the reduction of peptide bonds prone to enzymatic degradation, leads to peptidomimetics with longer half-lifes *in vitro,* compared to the unmodified peptide.[37] As a reduced amide bond does not provide a carbonyl carbon for hydrogen bonding, changes in structure and a possible loss of affinity towards other biomolecules is expected.

Fluoroalkenes are more lipophilic than amide functionalities, thus enhancing membrane permeability. A substantial dipole moment is given by the strong electronegativity of the fluorine mimicking the carbonyl oxygen of the amide functionality. Nevertheless, fluoroalkenes are unable to imitate essential characteristics of amide bonds like H-bonding properties. Altman et al. reported to replacement of the Tyr-Gly amide bond in leu-enkephalin and showed the excellent rat and human plasma stability of the analogue compared to its native form.[39]

With the incorporation of heterocycles, further variations for amide bond mimetics are available such as 2-imidazolidine, pyrazoles, tetrazoles as well as 1,2,4- and 1,2,3-triazoles. Especially 1,2,3-triazoles as replacement for amide bonds have gained importance and are frequently used in medicinal chemistry nowadays.[1]

1.5. 1,2,3-Triazoles as Amide Bond Isosteres

Triazoles are used as replacements for amide bonds in order to enhance the pharmacological characteristics and stability of peptides.[6] In comparison to amide bonds, the triazole surrogates are actually metabolically stable and are not cleaved by proteases. Moreover, 1,4- and 1,5-disubstituted 1,2,3-triazoles can imitate crucial properties of *trans*- and *cis*-amide bonds respectively, in a

satisfactory manner.[1,40] A comparison of an amide bond with a 1,4-disubstituted 1,2,3-triazole is shown in Figure 4.

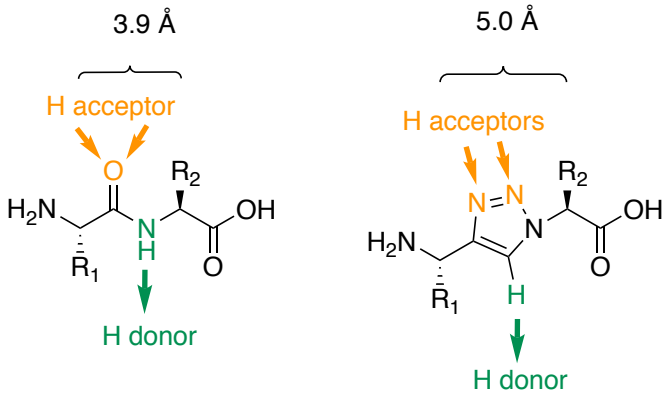

Figure 4: Comparison of a *trans* amide bond (left) with an 1,4-disubstituted 1,2,3-triazole (right) in terms of size and H-bonding capacities. Adapted from Mindt and co-workers.[8]

With regard to 1,4-disubstituted heterocycles, these properties include polarity, dipole moment, hydrogen bonding characteristics and size. When comparing the polarity of the two motifs, the triazole has a slightly higher dipole moment than the amide bond (~4.5 Debye vs. 3.5 Debye). Consequently, the aromatic heterocycle can interact with the dipole moment of other amino acids and in addition form intra- and intermolecular π-interactions with its peers. The dipole moment also leads to polarization of the heterocycle and allows the H of the C-5 atom to act as a proton-bond donor similar to the NH of the amide bond. The N-2 and N-3 in the triazole unit represent potential H-bond acceptors and thereby mimic the accepting properties of the carboxyl unit in the amide bond. In terms of structure and size, the triazole moiety slightly increases the distance between two neighboring amino acid side chains when incorporated into a peptide from ~3.9 Å (amide bond) to ~5.0 Å. Although 1,2,3-triazoles are more rigid due to their aromatic structure, they imitate the planarity of peptide bonds. To summarize, all the mentioned features present distinct advantages and make 1,2,3-triazoles suitable, highly stable amide bond bioisosteres.[1]

1.5.1. Synthesis of 1,4-Disubstituted 1,2,3-Triazoles

1,4-Disubstituted 1,2,3-triazoles can be synthesized regioselective by the Cu(I)-catalyzed azide-alkyne cycloaddition (CuAAC). This procedure was described by the groups of Meldal and Sharpless and categorized as click-reaction.[41,42] The concept of click-chemistry presents a simple procedure under mild conditions, with a wide scope leading to high yields.[41,42] Furthermore, only few and easily removable by-products are formed and it can be carried out in a variety of solvents

in solution as well as on solid phase.[43] The possibility to perform the reaction on solid phase makes it particularly useful for peptide synthesis and for the incorporation of triazoles into peptide sequences. In SPPS, the triazole is formed in two steps, presented in Scheme 2. First, the amino acid sequence attached to the resin needs to be transformed into its free amine form, by removing the protecting group.

Secondly, a diazo-transfer reaction has to be carried out to transform the amine into an azide.[1] Trifyl azide (TfN_3) and imidazole-1-sulfonyl azide hydrochloride (ISA.HCl) are among the most commonly used diazo-transfer reagents. ISA.HCl has been reported as a sufficient reagent for the synthesis of azido peptides on solid phase.[44] Trifyl azide is potentially explosive posing an additional risk for its users while ISA.HCl presents the more stable, safer and easier to handle option. To yield better conversions, $CuSO_4$ can be added to the diazo-transfer reaction in catalytic amounts.

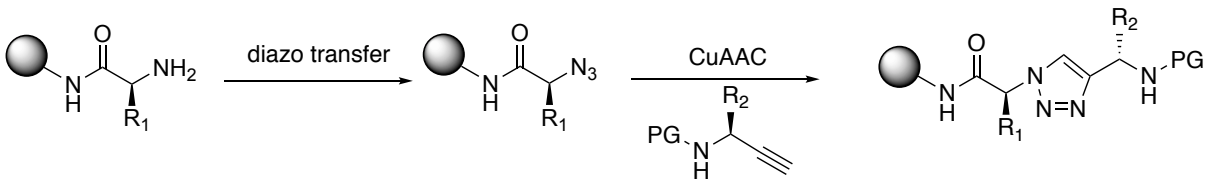

Scheme 2: Reaction scheme for the diazo-transfer and the CuAAC click reaction on solid phase starting from an unprotected amino acid on solid phase.

Subsequently, a CuAAC click-reaction is carried out by reacting the terminal azide attached to the amino acid sequence on the resin with a protected α-amino alkyne. The α-amino alkyne has to be synthesized in advance in solution within multiple steps. A prerequisite for a CuAAC reaction is the presence of a Cu(I) species in catalytic amounts.[45] Due to the thermodynamic instability of Cu(I), which can lead to oxidation to Cu(II) or disproportionation to Cu(0) and Cu(II), certain reaction conditions are required. Therefore, Cu(I) catalyzed reactions are usually carried out under inert and anhydrous conditions or in the presence of stabilizing agents. Ligands that are well suited as stabilizers include oligotriazole derivatives derived from propargylamine cores, such as TBTA (tris[(1-benzyl-1*H*-1,2,3-triazol-4-yl)methyl]amine).[46] Commonly used Cu(I) sources are copper salts like CuI, $Cu(Br(PPh_3)_3$ and $CuSO_4$ in combination with the reducing agent sodium ascorbate whereas $[Cu(CH_3CN)_4]PF_6$ is among the most widely used Cu(I) compelx. Solvents that are

frequently used for the diazo-transfer and CuAAC reactions are MeCN, MeOH, DCM, H_2O, DMSO and DMF whereas DMF is commonly used in SPPS with polystyrene based resins.[1,43,44]

Beckmann et al. reported a more time efficient procedure in solution where the diazo-transfer and the CuAAC click-reaction were carried out as a single step one-pot reaction. To obtain a copper(I) source for the CuAAC reaction, $CuSO_4$ was used in combination with sodium ascorbate as a reducing agent, with the additional function of $CuSO_4$ to catalyze the diazo-transfer.[45]

1.5.2. Applications of Triazolopeptidomimetics

Several examples for the synthesis and application of triazolopeptidomimetics are presented in literature.[47,48,49] The bombesin sequence BBN7-14 was subjected to amide-triazole scan. Bombesin is an agonistic ligand of the gastrin-releasing peptide receptor (GRPR) which is overexpressed in different tumors (*e.g.* prostate and lung cancer) and is studied in nuclear oncology and as vector to deliver radioactivity to the site of the disease. To find BBN7-14 derivatives with enhanced stability, every amide bond was systematically replaced to a triazole one at a time. From the nine different triazole containing derivatives, seven showed improved *in vitro* serum stability. The lipophilicity was not significantly altered for any of the compounds and three of them maintained their binding affinity compared to the unmodified reference.[1,50]

Another approach was performed by Grob et al. with the minigastrin analogue MG11, where the peptide was subjected to a triazole scan by successively replacing all the peptide bonds by triazoles individually. Minigastrin can be applied as delivery agent in nuclear medicine as it shows specific and high affinity towards the cholecystokinin-2 receptor which is overexpressed on tumors like stromal ovarian cancer.[7,51] Some of these derivatives showed significantly improved specific internalization. Additionally, six out of eight modified MG11 analogues showed enhanced resistance against proteases, leading to prolonged half-lifes.[7]

Fedorczyk et al. described the synthesis of 23 novel triazolopeptidomimetics as possible inhibitors for the interaction between neuropilin-1 (NRP-1) and vascular endothelial growth factor, as potential anticancer therapy. Several studies have reported *in situ* expression of NRP1 in cancer tissue of prostate, colorectal, breast and lung cancer as well as the relation between its overexpression and tumor malignancy. The study of Fedorczyk et al. showed that some of the synthesized triazolopeptidomimetics had remarkable resistance against proteolytic degradation in human plasma as well as half-lifes exceeding 48 hours.[52,47]

These examples confirm the effectiveness of the replacement of amide bonds with triazoles. This method leads to potential peptide-based drug candidates as well as resistant delivery agents with enhanced stability and other beneficial properties giving rise to a class of valuable peptidomimetics. The introduction of triazoles into peptides can be included in manual solid phase peptide synthesis but so far there is no method that describes the automation of this procedure. With the availability of automated peptide synthesizers, the development of a protocol for the fully automated synthesis of triazolopeptidomimetic shall be within reach.

2. Aim of the Thesis

The aim of this thesis was the automation of the synthesis of backbone modified triazolopeptidomimetics with an automated microwave assisted peptide synthesizer. Therefore, the triazole incorporation into peptides by the diazo-transfer and CuAAC reactions needed to be adapted from a manual to an automated setup which is compatible with SPPS. As the automated procedure requires the preparation of all reagent solutions in advance, the stability of the reagents for the triazole incorporation needed to be evaluated over time. In order to obtain the triazolopeptidomimetics in an efficient manner, the conditions for the triazole incorporation need to be optimized including reaction time, temperature and equivalents of the used reagents and reactants. To evaluate the robustness of the automated synthesis, different amino alkynes had to be tested to see possible impacts of amino acid side chain structures in terms of size, aromaticity and bulkiness. Therefore, amino alkynes with no side chain (Gly), aromatic side chain (Phe) and bulky, protected side chains (Arg, Glu, Tyr) should be inserted. To find out whether the solid support has an impact on the automated triazole incorporation and to show that different C-terminal functionalized peptides can be obtained with this protocol the synthesis were carried out using different resins (rink amide and wang resin). To test if the position of the incorporated triazole influences the efficacy of the procedure, especially for amino alkynes with side chains close to the resin in terms of steric hindrance, peptides bearing triazoles at different distances to the resin needed to be synthesized. Moreover, the insertion of two triazoles into one peptide needed to be carried out to prove that the protocol is also suitable for multiple triazole incorporations.

3. Materials and Methods

If not mentioned otherwise, all reagents and solvents were purchased from commercial suppliers and used without further purification. Routine monitoring of reactions was performed using precoated Merck-Kieselgel 60 F254 aluminium backed TLC plates. The spots were visualized by UV254 light and/or staining the plates with potassium permanganate followed by heating. Flash column chromatography was performed using silica gel (obtained from Sigma-Aldrich) as the adsorbent.

^{1}H- and ^{13}C-NMR spectra were recorded using either Bruker Avance Neo 500 MHz or Avance III 150 MHz Cryo instruments at 25°C. ^{1}H- and ^{13}C-NMR spectra were referenced to the residual solvent ($CDCl_3$, δ=7.26 ppm and δ=77.16 ppm respectively). All chemical shifts (δ) are reported in ppm and coupling constants (J) are in Hertz (Hz) and are reported to the nearest half integer.

High-Resolution Electrospray (ESI) mass spectra were recorded on a Bruker maXis UHR-TOF spectrometer in positive mode.

Chiral HPLC chromatograms were recorded on a Thermo Scientific Dionex UltiMate 3000 UHPLC using a ReproSil Chiral-NR column (r18.nr, 100Å, 8 µm, 250 x 4.6 mm, Dr. Maisch GmbH) and the mobile phase was MeCN in H_2O with 0.1% FA.

Peptide chromatograms were either recorded on a Thermo Scientific Dionex UltiMate 3000 UHPLC coupled to an Advion expression^{L} compact mass spectrometer or on an Agilent 1260 infinity II LC-MS system. The column used for the peptide analysis was an ACQUITY UPLC Peptide BEH C18 (300Å, 1.7 µm, 100 x 2.1 mm, Waters) and the mobile phase was MeCN in H_2O with 0.1% FA.

Peptide synthesis were carried out on a Biotage® Initiator+ Alstra™ Automated Microwave Peptide Synthesizer.

Peptide precipitates were centrifuged for 5 minutes at 4000 rpm with a Hettich centrifuge Rotina 380 R.

3.1. Synthesis of Building Blocks – General Procedure

The α-amino alkyne building blocks have been prepared by adapted procedures described by Grob et al.[7] and Valverde et al.[50] First, the α-amino acids were either converted into Weinreb amides (path 1) or reduced to the corresponding alcohol (path 2), depending on the side chain. In both cases they were subsequently reduced to the corresponding aldehyde. Then, a Seyferth-Gilbert homologation was carried out to obtain the α-amino alkyne.

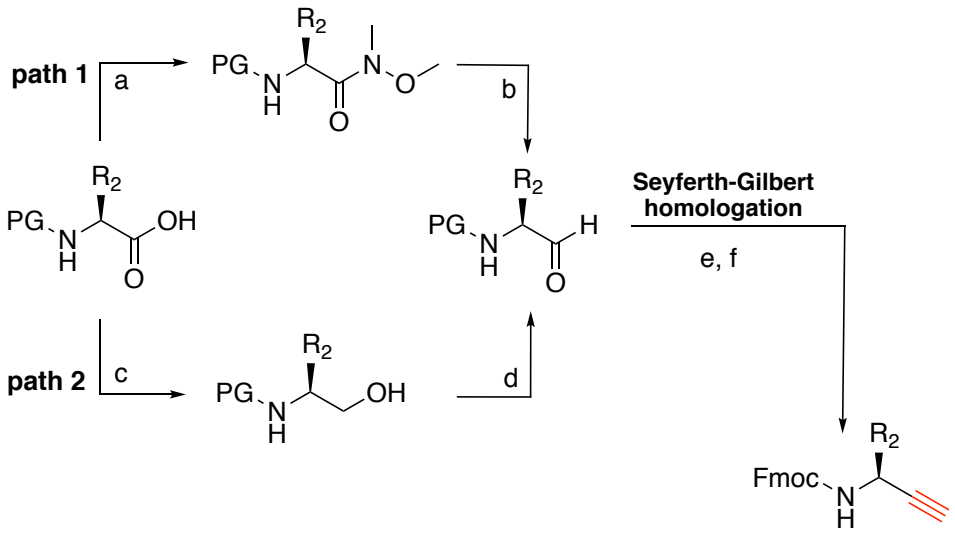

Scheme 3: Reaction scheme of the alkyne synthesis adapted from Grob et al.[7]. a) BOP, DIPEA, N,O-dimethylhydroxylamine hydrochloride; b) DIBAL-H; c) N-methylmorpholine, isobutyl chloroformate, $NaBH_4$; d) DMSO, oxalyl chloride, DIPEA; e) dimethyl-(1-diazo-2-oxopropyl)phosphonate, MeOH, K_2CO_3; f) if PG = Boc: TFA, DIPEA, Fmoc-OSu; if PG = Fmoc: DIPEA, Fmoc-OSu.

3.1.1. Synthesis of Fmoc-propargylamine

Fmoc chloride (1.3 g, 5 mmol, 1 equiv.) was dissolved in 10 mL acetone. The solution was added dropwise to a solution of propargylamine (275 mg, 5 mmol, 1 equiv.) and $NaHCO_3$ (840 mg, 10 mmol, 2 equiv.) in 10 mL water. After 30 min the completion of the reaction was verified by TLC and the precipitate was filtered and washed with water. For recrystallization 10 mL of hexane were added to the precipitate and heated to boil to 80°C. EtOAc was added dropwise until the crude product was dissolved completely. The solution was cooled and after crystallization in the fridge over night the product was filtered and washed with hexane.

3.1.2. Synthesis of Weinreb Amides from α-Amino Acids

The corresponding protected amino acid (1 equiv.), BOP (1 equiv.) and DIPEA (2.5 equiv.) were dissolved in DCM to obtain a 0.1 M solution. N,O-dimethylhydroxylamine hydrochloride (1.2 equiv.) was added and the reaction mixture was stirred at room temperature overnight. The

completion of the reaction was confirmed by TLC. The solution was diluted with EtOAc and washed with 1 M HCl (3x), saturated $NaHCO_3$ solution (3x), water and brine. The combined organic phases were dried over Na_2SO_4, filtered and concentrated under reduced pressure. The crude product was purified by flash chromatography on silica gel to obtain the corresponding Weinreb amide.

3.1.3. Synthesis of α-Amino Alcohols from α-Amino Acids

The corresponding Fmoc-protected amino acid (1 equiv.) was dissolved in anhydrous THF (0.2M) under argon and cooled to 0°C (ice bath). N-methylmorpholine (1.1 equiv.) and isobutyl chloroformate (1.05 equiv.) were added under inert conditions. The reaction was stirred at room temperature for 30 min (completion verified by TLC). The reaction mixture was added dropwise to a precooled (-78°C dry ice/acetone bath) suspension of $NaBH_4$ (2 equiv.) in THF:MeOH 3:1. The reaction was carried out for 30 min at -78°C. The excess of $NaBH_4$ was quenched with 10% acetic acid. The reaction mixture was concentrated under reduced pressure and the crude product was extracted with EtOAc. The Fmoc-protected α-amino alcohol was obtained by flash chromatography on silica gel.

3.1.4. Synthesis of α-Amino Alkynes from α-Amino Alcohols

A 1 M solution of DMSO (2.2 equiv.) in anhydrous DCM was cooled to -45°C (dry ice/MeCN bath). A 2 M solution of oxalyl chloride in DCM (1.2 equiv.) was added dropwise under inert conditions and the solution was stirred for 10 min. The Fmoc-protected α-amino alcohol (1 equiv.) was dissolved in anhydrous DCM (1.3 M), added dropwise to the reaction mixture and stirred for 30 min at -45°C under inert conditions. The reaction was warmed to -20°C (NaCl/ice bath), DIPEA (3 equiv.) was added dropwise and the reaction was carried out until completion (monitored by TLC). The solution was diluted with DCM and the organic layer was washed with 1 M $KHSO_4$ and water. The combined organic layers were dried over Na_2SO_4, filtered and the solvent removed under reduced pressure. The crude amino-aldehyde intermediate was subsequently dissolved in anhydrous MeOH (0.1 M according to the initial scale), K_2CO_3 (3 equiv.) and dimethyl-(1-diazo-2-oxopropyl)phosphonate (2 equiv.) were added and the reaction was stirred at room temperature overnight. The mixture was diluted with DCM and 10 mL of a saturated solution of Rochelle's salt were added. The reaction mixture was stirred until both phases became clear. The organic phase was washed with brine, dried over Na_2SO_4, filtered and the solvent removed under reduced

pressure. As cleavage of the Fmoc protecting group took place (verified by TLC) the unprotected crude amino alkyne was dissolved in 1 mL DCM. DIPEA (2.5 equiv.) and Fmoc-OSu (2 equiv.) were added and the reaction was stirred overnight at room temperature. The crude mixture was diluted with DCM and water. The aqueous phase was washed with DCM (3x) and the combined organic layers were dried over Na_2SO_4, filtered and the solvent removed under reduced pressure. The desired Fmoc-protected amino alkyne was obtained by flash chromatography using silica gel as a solid phase.

3.1.5. Synthesis of α-Amino Alkynes from Weinreb Amides

The corresponding protected Weinreb amide (1 equiv.) was dissolved in anhydrous DCM (0.1 M) and the solution was cooled to -78°C (acetone/dry ice bath). A solution of DIBAL-H (3 equiv., 1M in THF) was added dropwise with maintaining a temperature of -78 °C. The reaction was carried out under inert conditions and completed after 2 hours (verified by TLC). The excess of DIBAL-H was quenched by dropwise addition of anhydrous MeOH. After the reaction mixture was warmed to 0°C (ice/water bath), K_2CO_3 (3 equiv.) and dimethyl-(1-diazo-2-oxopropyl)phosphonate (2 equiv.) were added. The reaction was stirred at room temperature overnight. The reaction was diluted with 10 mL DCM and 10 mL of a saturated solution of potassium sodium tartrate were added. The reaction mixture was stirred until both phases became clear. The organic layer was washed with brine, dried over Na_2SO_4 and filtered. The solvent was removed under reduced pressure.

a) If the protecting group was Fmoc:

   As cleavage of the Fmoc protecting group took place (verified by TLC), the crude amino alkyne was dissolved in 1 mL DCM. DIPEA (2.5 equiv.) and Fmoc-OSu (2 equiv.) were added and the reaction was stirred overnight at room temperature. The crude mixture was diluted with DCM and water. The aqueous layer was washed with DCM (3x) and the combined organic layers were dried over Na_2SO_4, filtered and the solvent removed under reduced pressure. The desired Fmoc-protected amino alkyne was obtained by flash chromatography using silica gel.

b) If the protecting group was Boc:

Removal of the Boc protecting group was carried out by preparing a 0.5 M solution of the Boc-protected amino alkyne in DCM:TFA:H_2O (75:20:5). The reaction was stirred for 5 hours. The solvents were removed under reduced pressure by addition of toluene. Subsequently, the unprotected amino alkyne was dissolved in DCM. DIPEA (2.5 equiv.) and Fmoc-OSu (2 equiv.) were added and the reaction was stirred overnight at room temperature. The crude mixture was diluted with DCM and water. The aqueous layer was washed with DCM (3x) and the combined organic layers were dried over Na_2SO_4, filtered and the solvent removed under reduced pressure. The desired Fmoc-protected amino alkyne was obtained by flash chromatography using silica gel.

3.2. Synthesis of Triazolopeptidomimetics – General Procedure

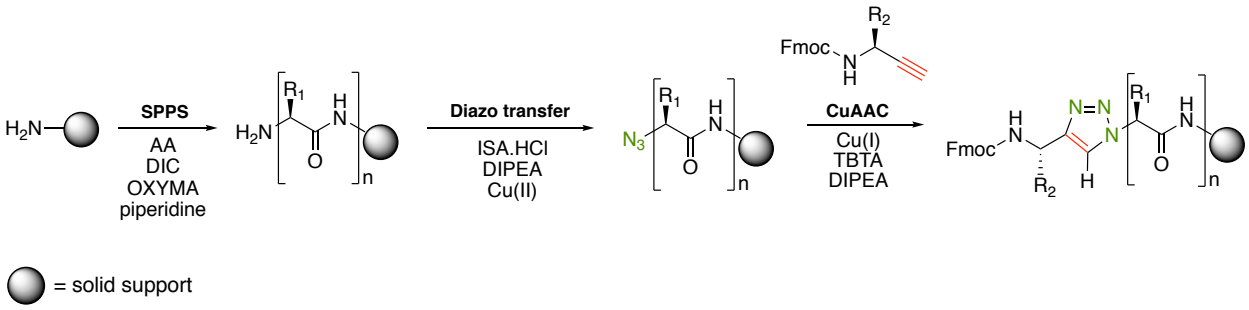

Scheme 4: General procedure for the synthesis of peptides and the incorporation of triazoles on solid phase. $R_{1/2}$ = amino acid specific side chain.

All triazole bearing peptide synthesis were performed automatically with the microwave assisted peptide synthesizer on solid phase following standard Fmoc chemistry. The reactions were carried out in 10 mL vials at a scale of 0.03 mmol. Rink amide MBHA (4-methylbenzylhydrylamine) resin (0.065 mmol/g loading, 100-200 mesh) and wang resin (0.99 mmol/g loading, 4-Benzyloxybenzyl alcohol polystyrene, 200-400 mesh) were used as solid supports. The resins were prepared by swelling in DMF at 70°C for 20'. Wang resin was preloaded using a loading cocktail consisting of the first amino acid (5 equiv.), DIC (5 equiv.), HOBt (5 equiv.) and DMAP (0.5 equiv.) in 6 mL DMF. The preloading was carried out at 75°C for 20 min. The cleavage of Fmoc protecting groups was accomplished using 2 x 4 .5 mL 20% piperidine in DMF for a 3' and a 10' reaction respectively at room temperature. The amino acids (5 equiv.) were prepared as 0.1 M solutions in DMF. For the coupling reactions the coupling reagents (5 equiv.) DIC (0.05 – 2 M in DMF) and OXYMA (0.2 M in DMF) were used. Coupling reactions were carried out for 5' at 75°C. For arginine a

double coupling with 5' and 75°C was carried out. The triazole incorporation was achieved by diazo-transfer followed by the CuAAC click reaction. For the diazo-transfer imidazole sulfonyl chloride (7 equiv.) was used as a 1.2 M solution in water. As a base DIPEA (14 equiv.) prepared as a 0.1 M solution in DMF was used. $CuSO_4$ was used with a catalytic charge of 0.02 equiv. and the reaction was carried out for 30' at 80°C. For the CuAAC click reaction $[Cu(CH_3CN)_4]PF_6$ (0.5 equiv.) was used as a copper source and TBTA (0.5 equiv.) as a stabilizing agent as 0.01 M solutions in DMF respectively. The corresponding amino alkyne (5 equiv.) was prepared as a 0.1 M solution in DMF and DIPEA (1 equiv.) in DMF was added to the reaction. The CuAAC reaction was run for 1 h at 70°C. After the synthesis a pre-cleavage wash was carried out with DCM. The sidechain protecting groups used were Boc (Trp), tBu (Tyr, Glu), Pbf (Arg) and Trt (Gln, His). The cleavage and the deprotection of the peptides were performed using TFA:H_2O:TIPS (95.5:0.5:0.5) for 2 h on the shaker. The cleaved peptides were dried under a stream of argon, precipitated with MTBE and analyzed by LC-MS and/or HPLC.

3.3. One-pot Triazole Synthesis

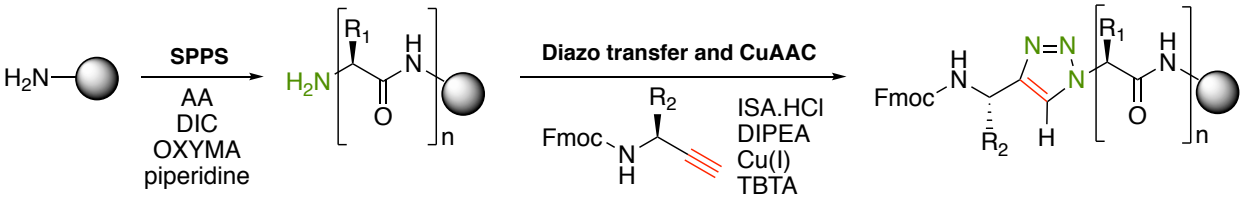

Scheme 5: Reaction scheme of the one-pot and one-step triazole synthesis.

One-pot triazole incorporation was carried out fully automatically with the peptide synthesizer by combining the diazo-transfer and the CuAAC click reaction in one single step. The procedure was adapted from methods described by Beckmann et al.[45] Therefore, the peptide sequence was synthesized as described in chapter 3.2 containing the free amine at the position where the triazole should be integrated. The reaction was performed in a 10 mL vial using 0.03 mmol of the peptide. The resin with the peptide on it was swollen in DMF for 20' at 70°C. Afterwards, the diazo-transfer reagent (5 equiv., 1.2 M in water), DIPEA (10 equiv., 0.1 M in DMF), $[Cu(CH_3CN)_4]PF_6$ and TBTA (2 equiv. respectively, 0.05 M in DMF) were added to the vial and the reaction was carried out for one hour at 80°C. After the synthesis a pre-cleavage wash was carried out with DCM. The cleavage and the deprotection of the peptide sequence were performed using TFA:H_2O:TIPS (95.5:0.5:0.5)

for 2 h on the shaker. The cleaved sequence was dried under a stream of argon, precipitated with MTBE and analyzed by LC-MS.

3.4. Stability of Reagents

3.4.1. Imidazole-1-sulfonylazide Hydrochloride

Three solutions of ISA.HCl in H_2O (1.2 M), ISA.HCl in DMSO (0.6 M) and ISA.HCl in DMF (0.6 M) were analyzed after 0', 60', 120', 240' and 24 hours. Therefore, 50 µL of the solution was diluted with 950 µL of a solution of 5% MeCN in water with 0,1% formic acid (starting conditions for the LC-MS run) and measured by LC-MS. For the measurements an Acquity UPLC BEH C18 7µm, 3x50mm column with a flow of 0.6 mL/min was used and the chromatograms recorded at 220 nm.

3.4.2. $[Cu(CH_3CN)_4]PF_6$ and TBTA

A solution of $[Cu(CH_3CN)_4]PF_6$ and TBTA in DMF (0.01 M) was prepared. After 0 and 24 hours an aliquot for the solution was drawn and the reaction was carried out. For the reaction 0.03 mmol of the azide functionalized peptide sequence N_3-His-Leu-NLe-NH_2 attached to the resin was used and prepared by swelling in DMF (20', 70°C). The CuAAC reaction was carried out for 1 h at 70°C as described in chapter 3.2. The cleavage and the deprotection of the triazole sequence were performed using TFA:H_2O:TIPS (95.5:0.5:0.5) for 2 h on the shaker. The cleaved sequence was dried under a stream of argon, precipitated with MTBE and analyzed by HPLC.

4. Results and Discussion

4.1. Synthesis and Characterization of Amino alkynes

Analytical data of the synthesized α-amino alkynes has found to be identical with data from literature reported by Grob et al.[7]

4.1.1. Fmoc-Gly-CCH

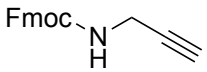

Figure 5: Structure of Fmoc-Gly-CCH ((9H-fluoren-9-yl)methyl prop-2-yn-1-ylcarbamate).

The Fmoc-protected propargylamine was synthesized as described in chapter 3.1.1 and obtained as light yellow-orange needle crystals with a yield of 78%.

ESI-MS: $[M+Na]^+$ *m/z* calculated for $C_{18}H_{15}NNaO_2$: 300.1000, found: = 300.0997.

^{1}H-NMR (500 MHz, $CDCl_3$) δ 7.77 (d, $_3$J = 7.5 Hz, 2H, arom. Fmoc), 7.59 (d, $_3$J = 7.1 Hz, 2H, arom. Fmoc), 7.41 (t, $_3$J = 7.5 Hz, 2H, arom. Fmoc), 7.32 (t, $_3$J = 7.0 Hz, 2H, arom. Fmoc), 4.96 (s, 1H, NH), 4.44 (d, $_3$J = 7.0 Hz, 2H, Fmoc-CH_2), 4.23 (t, $_3$J = 5.9 Hz, 1H, Fmoc-CH), 4.01 (d, $_3$J = 2.9 Hz, 2H, N-CH2), 2.26 (s, 1H, CCH) ppm.

^{13}C-NMR (150 MHz, $CDCl_3$) δ 156.03 (Fmoc-C=O), 143.93 (quart. C of Fmoc), 141.47 (quart. C of Fmoc), 127.88 (aromat. CH of Fmoc), 127.21 (aromat. CH of Fmoc), 125.16 (aromat. CH of Fmoc), 120.16 (aromat. C of Fmoc), 79.73 (quart. C of alkyne), 71.87 (tert. C of alkyne), 67.22 (Fmoc-CH_2), 47.29 (Fmoc-CH), 31.01 (N-CH_2) ppm.

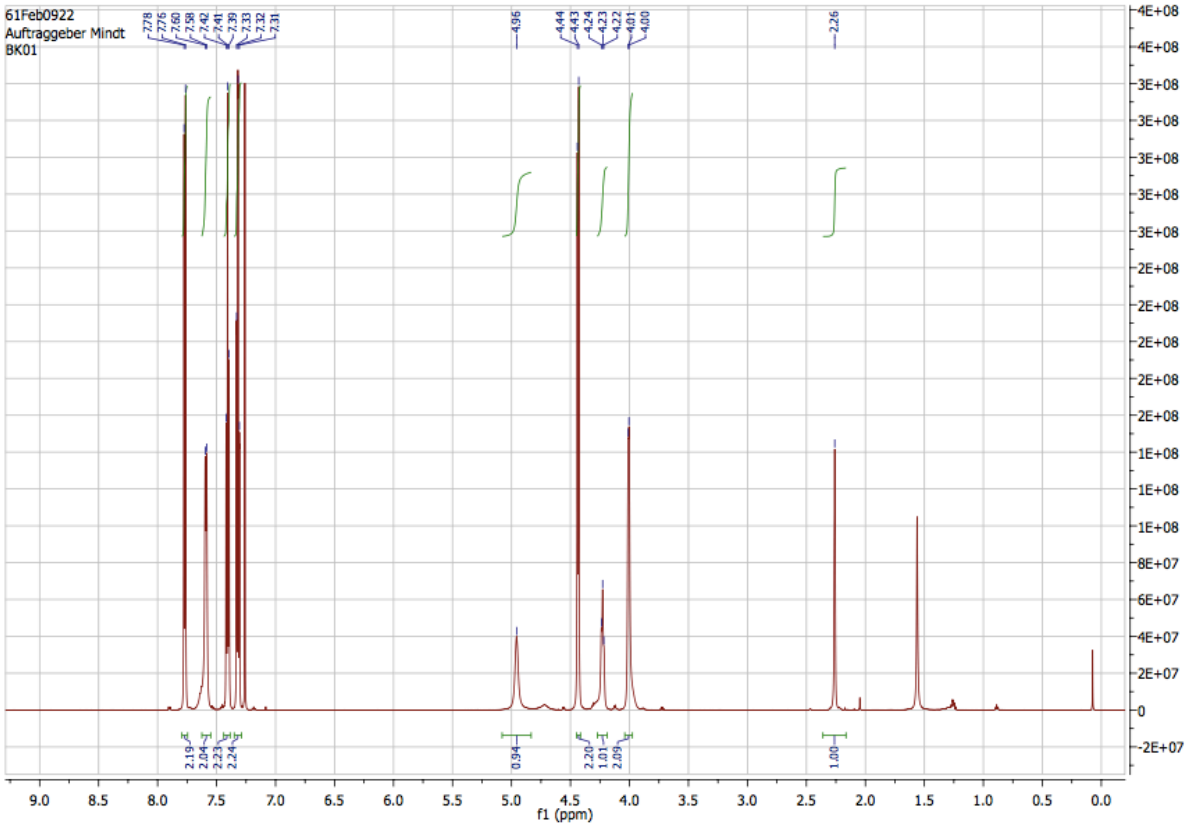

Figure 6: ^{1}H-NMR spectrum of Fmoc-Gly-CCH recorded with a 500 MHz instrument in $CDCl_3$.

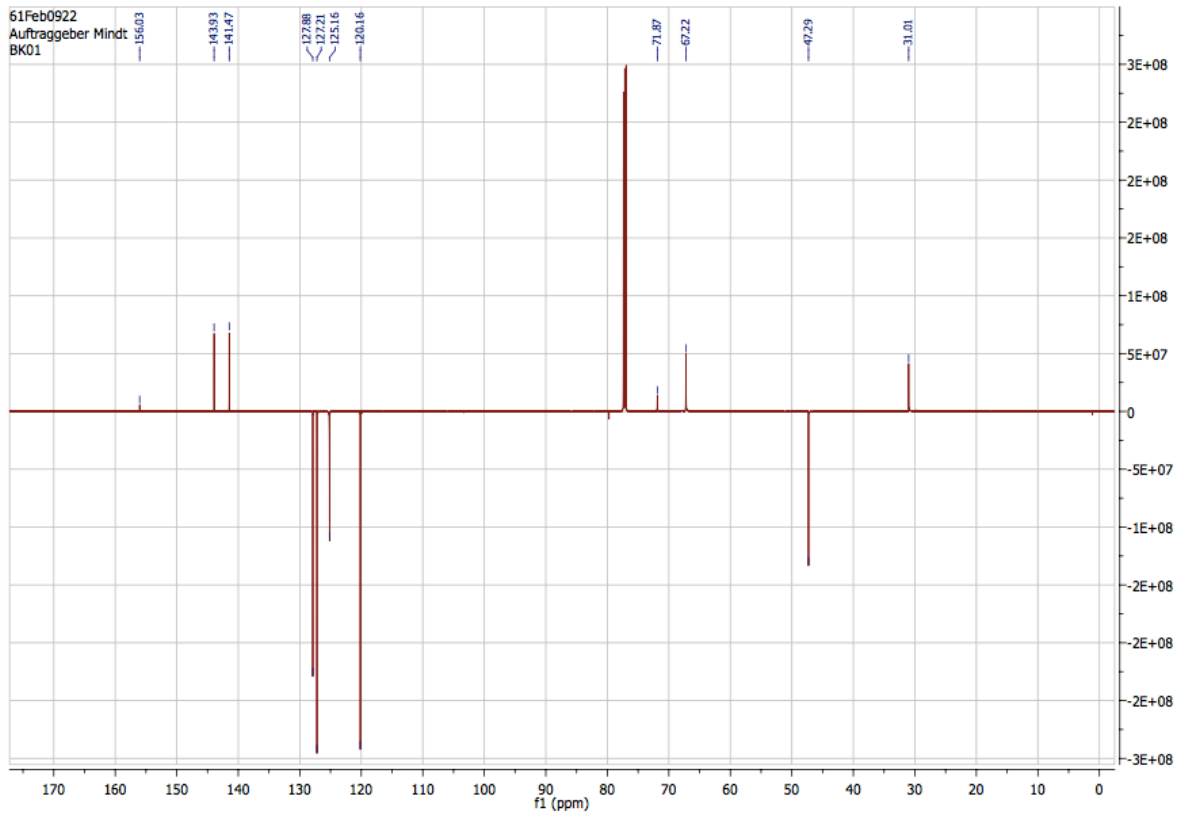

Figure 7: ^{13}C-NMR spectrum of Fmoc-Gly-CCH recorded with a 150 MHz instrument in $CDCl_3$.

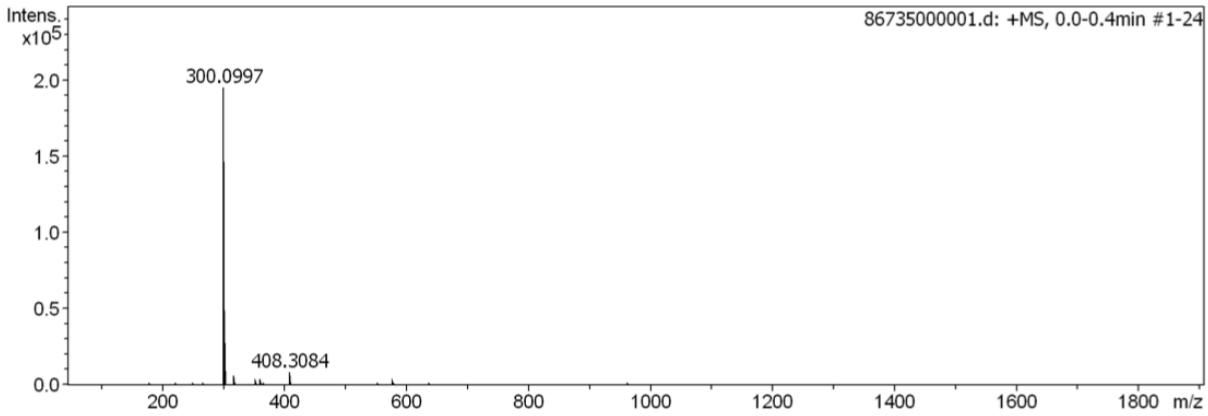

Figure 8: Mass spectrum of Fmoc-Gly-CCH showing the $[M+Na]^+$ m/z peak 300.0997. $[M+Na]^+$ m/z calculated for $C_{18}H_{15}NO_2Na$: 300.1000.

4.1.2. Fmoc-Tyr(OtBu)-CCH

4.1.2.1. Synthesis of Fmoc-Tyr(OtBu)-N(Me)O(Me)

The corresponding Fmoc-Tyr(OtBu) Weinreb amide was obtained from Fmoc-Tyr(OtBu)-COOH as described in chapter 3.1.2 and purified using hexane/EtOAc (1:1) as a mobile phase, with a yield of 89% as a white solid.

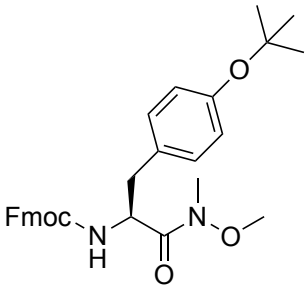

Figure 9: Structure of Fmoc-L-Tyr(OtBu)-N(Me)O(Me) ((9H-fluoren-9-yl)methyl (S)-(3-(4-(tert-butoxy)phenyl)-1-(methoxy(methyl)amino)-1-oxopropan-2-yl)carbamate).

ESI-MS: $[M+Na]^+$ *m/z* calculated for $C_{30}H_{34}N_2O_5Na$: 525.2360, found: = 525.2358.

^{1}H-NMR (500 MHz, $CDCl_3$) δ 7.76 (d, ^3J = 7.4 Hz, 2H, aromat. H Fmoc), 7.57 (t, ^3J = 7.3 Hz, 2H, aromat. H Fmoc), 7.40 (t, ^3J = 7.5 Hz, 2H, aromat. H Fmoc), 7.31 (t, ^3J = 7.5 Hz, 2H, aromat. H Fmoc), 7.07 (d, ^3J = 7.9 Hz, 2H, aromat. H Tyr), 6.90 (d, ^3J = 7.9 Hz, 2H, aromat. H Tyr), 5.49 (d, ^3J = 9.1 Hz, 1H, NH), 4.98 – 5.03 (m, 1H, α-CH), 4.33 – 4.37 (m, 2H, Fmoc-CH_2), 4.28 (t, ^3J = 7.3 Hz, 1H, Fmoc-CH), 3.62 (s, 3H, OMe), 3.16 (s, 3H, NMe), 3.02-3.06 (m, 1H, β-CH_2), 2.93-2.89 (m, 1H, β-CH_2), 1.29 (s, 9H, CH_3 of tBu) ppm.

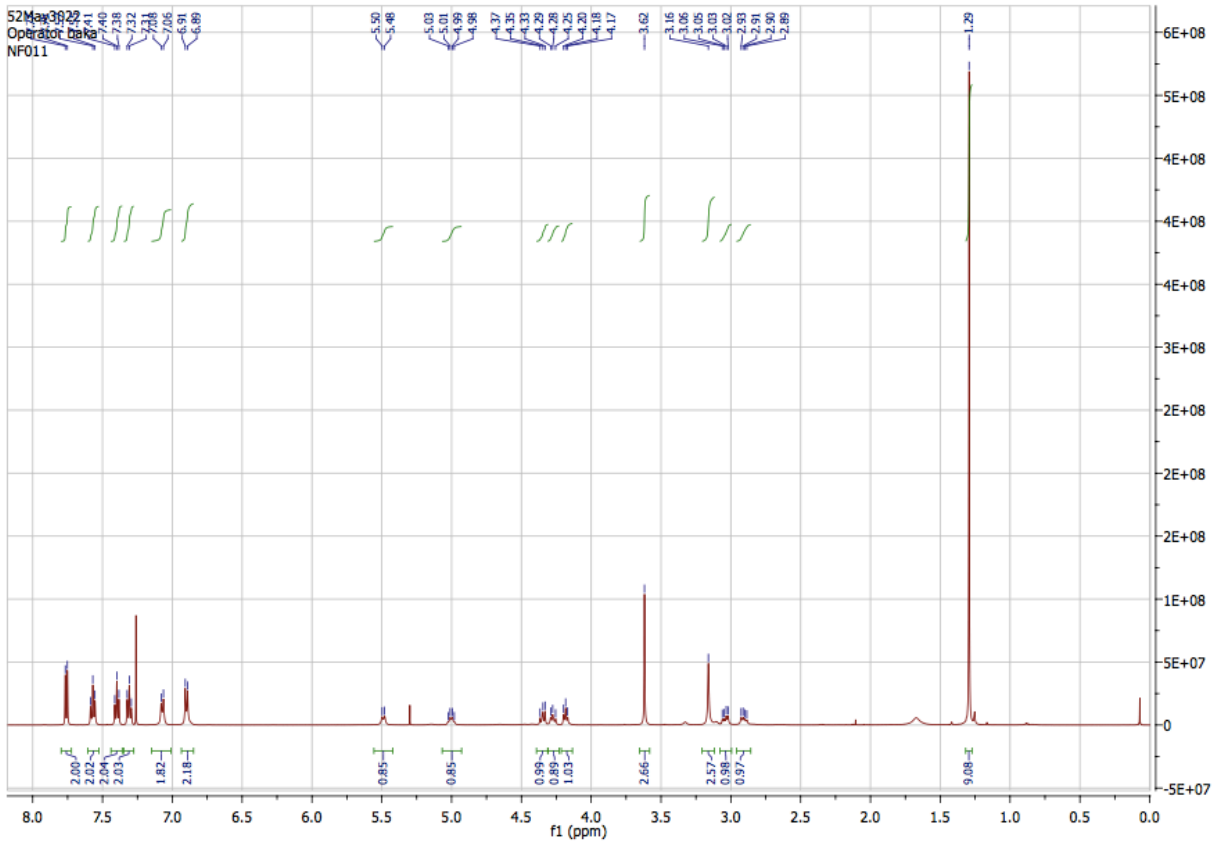

Figure 10: ^{1}H-NMR spectrum of Fmoc-Tyr(OtBu)-N(Me)O(Me) recorded with a 500 MHz instrument in $CDCl_3$.

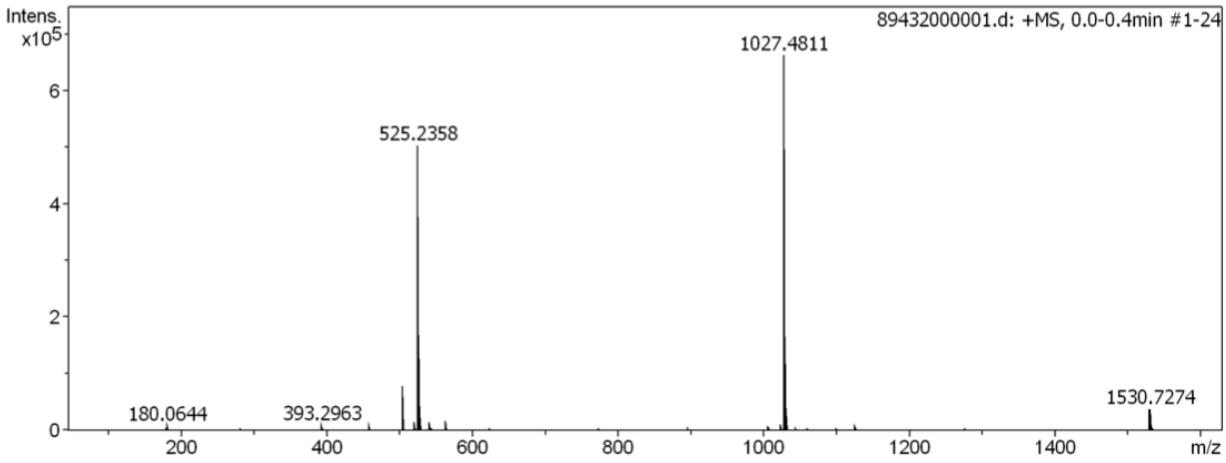

Figure 11: Mass spectrum of Fmoc-Tyr(OtBu)-N(Me)O(Me) showing the $[M+Na]^+$ m/z peak 525.2358. $[M+Na]^+$ m/z calculated for $C_{30}H_{34}N_2O_5Na$: 525.2360.

4.1.2.2. Synthesis of Fmoc-Tyr(OtBu)-CCH

The Weinreb amide (100 mg, 0.1989 mmol, 1 equiv.) was dissolved in 2 mL anhydrous DCM and the DIBAL-H reduction carried out for two hours with subsequent Seyferth-Gilbert homologation as described in chapter 3.1.5. Flash chromatography on silica gel (hexane/EtOAc 8:2) yielded the alkyne as white/clear crystals with 26%. The alkyne was isolated as a mixture of enantiomers in a 86:14 L/D ratio as demonstrated via chiral HPLC (Figure 16).

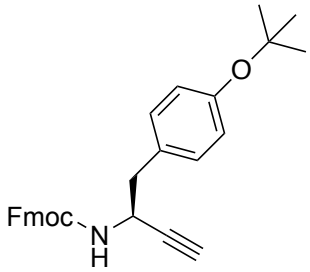

Figure 12: Structure of Fmoc-L-Tyr(OtBu)-CCH ((9H-fluoren-9-yl)methyl (S)-(1-(4-(tertButoxy)phenyl)but-3-yn-2-yl)carbamate).

ESI-MS: $[M+Na]^+$ *m/z* calculated for $C_{29}H_{29}NO_3Na$: 462.2040, found: = 462.2041.

^{1}H-NMR (500 MHz, $CDCl_3$) δ 7.77 (d, $_3J$ = 7.5 Hz, 2H, H Fmoc), 7.58 (d, $_3J$ = 6.8 Hz, 2H, H Fmoc), 7.41 (t, $_3J$ = 7.4 Hz, 2H, H Fmoc), 7.32 (td, $_3J$ = 7.1, $_4J$ = 0.5 Hz, 2H, H Fmoc), 7.13 (d, $_3J$ = 6.8 Hz, 2H, aromat. H Tyr), 6.92 (d, $_3J$ = 8.3, 2H, aromat. H Tyr), 4.95 (d, $_3J$ = 7.3 Hz, 1H, NH), 4.73 (d, $_3J$ = 3.9 Hz, 1H, α-CH), 4.50 – 4.34 (m, 2H, Fmoc-CH_2), 4.21 (t, $_3J$ = 6.6 Hz, 1H, Fmoc-CH), 3.01–2.89 (m, 2H, β-CH_2), 2.31 (d, $_4J$ = 2.3 Hz, 1H, CCH), 1.34 (s, 9H, CH_3 of tBu) ppm.

^{13}C NMR (150 MHz, $CDCl_3$) δ 155.31 (Fmoc-C=O), 154.61 (quart. C-O phenol), 143.91 (quart. C of Fmoc), 141.47 (quart. C of Fmoc), 130.86 (quart. C-C phenol), 130.36 (aromat. CH of phenol), 127.87 (aromat. CH of Fmoc), 127.20 (aromat. CH of Fmoc), 125.14 (aromat. CH of Fmoc), 124.09 (aromat. CH of phenol), 120.14 (aromat. CH of Fmoc), 82.56 (quart. C of CCH), 78.50 (quart. C of tBu), 72.67 (tert. C of CCH), 67.02 (Fmoc-CH_2), 47.34 (Fmoc-CH), 44.46 (α-CH), 40.95 (β-CH_2), 28.99 (CH_3 of tBu) ppm.

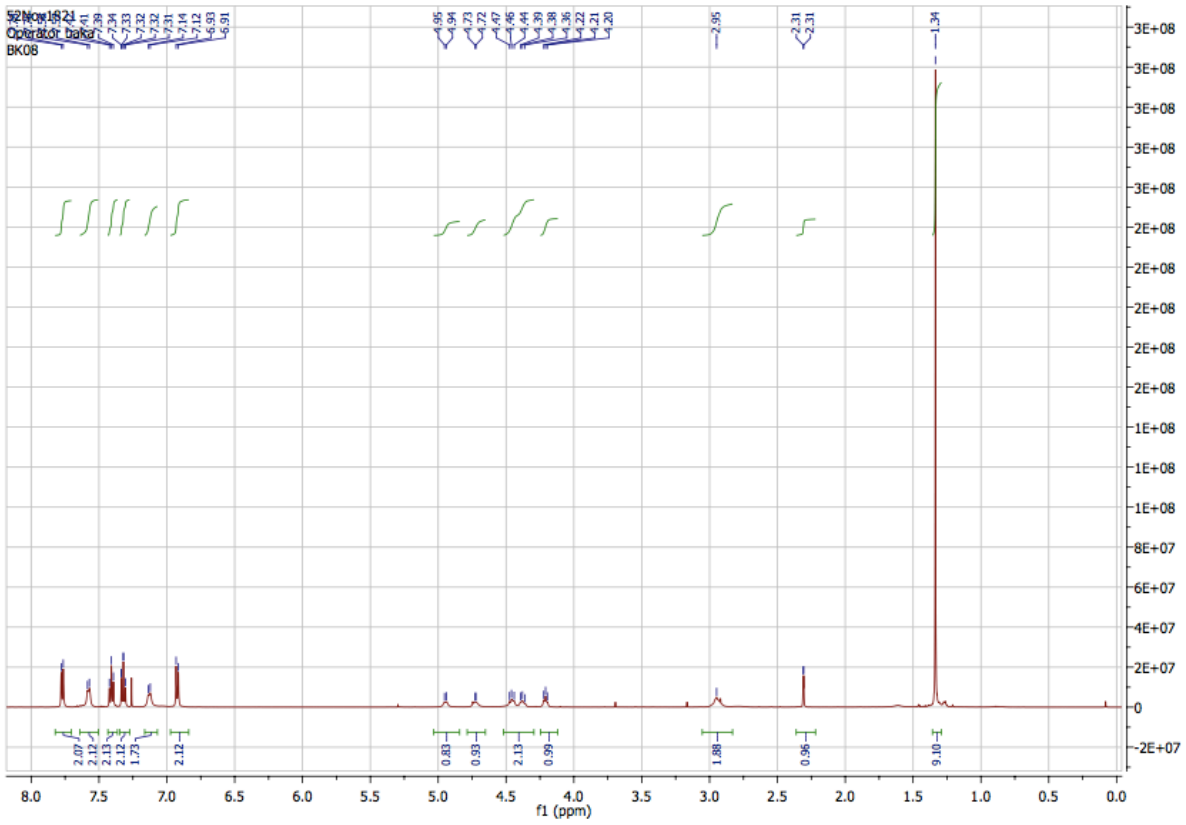

Figure 13: ^{1}H-NMR spectrum of Fmoc-Tyr(OtBu)-CCH recorded with a 500 MHz instrument in $CDCl_3$.

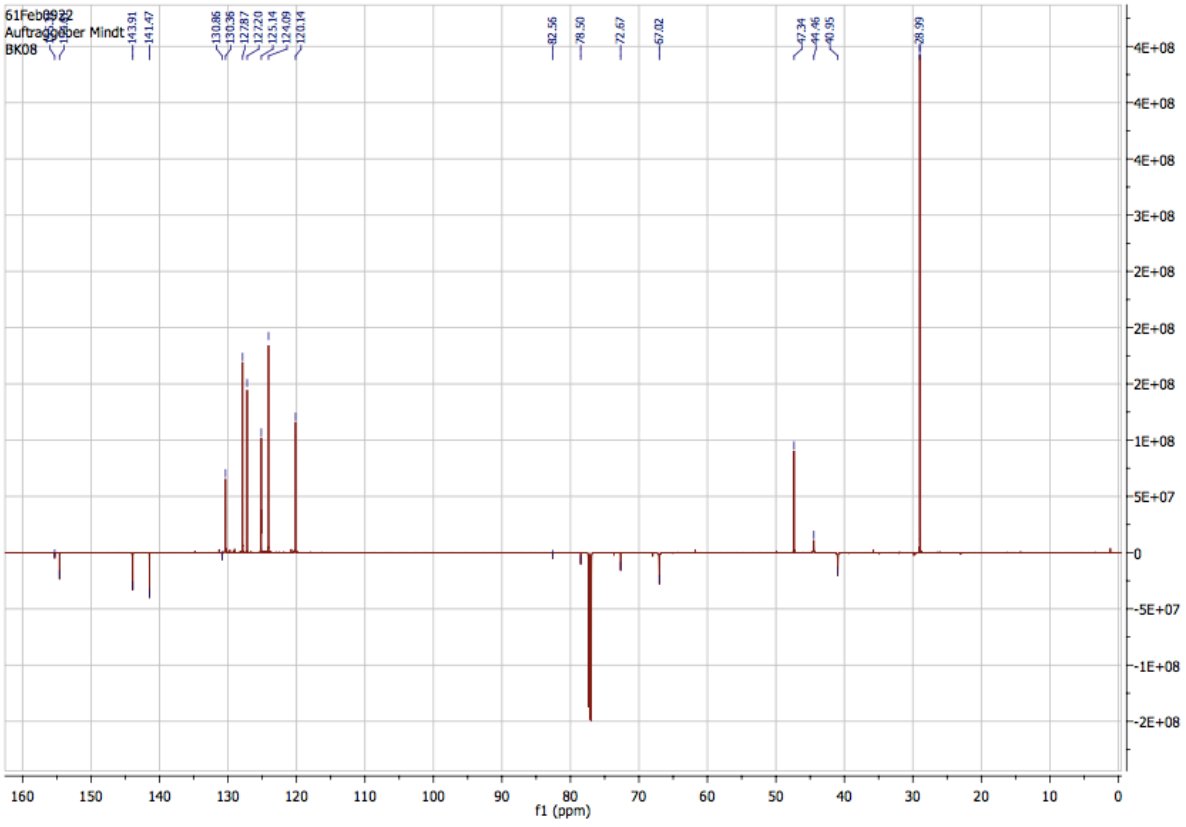

Figure 14: ^{13}C-NMR spectrum of Fmoc-Tyr(OtBu)-CCH recorded with a 150 MHz instrument in $CDCl_3$.

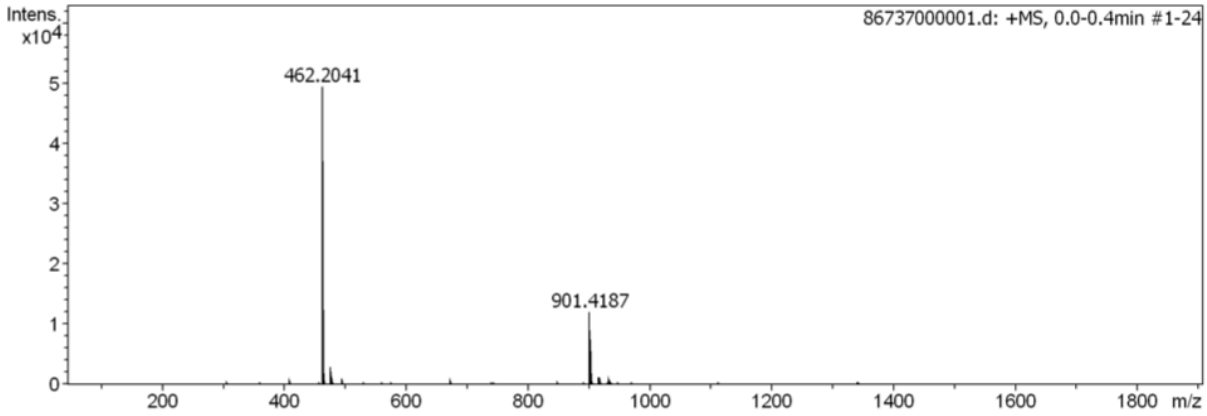

Figure 15: Mass spectrum of Fmoc-Tyr(OtBu)-CCH showing the $[M+Na]^+$ m/z peak 462.2041. $[M+Na]^+$ m/z calculated for $C_{29}H_{29}NO_3Na$: 462.2040.

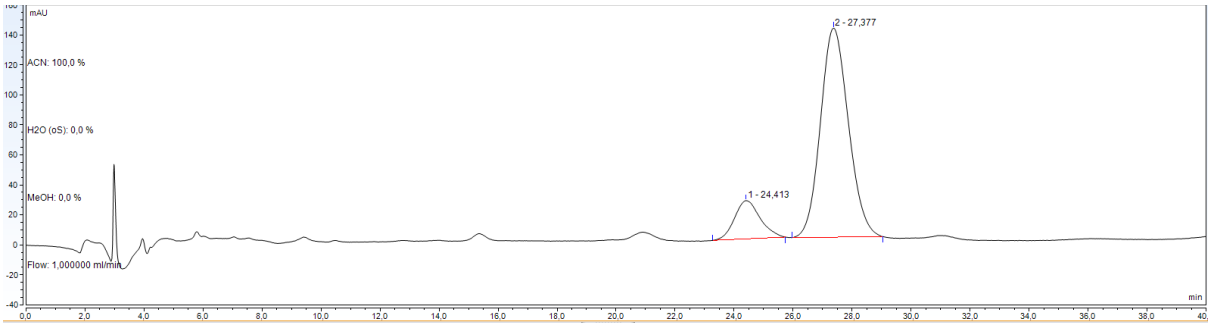

Figure 16: Chiral HPLC chromatogram of Fmoc-Tyr(tBu)-CCH recorded at 220 nm with an isocratic flow of 1 mL/min using 20% isopropanol in hexane as a mobile phase. The chromatographic peak at t_r = 24.413' shows the D-enantiomer (14%) and the peak at t_r = 27.377' shows the L-enantiomer (86%).

4.1.3. Fmoc-Phe-CCH

4.1.3.1. Synthesis of Boc-Phe-N(Me)O(Me)

The corresponding Weinreb amide was obtained from Boc-Phe-COOH (286 mg, 1.0780 mmol, 1 equiv.) as described in chapter 3.1.2 and purified by flash chromatography using hexane/EtOAc (2:1) as a mobile phase. The Weinreb amide was yielded with 76% as a viscous, colorless oil.

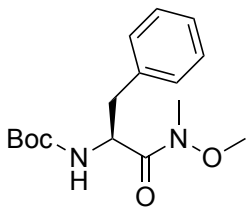

Figure 17: Structure of Fmoc-L-Phe-N(Me)O(Me) (tert-butyl (S)-(1-(methoxy(methyl)amino)-1-oxo-3-phenylpropan-2-yl)carbamate).

ESI-MS: $[M+Na]^+$ *m/z* calculated for $C_{16}H_{24}N_2O_4Na$: 331.1628, found: = 331.1620.

^{1}H-NMR (500 MHz, $CDCl_3$) δ 7.27 – 7.09 (m, 5H, aromat. CH), 5.13 (d, $_3J$ = 7.2 Hz, 1H, NH), 4.88 – 4.87 (m, 1H, α-CH), 3.58 (s, 3H, OMe), 3.09 (s, 3H, NMe), 3.00 - 2.96 (m, 1H, β-CH_2), 2.82 - 2.78 (m, 1H, β-CH_2), 1.31 (s, 9H, CH_3 of tBu) ppm.

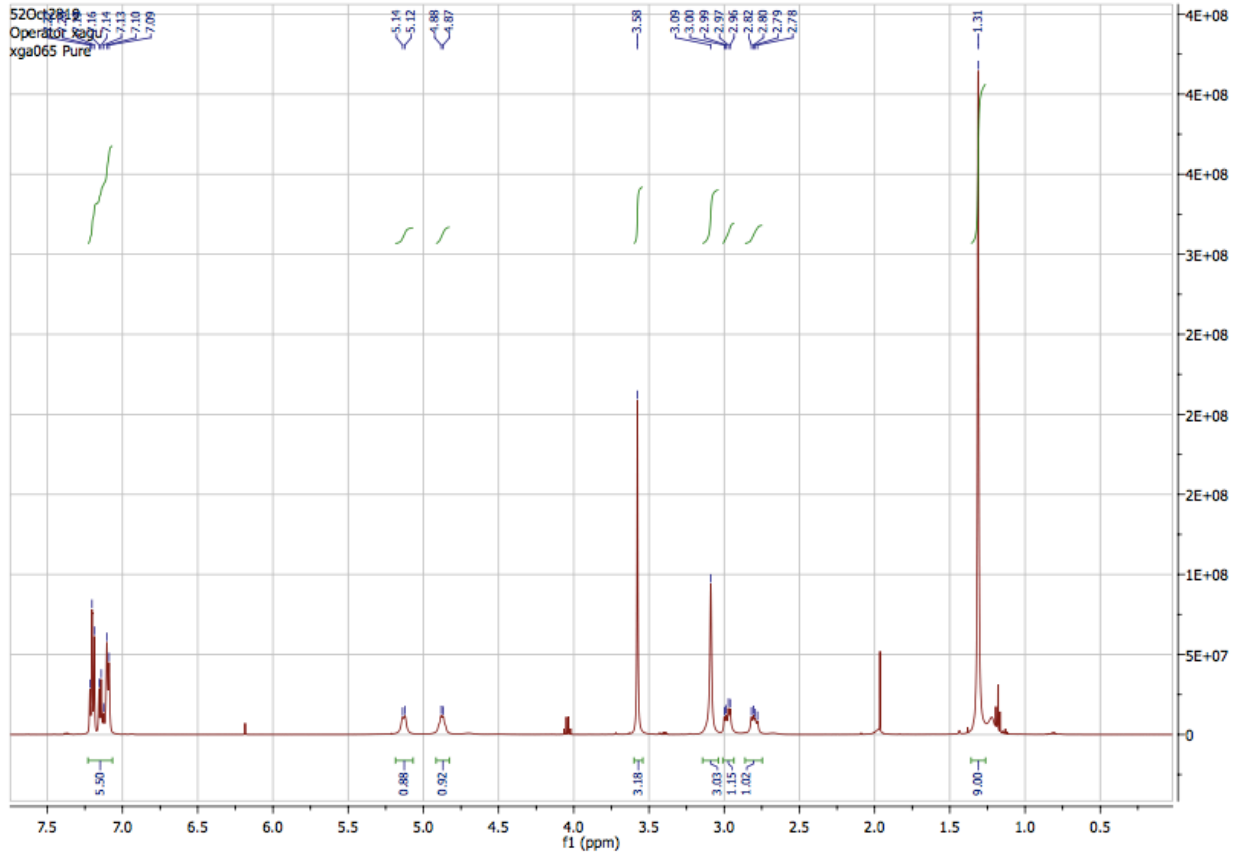

Figure 18: ^{1}H-NMR spectrum of Boc-Phe-N(Me)O(Me) recorded with a 500 MHz instrument in $CDCl_3$.

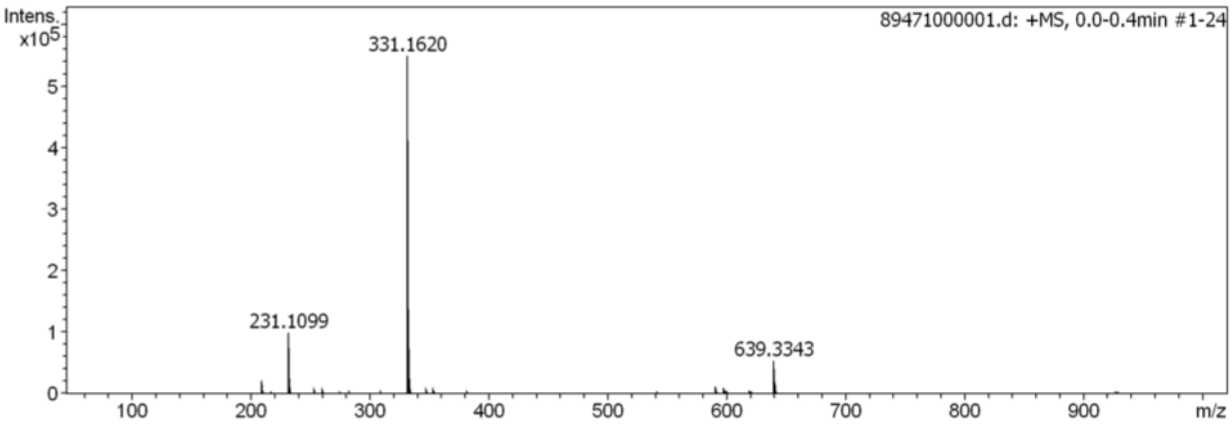

Figure 19: Mass spectrum of Boc-Phe-N(Me)O(Me) showing the $[M+Na]^+$ m/z peak 331.1620. $[M+Na]^+$ m/z calculated for $C_{16}H_{24}N_2O_4Na$: 331.1628.

4.1.3.2. Synthesis of Fmoc-Phe-CCH

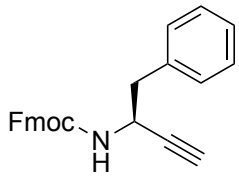

Figure 20: Structure of Fmoc-L-Phe-CCH ((9H-fluoren-9-yl)methyl (S)-(1-phenylbut-3-yn-2-yl)carbamate).

The corresponding Boc protected amino alkyne was obtained from the Weinreb amide (290 mg, 0.9403 mmol, 1 equiv.) as described in chapter 3.1.5. Replacement of the Boc protecting group to a Fmoc group was carried out as described in chapter 3.1.5. The corresponding amino alkyne was obtained as a yellow solid after purification by flash chromatography on silica gel (hexane/EtOAc 5:1) with a yield of 77%. The alkyne was isolated as a mixture of enantiomers in a 96:4 L/D ratio as demonstrated via chiral HPLC (**Fehler! Verweisquelle konnte nicht gefunden werden.**).

ESI-MS: $[M+Na]^+$ *m/z* calculated for $C_{25}H_{21}NO_2Na$: 390.1464, found: = 390.1471.

^{1}H-NMR (500 MHz, $CDCl_3$) δ 7.76 (d, $_3J$ = 7.5 Hz, 2H, Fmoc), 7.59 – 7.54 (m, 2H, Fmoc), 7.40 (t, $_3J$ = 7.5, 2H, Fmoc), 7.34 – 7.21 (m, 2H Fmoc and 5H Phe), 5.02 (d, $_3J$ = 6.9 Hz, 1H, NH), 4.81 – 4.73 (m, 1H, α-CH Phe), 4.52 – 4.32 (m, 2H, Fmoc-CH_2), 4.19 (t, $_3J$ = 6.8 Hz, 1H Fmoc-CH) 3.05 – 2.91 (m, 2H, β-CH_2Phe), 2.29 (d, $_4J$ = 2.2 Hz, 1H, CCH) ppm.

^{13}C-NMR (150 MHz, $CDCl_3$) δ 155.29 (Fmoc-C=O), 143.85 (quart. C of Fmoc), 141.42 (quart. C of Fmoc), 136.09 (quart. aromat. C of Phe), 129.91, 128.46, 127.82, 127.15, 125.15, 125.09, 120.10 (7 aromat. CH), 82.40 (quart. C of alkyne), 72.75 (tert. C of alkyne), 66.96 (Fmoc-CH_2), 47.27 (Fmoc- CH), 44.36 (α-CH), 41.52 (β-CH_2) ppm.

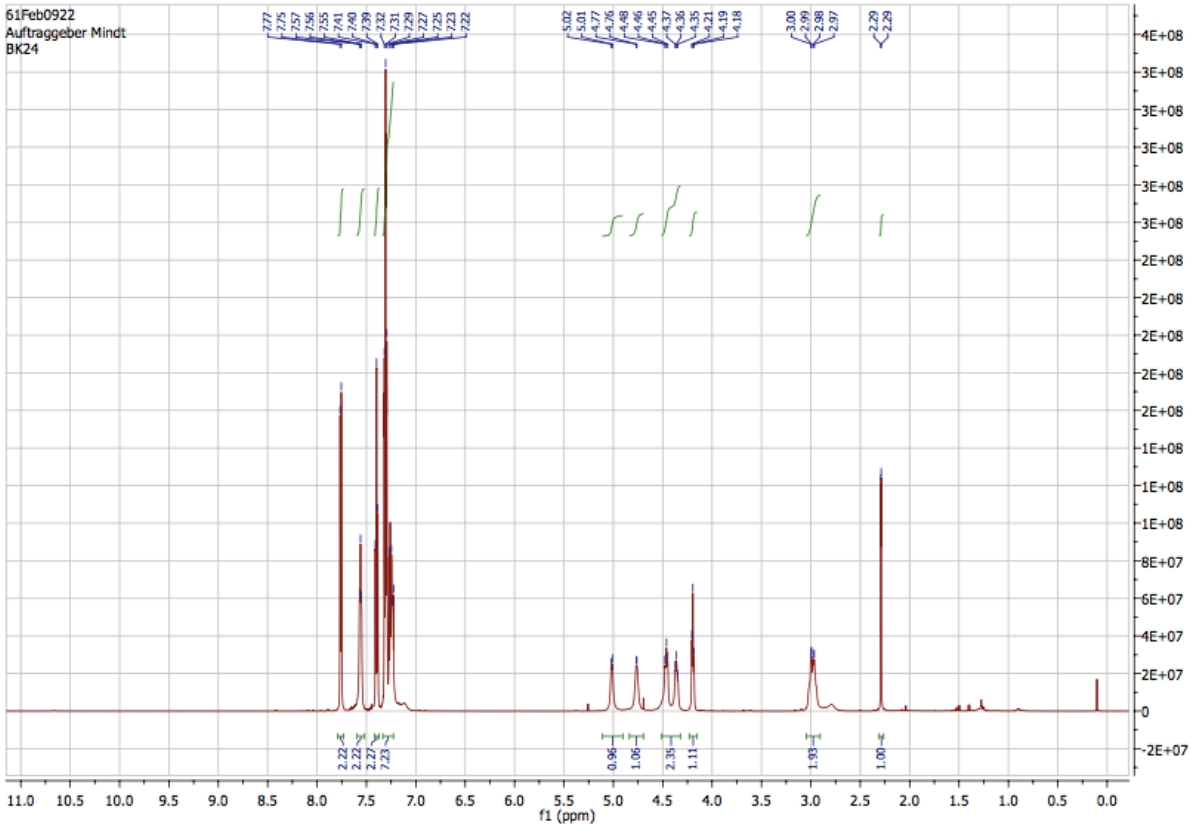

Figure 21: ^{1}H-NMR spectrum of Fmoc-Phe-CCH recorded with a 500 MHz instrument in $CDCl_3$.

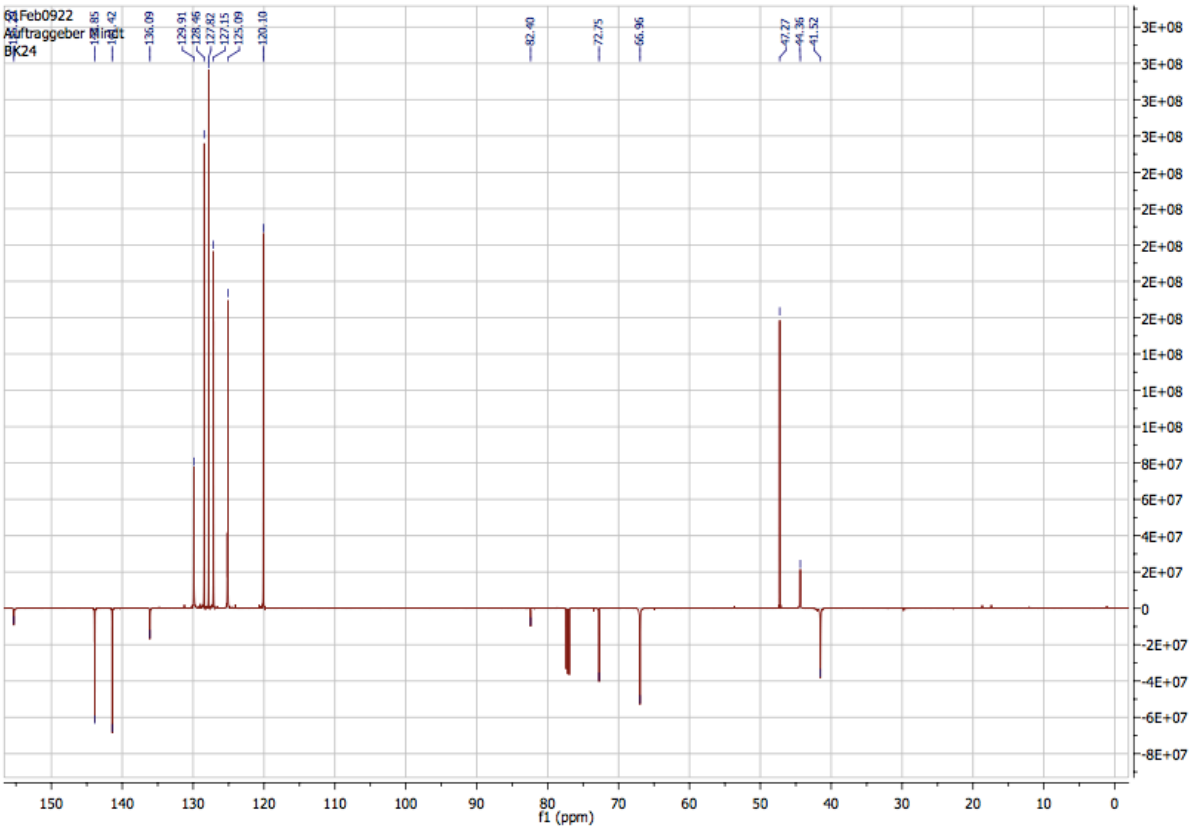

Figure 22: ^{13}C-NMR spectrum of Fmoc-Phe-CCH recorded with a 150 MHz instrument in $CDCl_3$.

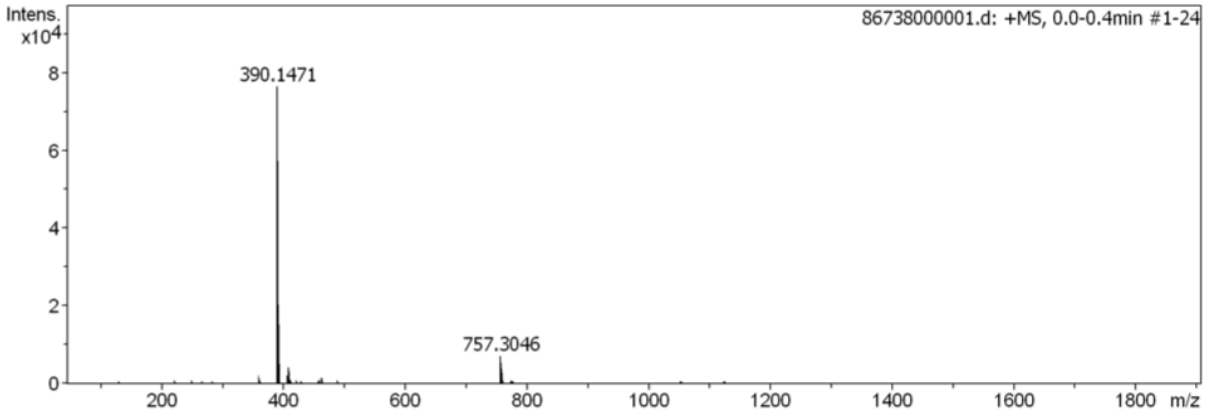

Figure 23: Mass spectrum of Fmoc-Phe-CCH showing the $[M+Na]^+$ *m/z* peak 390.1471. $[M+Na]^+$ m/z calculated for $C_{25}H_{21}NO_2Na$: 390.1464.

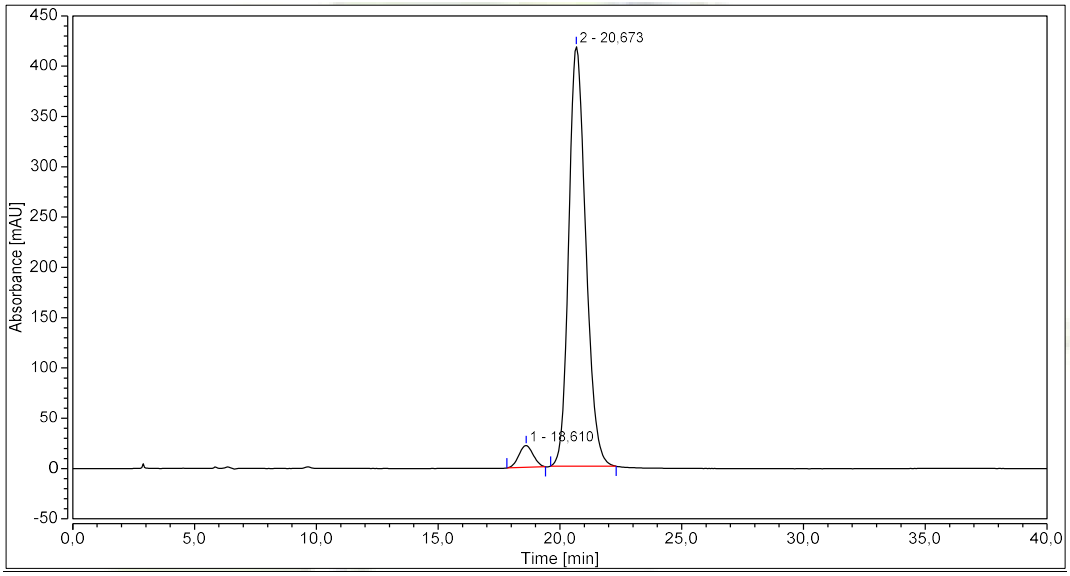

Figure 24: Chiral HPLC chromatogram of Fmoc-Phe-CCH recorded at 250 nm with an isocratic flow of 1 mL/min using 20% isopropanol in hexane as a mobile phase. The chromatographic peak at t_r = 16.610' shows the D-enantiomer (4%) and the peak at t_r = 20.673' shows the L-enantiomer (96%).

4.1.4. Fmoc-Glu(OtBu)-CCH

4.1.4.1. Synthesis of Fmoc-Glu(OtBu)-OH

The corresponding amino alcohol was obtained from Fmoc-Glu(OtBu)-COOH (700 mg, 1.7 mmol, 1 equiv.) as described in chapter 3.1.3. Fmoc-Glu(OtBu)-COOH was dissolved in 8.5 mL dry THF and the reaction was carried out for 30 min at room temperature. The excess of $NaBH_4$ was quenched with 7 mL of 10% acetic acid. The corresponding Fmoc-protected amino alcohol

was purified by flash chromatography on silica gel (hexane/EtOAc 1:1) and yielded with 83% as a colorless solid.

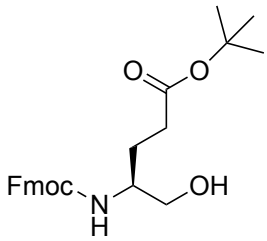

Figure 25: Structure of Fmoc-L-Glu(OtBu)-OH (tert-butyl (S)-4-((((9H-fluoren-9-yl)methoxy)carbonyl)amino)-5-hydroxypentanoate).

ESI-MS: $[M+Na]^+$ *m/z* calculated for $C_{24}H_{29}NO_5Na$: 434.22, found: = 434.24.

^{1}H-NMR (500 MHz, $CDCl_3$) δ 7.73 (d, ^3J = 7.5 Hz, 2H, aromat. H of Fmoc), 7.60 (d, ^3J = 7.4 Hz, 2H, aromat. H of Fmoc), 7.40 (t, ^3J = 7.5 Hz, 2H, aromat. H of Fmoc), 7.32 (t, ^3J = 7.5, 2H, aromat. H of Fmoc), 5.17 (d, ^3J = 8.2 Hz, 1H, NH), 4.42 – 4.40 (m, 2H, Fmoc-CH_2), 4.22 – 4.19 (m, 1H Fmoc-CH), 3.67 – 5.59 (m, 3H, CH_2 of CH_2OH and α-CH), 2.99 – 2.03 (m, 1H, OH), 2.34 – 2.32 (m, 2H, γ-CH_2), 1.88 – 1.79 (m, 2H, β-CH_2), 1.45 (s, 9H, CH_3 of tBu) ppm.

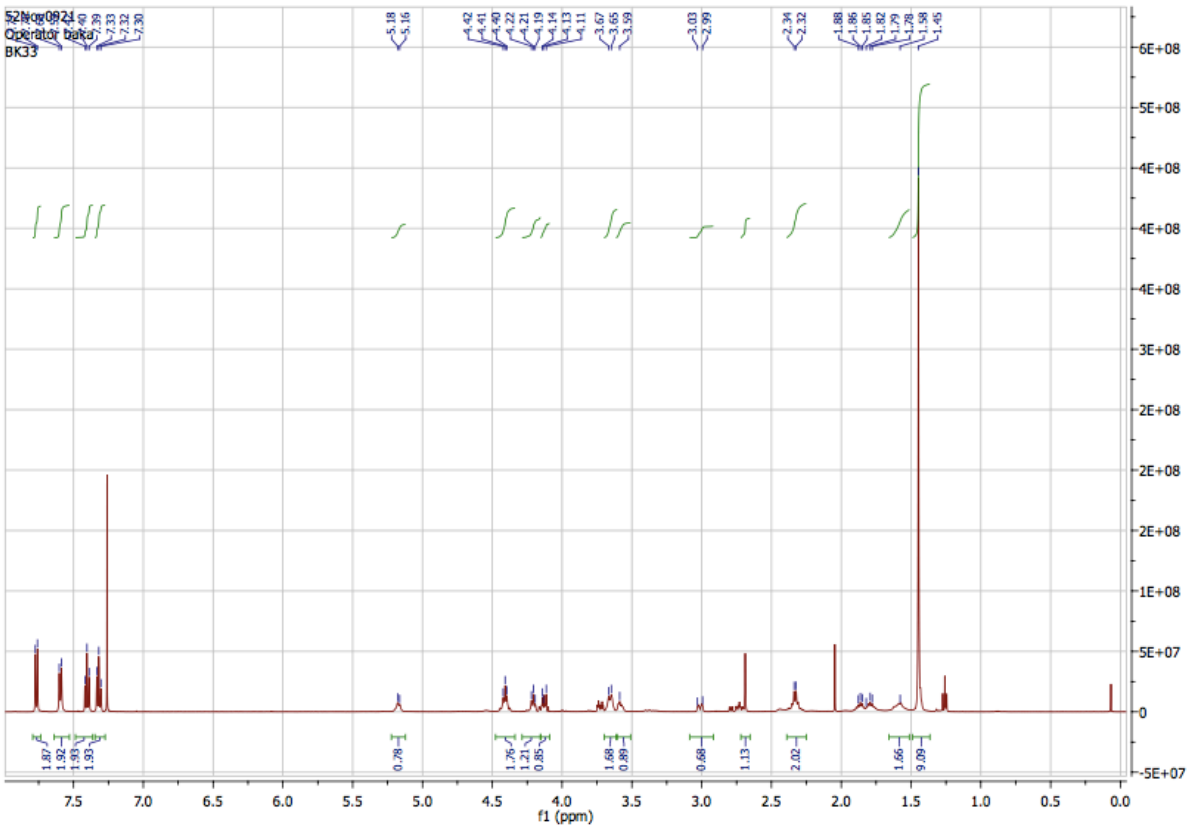

Figure 26: ^{1}H-NMR spectrum of Fmoc-Glu(OtBu)-OH recorded with a 500 MHz instrument in $CDCl_3$.

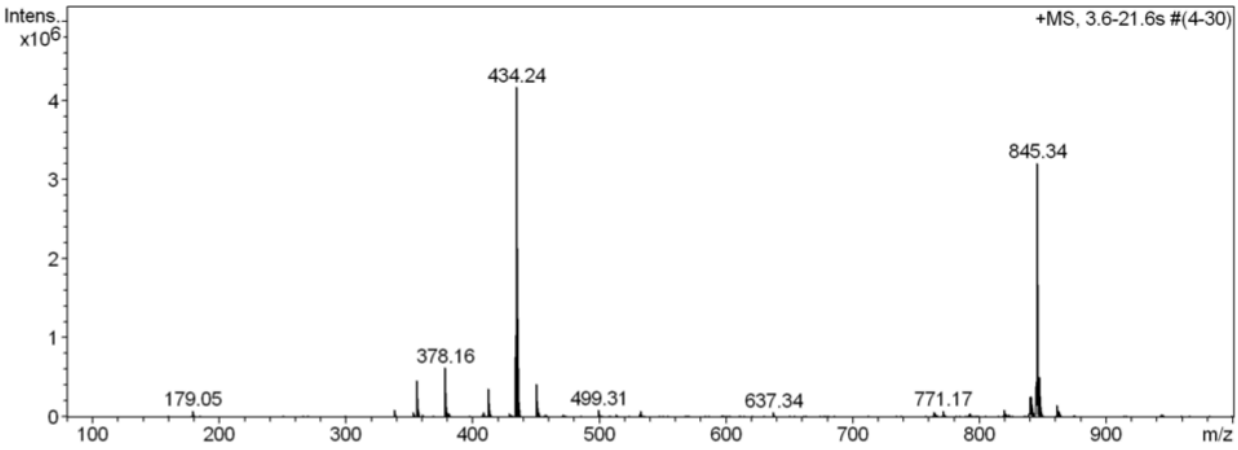

Figure 27: Mass spectrum of Fmoc-Glu(OtBu)-OH showing the $[M+Na]^+$ *m/z* peak 434.24. $[M+Na]^+$ m/z calculated for $C_{24}H_{29}NO_5Na$: 434.22.

4.1.4.2. Synthesis of Fmoc-Glu(OtBu)-CCH

The Fmoc-protected amino-alkyne was obtained from Fmoc-Glu(OtBu)-OH (100 mg, 0.2430 mmol, 1 equiv.) following procedure in chapter 3.1.4. The corresponding amino alkyne was isolated by flash chromatography on silica gel (hexane/EtOAc 8:2) as a white solid with a yield of 24%. The alkyne was obtained as a mixture of enantiomers in a 85:15 L/D ratio as demonstrated via chiral HPLC (Figure 32).

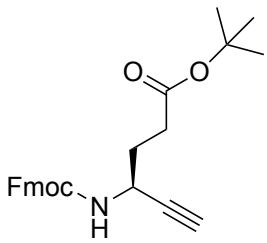

Figure 28: Structure of Fmoc-L-Glu(OtBu)-CCH (tertButyl (S)-4-((((9H-fluoren-9-yl)methoxy)carbonyl)amino)hex-5-ynoate).

ESI-MS: $[M+Na]^+$ *m/z* calculated for $C_{25}H_{27}NO_4Na$: 428.1832, found: = 428.1836.

^{1}H-NMR (500 MHz, $CDCl_3$) δ 7.77 (d, $_3$J = 7.5 Hz, 2H, Fmoc), 7.59 (d, $_3$J = 7.2 Hz, Fmoc), 7.40 (t, $_3$J = 7.4 Hz, 2H, Fmoc), 7.32 (t, $_3$J = 7.9 Hz, 2H, Fmoc), 5.18 (d, $_3$J = 7.7 Hz, 1H, NH), 4.53 (d, $_3$J = 6.7 Hz, 1H, α-CH_2), 4.42 (d, $_3$J = 7.0 Hz, 2H, Fmoc-CH_2), 4.22 (t, $_3$J = 6.5 Hz, 1H Fmoc-CH), 2.49 – 2.34 (m, 2H, β-CH_2), 2.33 (d, $_4$J = 2.3 Hz, 1H, CCH), 2.00 (m, 2H, γ-CH_2), 1.46 (s, 9H, CH_3 of tBu) ppm.

^

^{13}C NMR (150 MHz, $CDCl_3$) δ 172.14 (sidechain C=O), 155.40 (Fmoc C=O), 143.75 (quart. C of Fmoc), 141.29 (quart. C of Fmoc), 127.70 (aromat. CH of Fmoc), 127.05 (aromat. CH of Fmoc), 125.04 (aromat. CH of Fmoc), 119.97 (aromat. CH of Fmoc), 82.29 (quart. C of CCH), 80.77 (quart. C of tBu), 72.00 (tert. C of CCH), 66.93 (Fmoc-CH_2), 47.16 (Fmoc-CH), 42.84 (α-CH), 31.64 (γ-CH_2), 30.72 (β-CH_2), 28.06 (CH_3 of tBu) ppm.

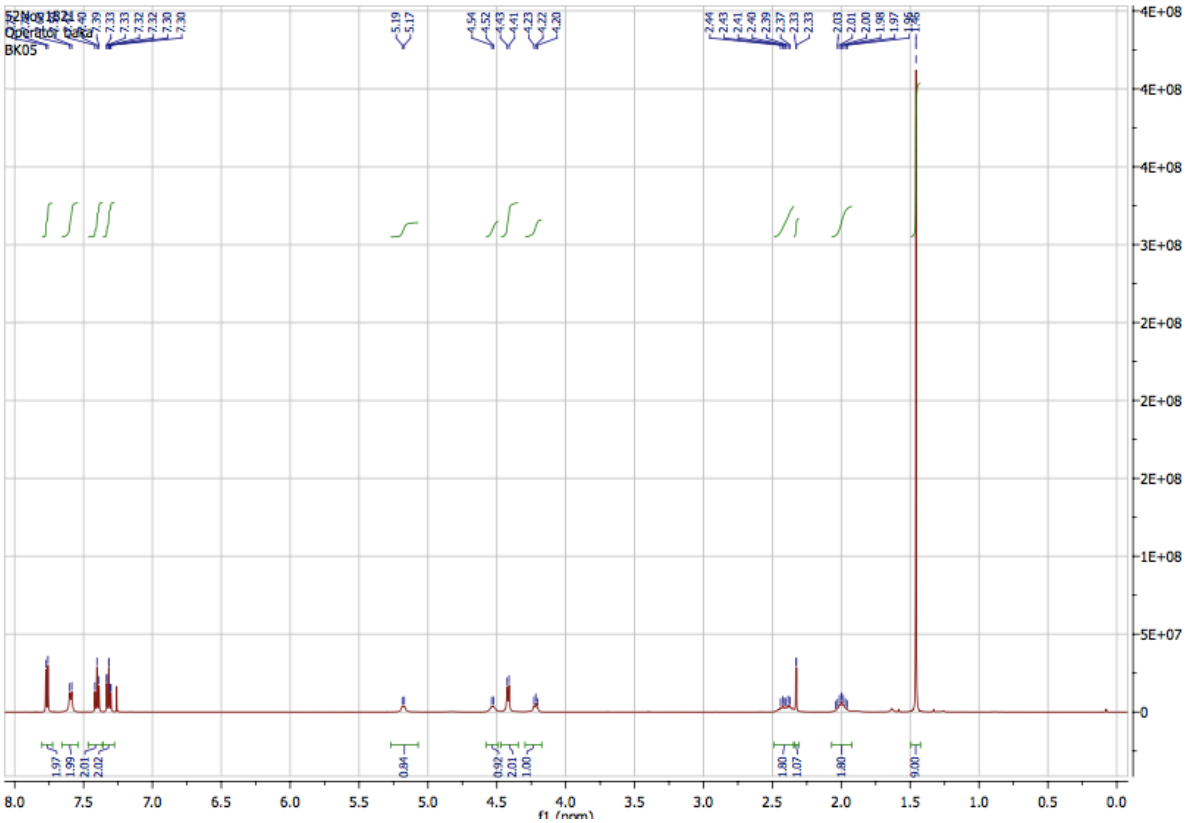

Figure 29: ^{1}H-NMR spectrum of Fmoc-Glu(OtBu)-CCH recorded with a 500 MHz instrument in $CDCl_3$.

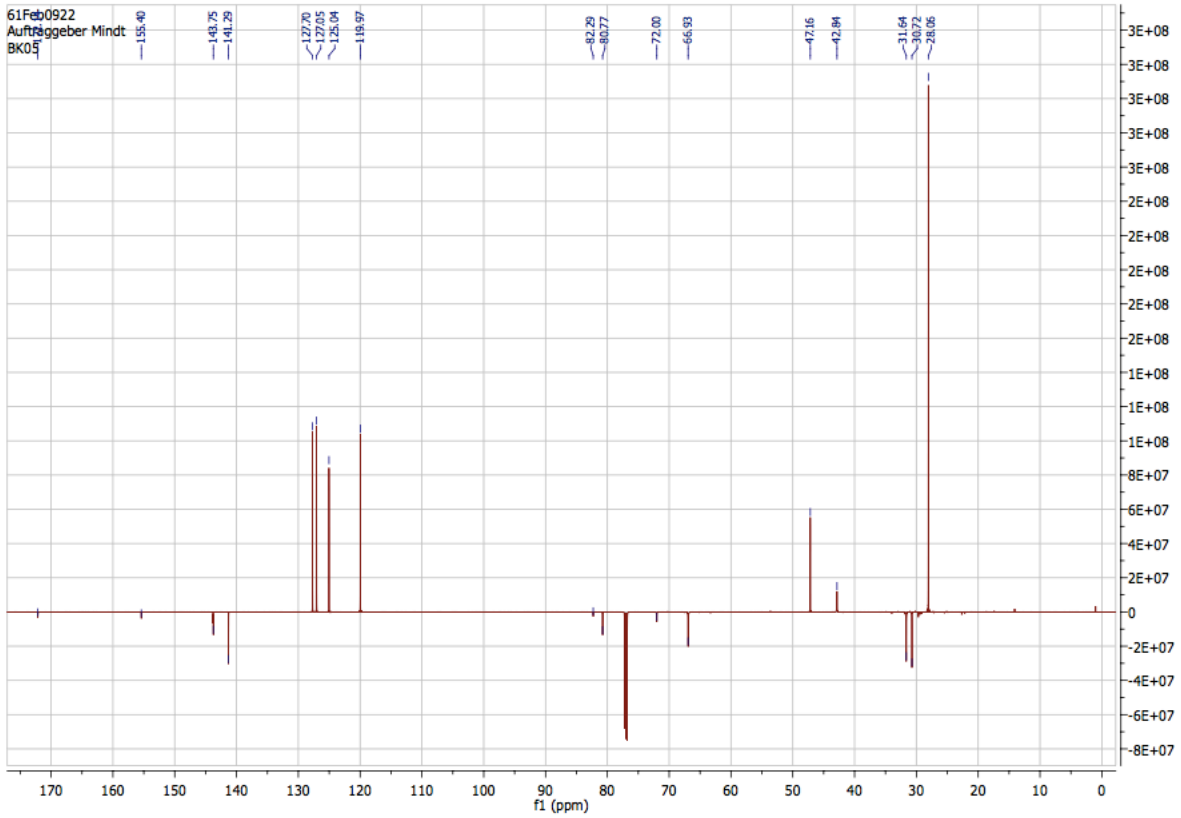

Figure 30: ^{13}C-NMR spectrum of Fmoc-Glu(OtBu)-CCH recorded with a 150 MHz instrument in $CDCl_3$.

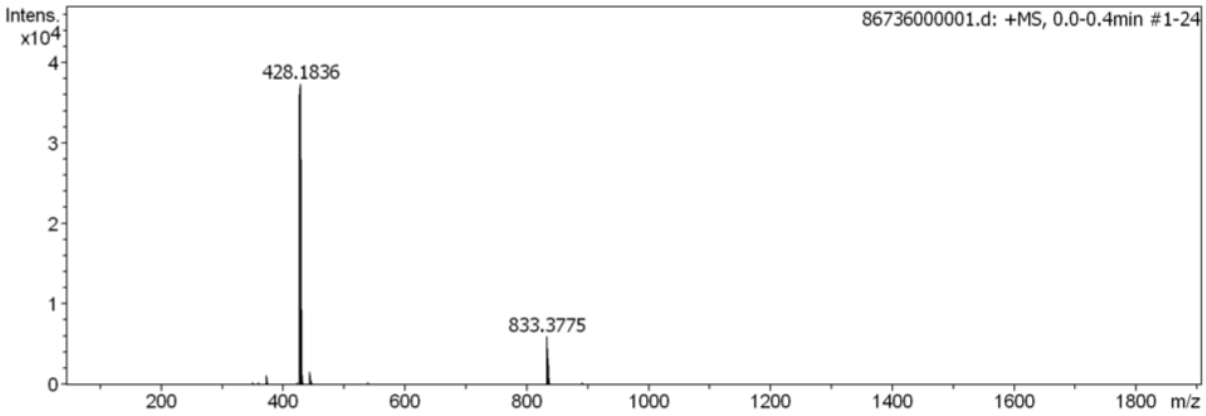

Figure 31: Mass spectrum of Fmoc-Glu(OtBu)-CCH showing the $[M+Na]^+$ *m/z* peak 428.1836. $[M+Na]^+$ *m/z* calculated for $C_{25}H_{27}NO_4Na$: 428.1832.

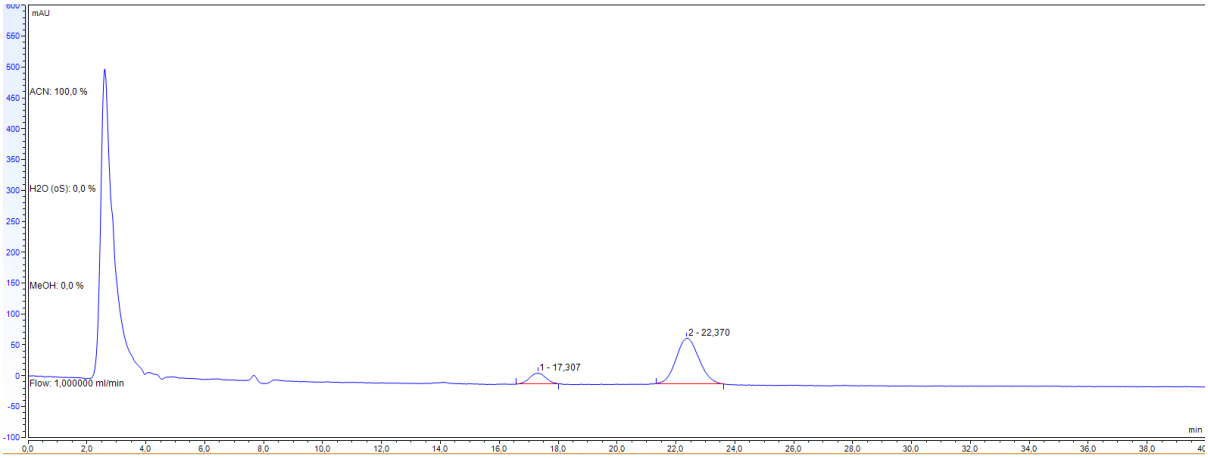

Figure 32: Chiral HPLC chromatogram of Fmoc-Glu(OtBu)-CCH recorded at 220 nm with an isocratic flow of 1 mL/min using 20% isopropanol in hexane as a mobile phase. The chromatographic peak at t_r = 17.307' shows the D-enantiomer (15%) and the peak at t_r = 22.370' shows the L-enantiomer (85%).

4.1.5. Fmoc-Arg(Boc)$_2$-CCH

4.1.5.1. Synthesis of Fmoc-Arg(Boc)$_2$-N(Me)O(Me)

The Weinreb amide was obtained from Fmoc-Arg(Boc)$_2$-COOH (500 mg, 0.8430 mmol, 1 equiv.) as described in chapter 3.1.2 and purified by flash chromatography using hexane/EtOAc (1:1) as a mobile phase with a yield of 62% a light yellow solid.

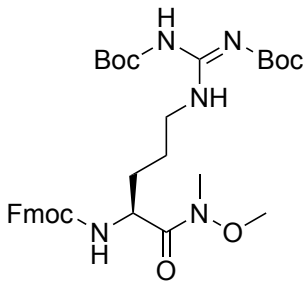

Figure 33: Structure of Fmoc-L-Arg(Boc)$_2$-N(Me)O(Me).

ESI-MS: $[M+H]^+$ *m/z* calculated for $C_{33}H_{46}N_5O_8$: 640.3310, found: = 640.3347.

^{1}H-NMR (500 MHz, $CDCl_3$) δ 11.50 (s, 1H, NH-Boc) 8.34 (s, 1H, NH bei Fmoc) 7.75 (t, $_3$J = 7.0 Hz, 2H, arom. H Fmoc), 7.62 - 7.60 (m, 2H arom. H Fmoc), 7.39 (t, $_3$J = 7.4 Hz, 2H, arom. H Fmoc), 7.33 - 7.30 (m, 2H, arom. H Fmoc), 5.61 (d, 1H, CH or NH from Arg chain), 4.51 (s, 1H, NH oder CH from Arg chain), 4.40 – 4.37 (m, 2H, Fmoc-CH_2), 4.22 (t, $_3$J = 6.3 Hz, 1H, Fmoc-CH), 4.14 – 4.11 (m, 2H, CH_2 bei NH), 1.82 – 1.82 (m, 4H, aliphatische CH_2 Arg chain), 1.50 (d, 18H, $_4$J = 2.3 Hz, CH_3 of tBu) ppm.

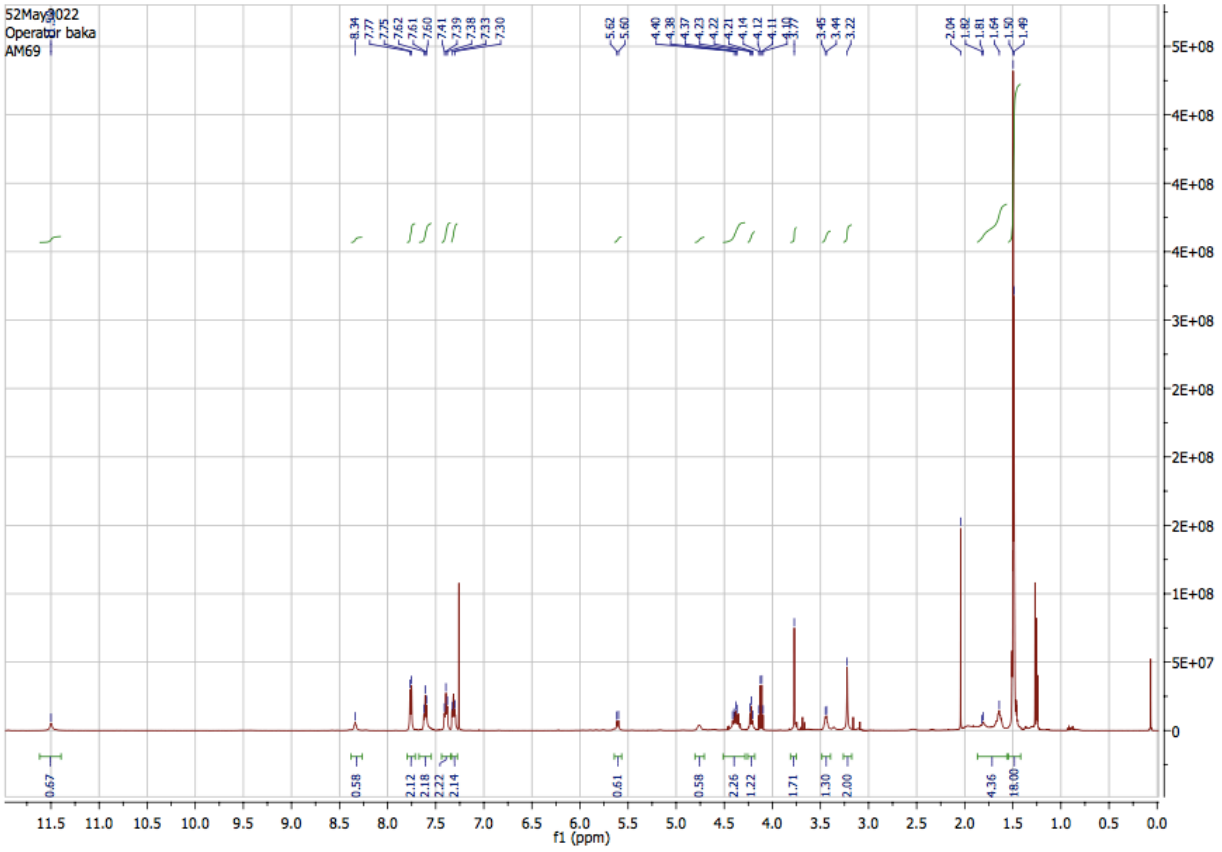

Figure 34: ^{1}H-NMR spectrum of Fmoc-Arg(Boc)$_2$-N(Me)O(Me) recorded with a 500 MHz instrument in $CDCl_3$.

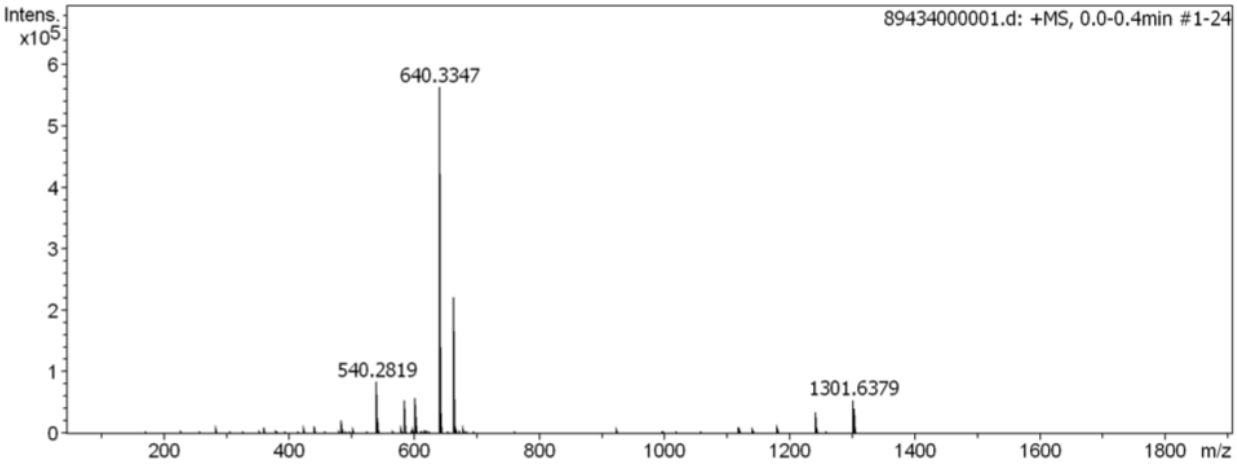

Figure 35: Mass spectrum of Fmoc-Arg(Boc)$_2$-N(Me)O(Me) showing the $[M+H]^+$ *m/z* peak 640.3347. $[M+H]^+$ m/z calculated for $C_{33}H_{46}N_5O_8$: 640.3310.

4.1.5.2. Synthesis of Fmoc-Arg(Boc)$_2$-CCH

The amino alkyne was obtained from the corresponding Weinreb amide (322 mg, 1.5791 mmol, 3 equiv.) following procedure in chapter 3.1.5 whereas the Seyferth-Gilbert homologation was carried out over 72 h. The corresponding amino alkyne was isolated by flash chromatography on silica gel (hexane/EtOAc 2:5) as a white solid with a yield of 11%. The alkyne was obtained as a mixture of enantiomers with a 88:12 L/D ratio as demonstrated via chiral HPLC (Figure 40).

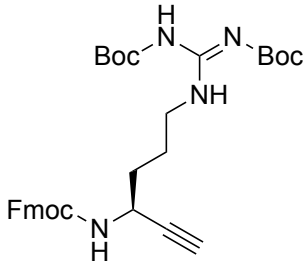

Figure 36: Structure of Fmoc-L-Arg(Boc)$_2$-CCH.

ESI-MS: $[M+H]^+$ *m/z* calculated for $C_{32}H_{41}N_4O_6$: 577.3021, found: = 577.3019.

^{1}H-NMR (500 MHz, $CDCl_3$) δ 11.50 (s, 1H, NH-Boc) 8.37 (s, 1H, NH bei Fmoc) 7.77 (t, $_3$J = 7.0 Hz, 2H, arom. H Fmoc), 7.59 - 7.63 (m, 2H arom. H Fmoc), 7.40 (t, $_3$J = 7.5 Hz, 2H, arom. H Fmoc), 7.35 - 7.32 (m, 2H, arom. H Fmoc), 5.33 (d, 1H, CH or NH from Arg chain), 4.51 (s, 1H, NH oder CH from Arg chain), 4.48 – 4.39 (m, 2H, Fmoc-CH_2), 4.22 (t, $_3$J = 6.4 Hz, 1H, Fmoc-CH), 3.59 – 3.33 (m, 2H, CH_2 bei NH), 2.30 (d, $_4$J = 2.1 Hz, 1H, CCH), 1.81 – 1.63 (m, 4H, aliphatische CH_2 Arg chain), 1.50 (d, 18H, $_4$J = 2.3 Hz, CH_3 of tBu) ppm.

^{13}C-NMR (150 MHz, $CDCl_3$) δ 155.6 (quart. C between 3 N), 153.60-143.92 (3 quart. C=O), 141.67 (2 quart. C of Fmoc), 141.48 (2 quart. C of Fmoc), 127.85-120.12 (aromat. CH of Fmoc), 67.83 (quart. C of CCH), 66.99 (Fmoc-CH_2), 65.33 (quart. C of tBu), 50.51 (tert. C of CCH), 47.38 (Fmoc-CH), 43.31 (CH), 32.82 (CH_2), 29.84 (CH_2), 28.42/28.22 (CH_3 of tBu), 25.65 (CH_2) ppm.

162.6, 36.62, 31.58 ppm → DMF impurity

Analytical data has found to be identical with data from literature reported by Mascarin et al.[48]

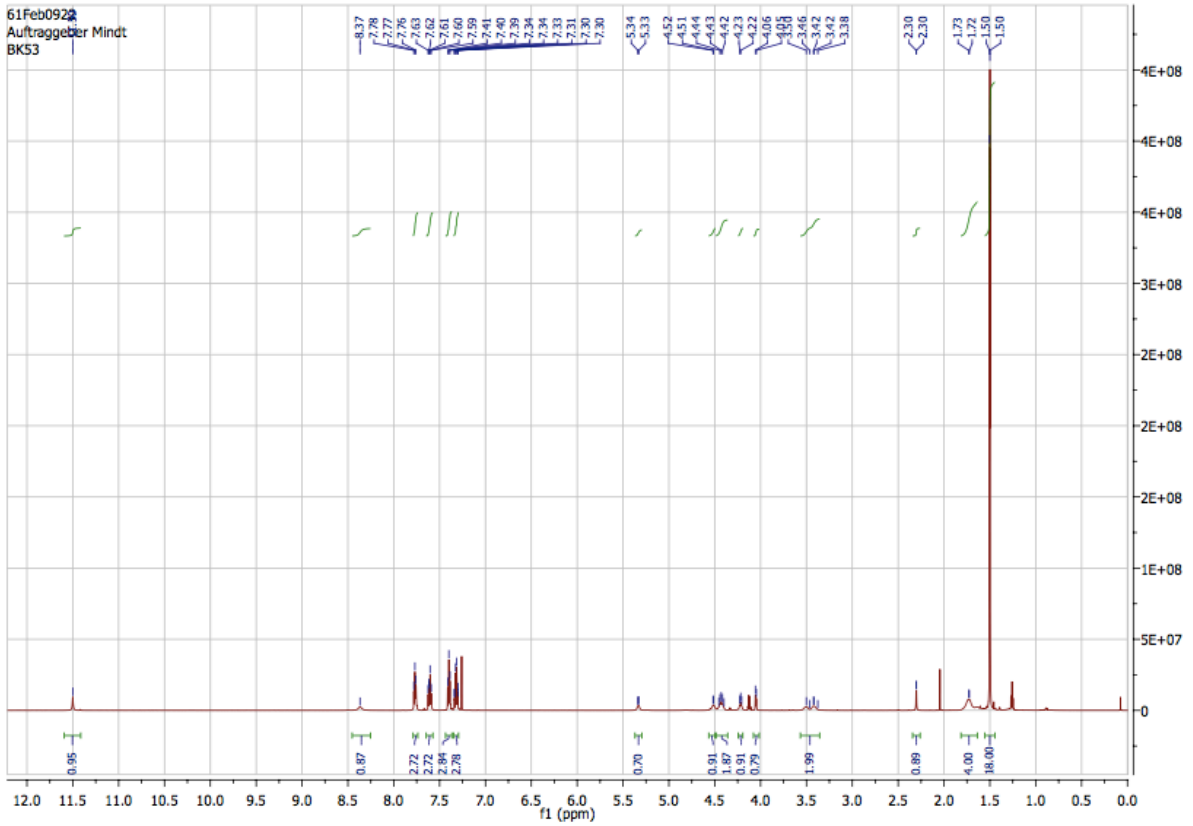

Figure 37: ^{1}H-NMR spectrum of Fmoc-Arg(Boc)$_2$-CCH recorded with a 500 MHz instrument in $CDCl_3$.

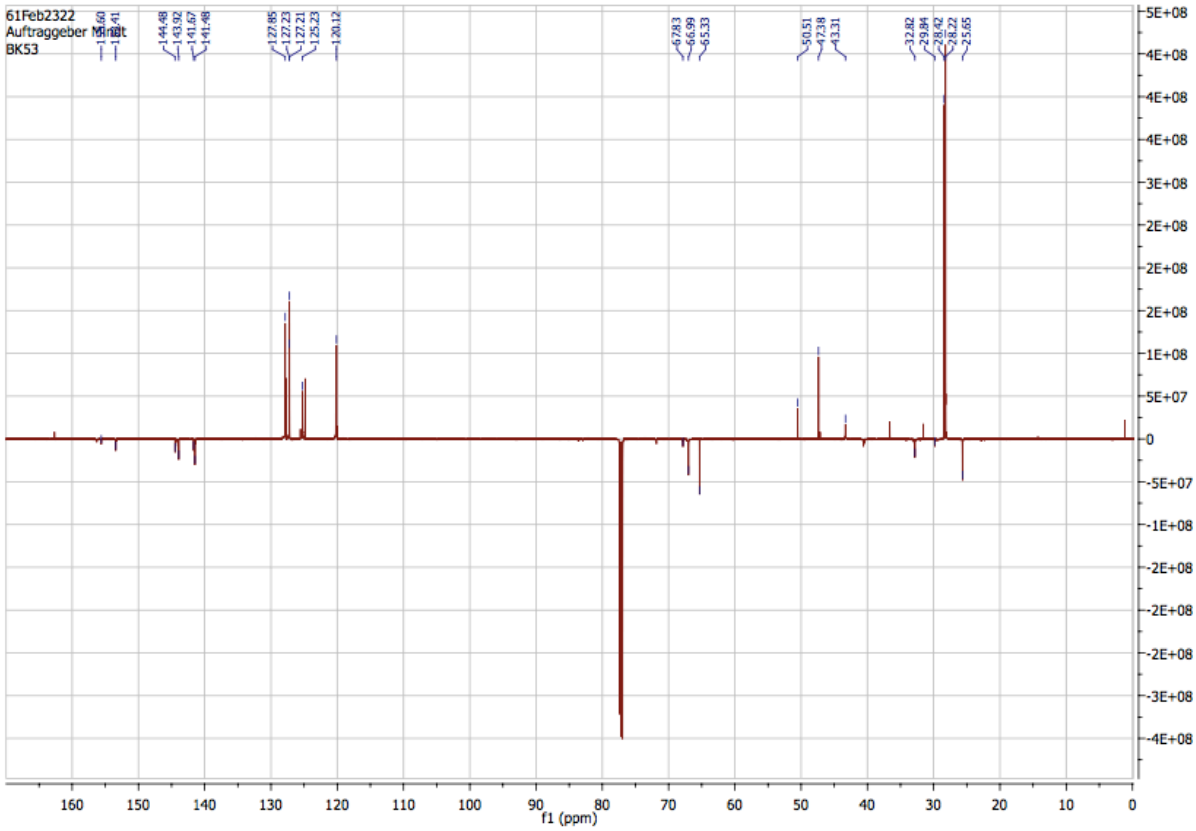

Figure 38: ^{13}C-NMR spectrum of Fmoc-Arg(Boc)$_2$-CCH recorded with a 150 MHz instrument in $CDCl_3$.

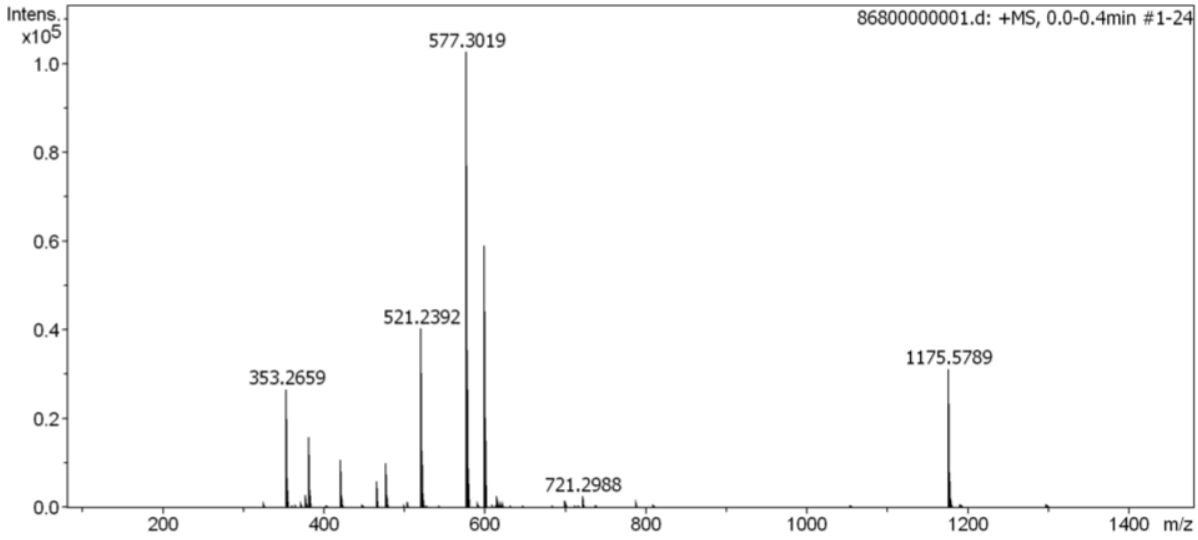

Figure 39: Mass spectrum of Fmoc-Arg(Boc)$_2$-CCH showing the $[M+H]^+$ *m/z* peak 577.3019. $[M+H]^+$ *m/z* calculated for $C_{32}H_{41}N_4O_6$: 577.3021.

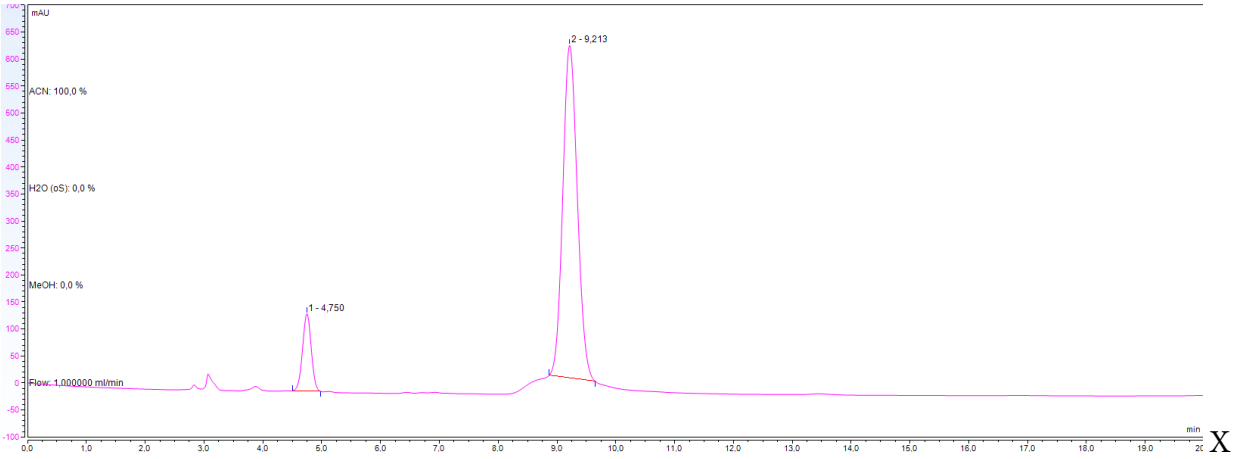

Figure 40: Chiral HPLC chromatogram of Fmoc-Arg(Boc)$_2$-CCH recorded at 220 nm with an isocratic flow of 1 mL/min using 10% iso-propanol in hexane as a mobile phase. The chromatographic peak at t_r = 4.750' shows the D-enantiomer (12%) and the peak at t_r = 9.213' shows the L-enantiomer (88%).

4.2. Diazo-Transfer

Imidazole-1-sulfonylazide hydrochloride (ISA.HCl) was used as a diazo-transfer reagent to obtain the azide functionalized peptide for the subsequent CuAAC. ISA.HCl is a safe, efficient and potent reagent for the conversion of amides into azides and its application within manual SPPS has already been reported.[44] First, the diazo-transfer reaction had to be adapted from a manual to an automated setup to implement it into the peptide synthesis-procedure. The automated setup requires the preparation of all the reagent solutions in advance. This means that the reagents are in solution for longer periods, thus potentially limiting their preservation and stability.

In a first trial for the diazo-transfer 5 equivalents of ISA.HCl and 10 equivalents of DIPEA were used and the reaction was carried out for 60 minutes at room temperature in DMF. This approach

did not yield the desired product. The instability of the diazo-transfer reagent in the solvent was suspected to be the limiting factor which was confirmed by stability studies in DMF described in chapter 4.2.1. The stability of the diazo-transfer reagent has to be ensured since an intact reagent is essential for the successful incorporation of triazoles and its stability has to be guaranteed over a certain period for the automated setup. Therefore, the storage stability in solution of the used diazo-transfer reagent was investigated over time.

4.2.1. Stabilitiy of Imidazole-1-sulfonylazide Hydrochloride

In order to find solvents that are compatible with SPPS, suitable for solving the diazo-transfer reagent ISA.HCl and keeping it intact, different options were tested. Additionally, it had to be considered that some solvents, such as water, show poor swelling properties when used with polystyrene based resins.[15] Therefore, a solvent suitable for the solution and preservation of ISA.HCl but not interfering with the resin had to be found.

DMF is a conventionally used solvent for SPPS providing good swelling properties.[15] Consequently, the stability of the diazo-transfer reagent was investigated in DMF and additionally in two alternative solvents; water and DMSO. To determine the degradation, the incubated solutions were analyzed by LC-MS at different timepoints. In DMF, a rapid degradation of ISA.HCl was observed over time as well as the formation of the side product imidazole-1-sulfonylamide (Scheme 6; $[M+H]^+$ *m/z* found: 147.1) corresponding to the peak at t_r = 0.734' shown in Figure 42. The chromatographic peak corresponding to ISA.HCl ($[M+H]^+$ *m/z* 174.0) was found at t_r = 3.975'. The peak at t_r = 0.497' corresponds to the solvent.

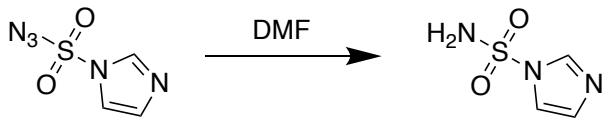

Scheme 6: Schematic formation of the side product imidazole-1-sulfonylamide from imidazole-1-sulfonylazide in DMF.

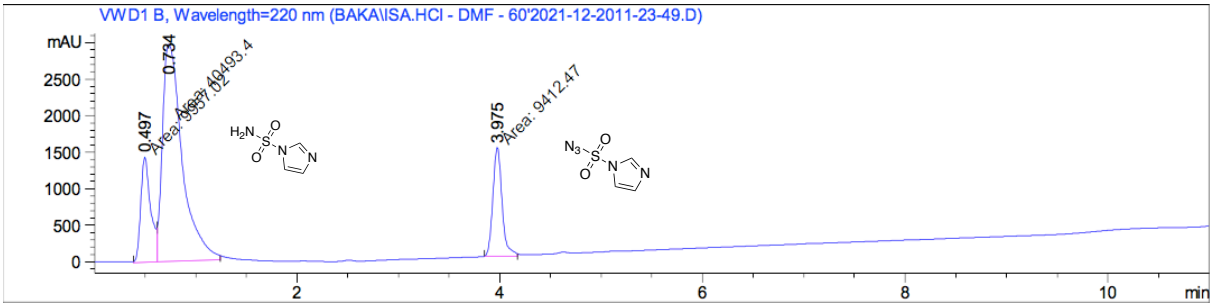

Figure 41: Analytical LC profile of ISA.HCl in DMF after 60 minutes incubation time. 5 to 80% MeCN in H_2O with 0.1% FA in 10 minutes with an Acquity UPLC BEH C18 7µm, 3x50mm column with a flow of 0.6 mL/min recorded at 220 nm. The chromatogram shows the solvent peak at t_r = 0.497', the peak corresponding to the side product imidazole-1-sulfonylazide at t_r = 0.734' and the peak corresponding to ISA.HCl at t_r = 3.975'.

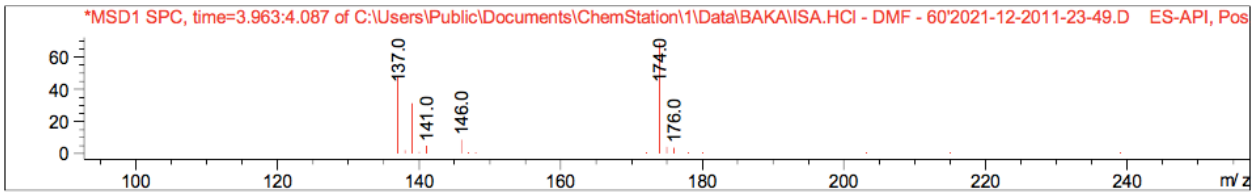

Figure 42: Mass spectrum of the imidazole-1-sulfonylazide peak in DMF; showing the $[M+H]^+$ *m/z* peak for $C_3H_4N_5O_2S$: 174.0. $[M+H]^+$ *m/z* calculated: 174.0.

An overview of the ISA.HCl stability analysis is given in Figure 43, displaying the decreasing amount of ISA.HCl in the different solvents over 24 hours. After four hours of incubation only 30% of the diazo-transfer reagent remained intact in DMF. In DMSO, ISA.HCl was more degraded and only 13% of the azide was left after four hours. Compared to the other tested solvents, the diazo-transfer reagent showed to be very stable in water as after four hours still 98% of the ISA peak remained and no side products were detected.

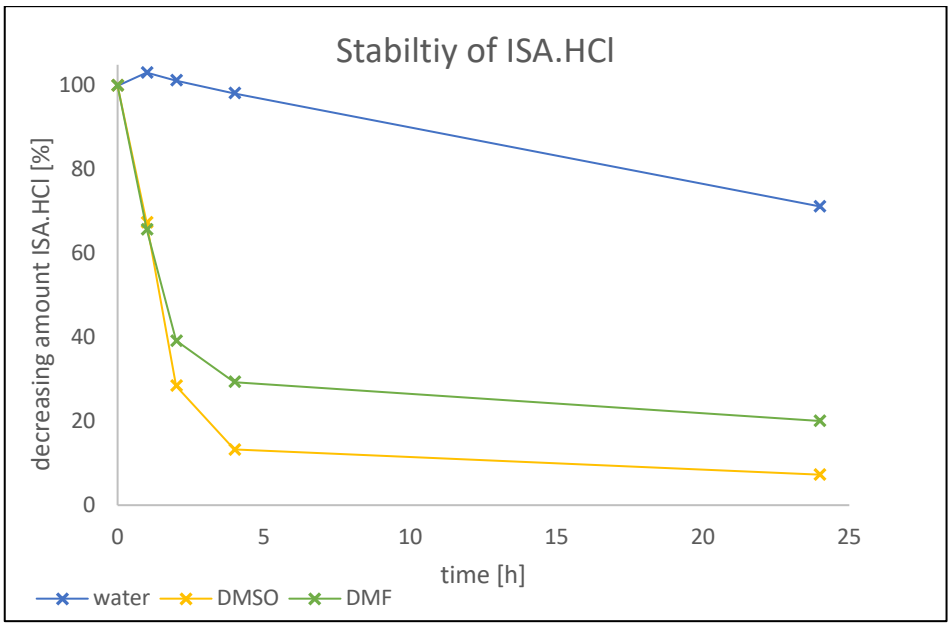

Figure 43: Decreasing amount of ISA.HCl in water (blue), DMSO (yellow) and DMF (green) over 24 hours.

Based on the findings, the solvent that preserves the azide best is water. A limiting factor is that water shows poorer swelling properties for polystyrene based resins compared to solvents like DMF, DMSO and DCM.[15] To keep the amount of water in the final solution to a minimum and thereby minimize the interference of water with the swelling of the resin, a concentrated solution of ISA.HCl (1.2 M) was prepared for the diazo-transfer reaction. Using the concentrated solution results in a DMF to water ratio of 9:1 in the final reaction. DMF and DMSO do not provide the preservation of ISA.HCl making their application as solvents for the diazo-transfer impossible as triazoles can be incorporated in different positions of the sequence. This means that the reagents have to be stable in solution in the peptide synthesizer for up to several hours.

4.2.2. Optimization of the Diazo-Transfer

First, the diazo-transfer reaction needed to be adapted from a manual to an automated setup. To obtain the triazolopeptidomimetics in a pure and efficient manner, the setting for the automated triazole incorporation was optimized using a bombesin derivative. The screening of the diazo-transfer reaction was carried out varying time, temperature and the concentrations of reactants as described in chapter 3.2, using the microwave assisted peptide synthesizer.

For the screening the sequence H_2N-His-Leu-Nle-NH_2 (Scheme 7) was synthesized on rink amide resin in a scale of 0.15 mmol and aliquots (0.03 mmol) were taken for the diazo-transfer reactions.

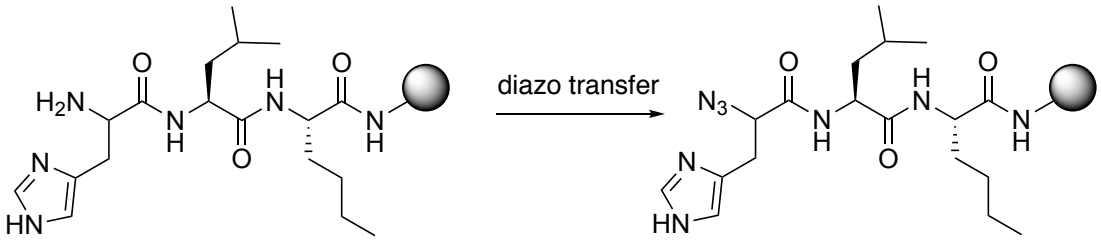

Scheme 7: Reaction scheme and part of the bombesin sequence used for the diazo-transfer screening.

The applied conditions for the diazo-transfer are listed in Table 1. It was noticed that a higher conversion could not be obtained by increasing the amounts of DIPEA and ISA.HCl at room temperature. To shorten the reaction time, higher temperatures (70 and 80°C) were applied leading to lower conversions in both cases. The use of catalytic amounts of Cu(II) salts has shown to improve the conversion for diazo-transfer reactions.[53] This could also be proven by the screening as the conversion could be significantly increased by adding $CuSO_4$ as a catalyst. The screening showed that the reaction is most efficient with a high conversion by using 7 equivalents of the diazo-transfer reagent, 14 equivalents of DIPEA, 0.01 equivalents of $CuSO_4$ and performing the

reaction for 30' at 70°C (entry 5 in Table 1). The result of the optimized diazo-transfer reaction is displayed in the chromatogram in Figure 44.

Table 1: Different reaction conditions for the diazo-transfer screening. The most efficient one is highlighted.

reaction	ISA.HCl [equiv.]	DIPEA [equiv.]	reaction time	temperature (MW)	$CuSO_4$ [equiv.]	conversion
1	5	10	60'	rt	-	85%
2	7	14	60'	rt	-	86%
3	7	14	30'	70°C	-	68%
4	7	14	30'	80°C	-	68%
5	**7**	**14**	**30'**	**70°C**	**0.01**	**90%**
6	5	10	30'	70°C	0.01	70%

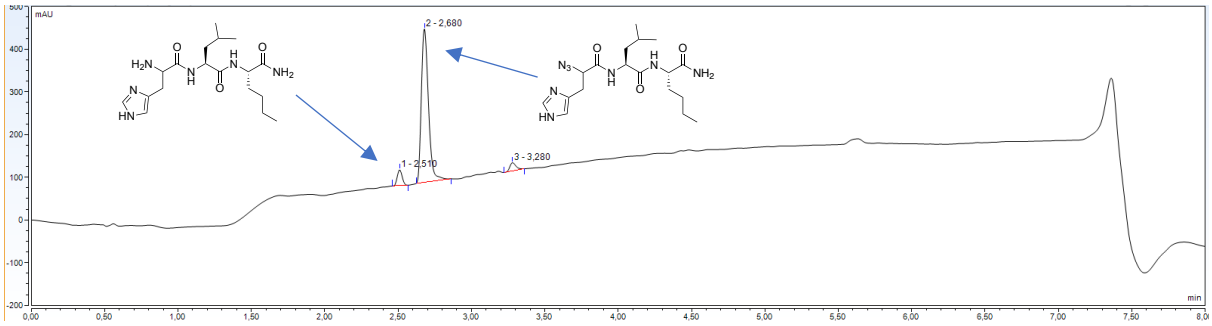

Figure 44: Analytical profile of N_3-His-Leu-Nle-NH_2 (t_r = 2.680', 90%) synthesized on solid support with conditions of reaction 5(Table 1, entry 5). Gradient of 5 to 95 % MeCN in H_2O with 0.1% FA in 5 minutes with a 0.6 mL/min flow recorded at 220 nm. The peak at t_r = 2.510' corresponds to the amine and the peak at t_r = 3.280' shows an impurity.

4.3. CuAAC

To obtain the triazole starting from the azide, $[Cu(CH_3CN)_4]PF_6$ was used as a copper(I) source. As with the diazo-transfer the CuAAC reaction first needed to be adapted from a manual to an automated setup. To ensure the stability of the Cu(I)-complex over time and to prevent its oxidation to Cu(II), the stabilizer TBTA was added as it performs well as a stabilizing ligand in Cu(I) mediated reactions leading to satisfying results.[46]

4.3.1. Stability of $[Cu(CH_3CN)_4]PF_6$ and TBTA

In order to make sure that the CuAAC reagent $[Cu(CH_3CN)_4]PF_6$ is stable in the used solvent DMF over time and it does not get oxidized to Cu(II), stability studies were carried out.

In general, $[Cu(CH_3CN)_4]PF_6$ is stable against oxidation by air and only minor surface oxidation takes place due to the slightly hygroscopic nature of the complex.[54] The coordinating acetonitrile ligands are supposed to protect the Cu(I) from oxidation but are not strongly bound to the central ion making the Cu(I) easily available for reactions in solution. In the presence of other solvents than MeCN, a ligand exchange is possible. In the presence of water, disproportionation and/or oxidation of the Cu(I) species takes place.[54,55] The solvent used in this SPPS approach was DMF. As the used DMF was not anhydrous, the loss of Cu(I) species was expected to a certain extent. To prevent this, the stabilizing agent TBTA was added to the $[Cu(CH_3CN)_4]PF_6$ solution.

To gain information about the effect of TBTA on the Cu(I)-complex, the stabilizer and the complex were investigated by NMR. Therefore, TBTA was dissolved in deuterated DMF and a ^{1}H-NMR spectrum recorded. All signals were sharp, could be assigned and compared with literature.[56]

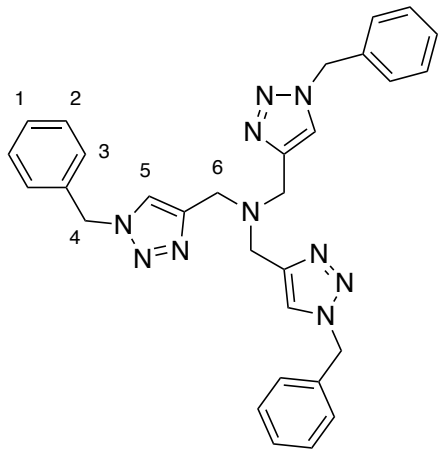

Figure 45: Structure of the stabilizing agent TBTA.

^{1}H-NMR (500 MHz, dDMF) δ 8.17 (s, 3H, triazole), 8.02 (HCO DMF), 7.47-7.26 (m, 15H, benzyl), 5.69 (s, 6H, CH_2 benzyl), 3.71 (s, 6H, NCH_2), 3.49 (H_2O), 2,91 & 2,74 (CH_3 DMF) ppm.

Then, the $[Cu(CH_3CN)_4]PF_6$ was added to the TBTA solution and another ^{1}H-NMR spectrum recorded. The spectrum changed significantly as all the TBTA signals were shifted, broadened or

not visible anymore. The red spectrum shows the TBTA solution and the blue spectrum shows the TBTA + $[Cu(CH_3CN)_4]PF_6$ solution (Figure 46).

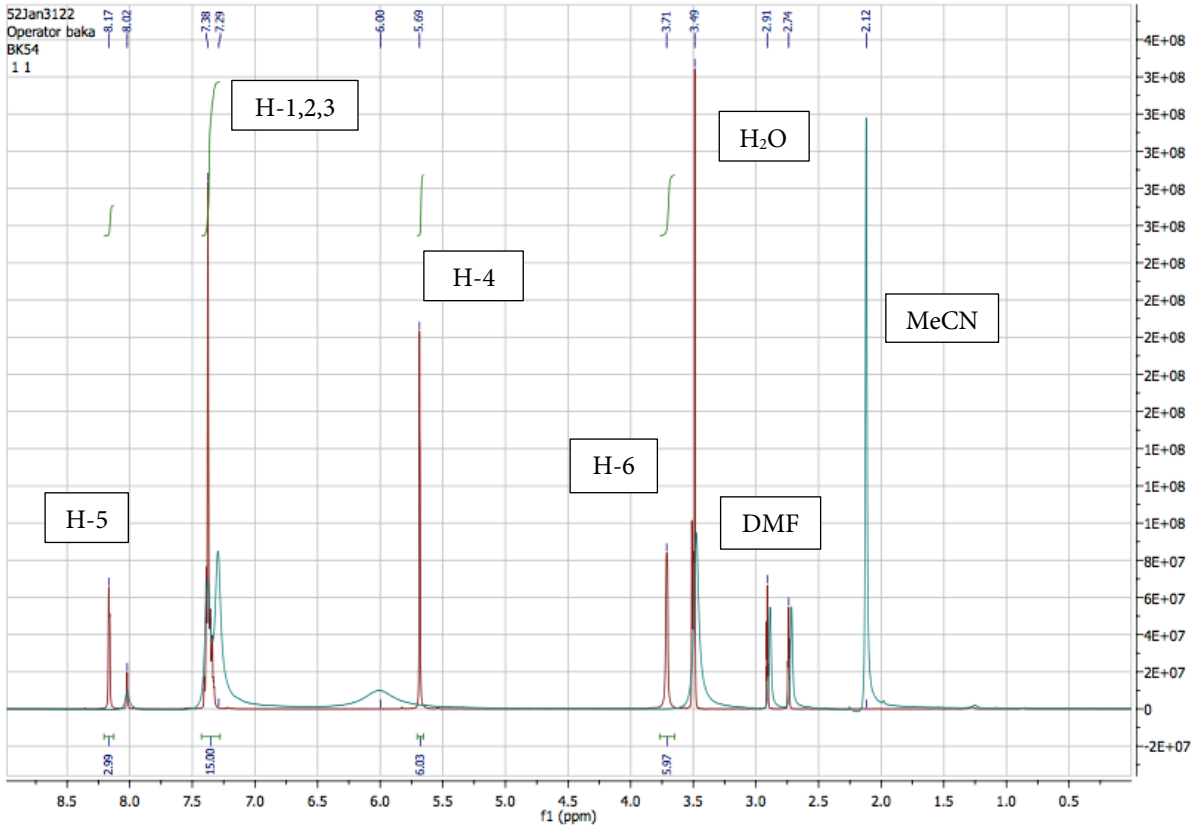

Figure 46: ^{1}H-NMR spectra of TBTA in dDMF alone (red) and of TBTA and $[Cu(CH_3CN)_4]PF_6$ in dDMF (blue). The signals were assigned to the atoms of TBTA, the solvent and acetonitrile.

The triazole signal at 8.17 ppm (H-2) and the signal at 3.71 ppm (H-6) of TBTA disappeared completely. The aromatic signals at 7.38 ppm changed from a multiplet to a duplet and broadened. The CH_2 signals of the benzyl groups broadened and shifted from 5.69 to 6.00 ppm. The peak at 2.16 ppm shows the signal of free MeCN. As the changes in the NMR spectrum are very significant, coordination of the copper by TBTA is assumed as expected. Information about the oxidation state of the copper could not be gained.

To test the stability of the CuAAC reagents in solution over time for the preparation for the automated triazole incorporation on solid phase, a 24 h stability study was carried out. The $[Cu(CH_3CN)_4]PF_6$ and TBTA solution was prepared and stored for 0 and 24 hours, as described in chapter 3.4.2. A CuAAC reaction with the sequence H_2N-His-Leu-Nle-NH_2 was carried out after 0 and 24 hours, using the stored solution. The triazole conversion for the CuAAC after directly preparing the solution was 82%, as shown in (Figure 47). After 24 hours 25% of the triazole could

be obtained by applying the same conditions and the formation of many by-products occurred (Figure 48).

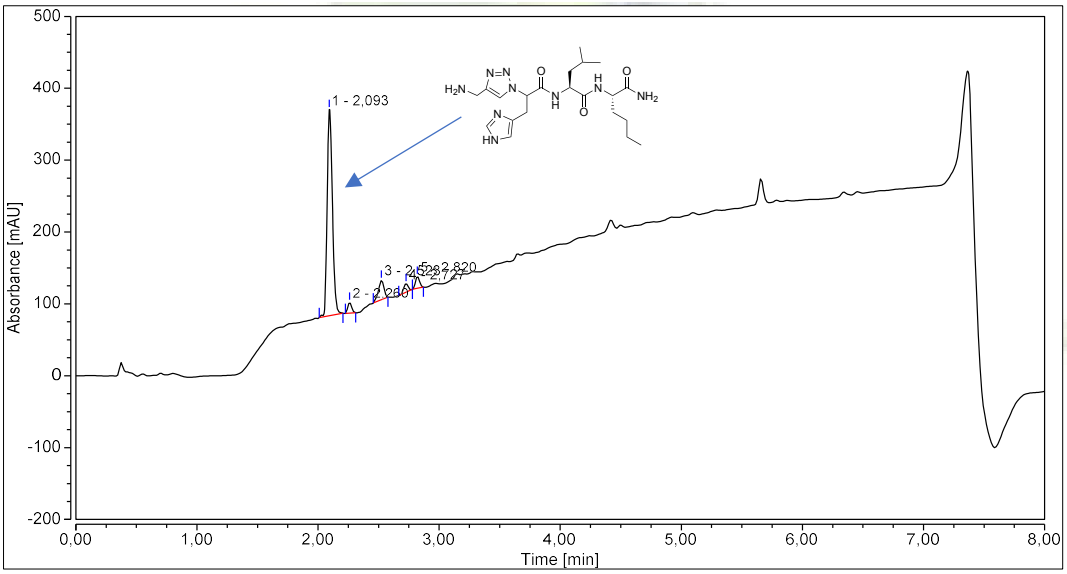

Figure 47: Analytical profile of NH_2-Glyψ[Tz]His-Leu-Nle-NH_2 (t_r = 2.093', 82%) synthesized with a freshly prepared $[Cu(CH_3CN)_4]PF_6$/TBTA solution. Gradient from 5 to 95 % MeCN in H_2O in 5 minutes with a 0.6 mL/min flow, recorded at 220 nm.

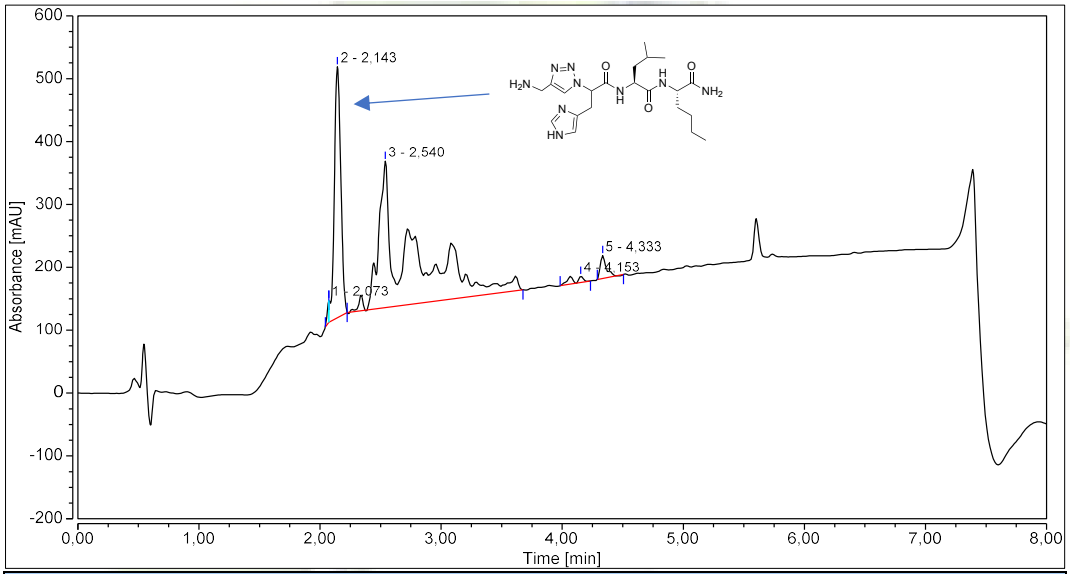

Figure 48: Analytical profile of NH_2-Glyψ[Tz]His-Leu-Nle-NH_2 (t_r = 2.143', 25%) synthesized with a 24 hours old $[Cu(CH_3CN)_4]PF_6$/TBTA solution. Gradient from 5 to 95 % MeCN in H_2O in 5 minutes with a 0.6 mL/min flow, recorded at 220 nm.

The result of the triazolopeptidomimetic synthesis of minigastrin proves, that the reagents are stable enough to be stored for the automated incorporation of a triazole 9 hours after preparation of the solution (chapter 4.5.4). In this case, a very good conversion of almost 80% of the final triazolopeptidomimetic could be obtained. Nevertheless, regarding to the results of the 24 hours

stability study, the storage seems to a be a limited for the stability of the CuAAC reagents in solution.

4.3.2. Optimization of the CuAAC

To obtain ideal outcomes for the triazoles, a screening of the CuAAC reaction was carried out varying time, temperature and the concentrations of reactants as described in chapter 3.2, using the microwave assisted peptide synthesizer. The reaction was first carried out using 0.5 equivalents of Cu(I) and TBTA, 5 equivalents of the amino-alkyne and 1 equivalent of DIPEA for 60 minutes at 70°C, resulting in the desired product. For the CuAAC screening, aliquots of 0.03 mmol of the azide-tripeptide N_3-His-Leu-Nle-NH_2 (attached to the resin) that was synthesized within the diazo-transfer screening (see chapter 4.2.2.) and the Fmoc-protected propargylamine were used and different conditions applied (shown in Table 2).

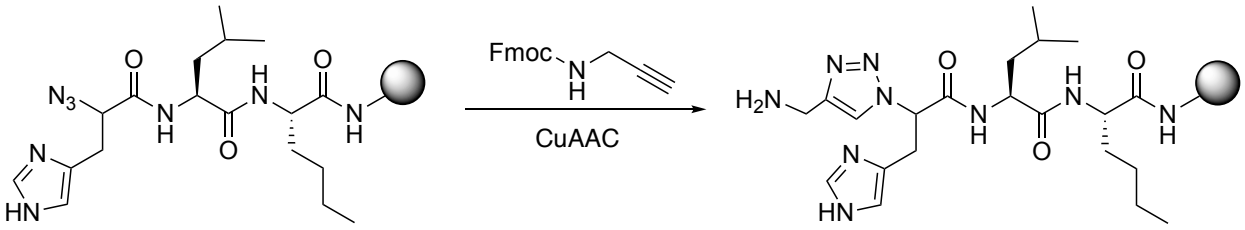

Scheme 8: Reaction scheme and part of the azide-functionalized bombesin sequence used for the CuAAC screening.

No improvements were observed by increasing the temperature of the reaction or the equivalents of the copper(I) source. The screening showed that the most suitable conditions for the CuAAC reaction are the conditions of reaction 7 (entry 7 in Table 2).

Table 2: Reaction conditions for the CuAAC screening. The most efficient one is highlighted.

reaction	$[Cu(CH_3CN)_4]PF_6$ [equiv.]	TBTA [equiv.]	DIPEA [equiv.]	amino alkyne [equiv.]	reaction time	temperature (MW)	conversion
7	**0.5**	**0.5**	1	5	**60'**	**70°C**	**82%**
8	0.5	0.5	1	5	30'	70°C	71%
9	1.5	1.5	1	5	30'	70°C	72%
10	1	1	1	5	30'	80°C	72%

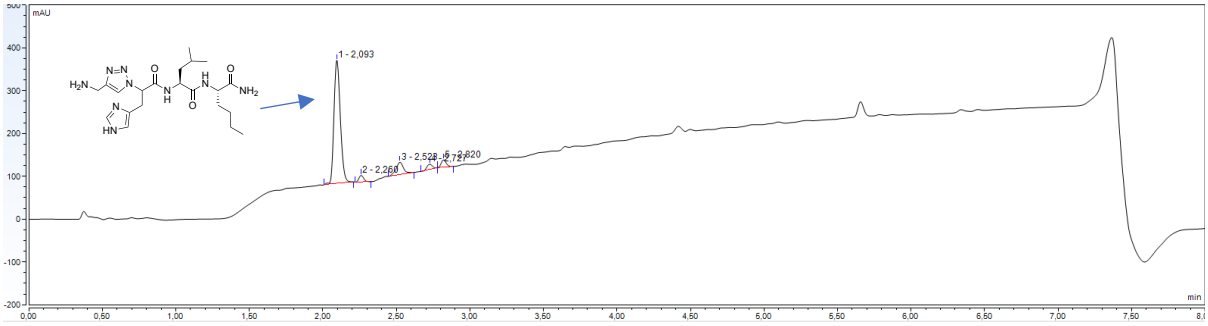

Figure 49: Analytical profile of NH_2-Glyψ[Tz]His-Leu-Nle-NH_2 (t_r = 2.093', 82%) synthesized with conditions of reaction 7 (Table 2, entry 7). Gradient of 5 to 95 % MeCN in H_2O with 0.1% FA in 5 minutes with a 0.6 mL/min flow recorded at 220 nm.

4.4. One-pot diazo-transfer and CuAAC

To optimize the triazole incorporation into the peptide sequence a one-pot one-step diazo-transfer and CuAAC reaction was attempted. A one-pot procedure in solution using different amines has been reported by Beckman et al. using 1 equivalent of the amino alkyne, 0.1 equivalents of $CuSO_4$ and the twofold of sodium ascorbate, 0.25 equivalents of TBTA and used $NaHCO_3$ as a base.[45] They carried out the reaction in a water methanol mixture at 80°C (microwave heating) until completion of conversion using triflyl azide as a diazo-transfer reagent, yielding more than 90% of the triazole. To find suitable conditions for the one-pot one-step incorporation of triazoles into peptides on solid support, a screening (displayed in Table 3) with different conditions was accomplished applying adapted procedures described by Beckman et al.[45]

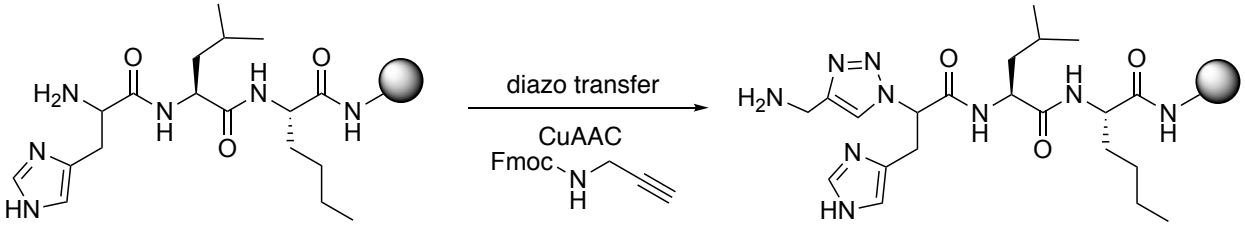

Scheme 9: Reaction scheme and part of the bombesin sequence used for the one-pot screening.

For the one-pot screening, aliquots (0.03 mmol) of the tripeptide H_2N-His-Leu-Nle-NH_2 (attached to the resin), synthesized and described in chapter 4.2.2, were used. The first two trials were unsuccessful leading to the azide-tripeptide as the reaction stopped at this step. After increasing the equivalents of the CuAAC reagents $[Cu(CH_3CN)_4]PF_6$ and TBTA the reaction resulted in 12 and 18% of the desired triazolo-tripeptide (t_r = 2.113') with significant amounts of the amine (t_r = 2.010') and the azide (t_r = 2.713') left (Figure 50). Another approach consisted on replacing the Cu(I)-complex by a $CuSO_4$/sodium ascorbate system. However, this resulted only in the azide. In

light of the less promising results of this series, the optimization of the one-pot one-step triazole synthesis was not pursued any further.

Table 3: Reaction conditions for the one-pot one-step triazolo-peptide synthesis. The most efficient one is highlighted.

reaction	Cu(I)[a] [equiv.]	TBTA [equiv.]	amino alkyne [equiv.]	DIPEA [equiv.]	ISA.HCl [equiv.]	$CuSO_4$ [equiv.]	Na-asc. [equiv.]	reaction time	temp. (MW)	con-version
11	0.5	0.5	2	10	5	-	-	30’	80°C	0%
12	0.5	0.5	2	10	5	-	-	60’	80°C	0%
13	**1**	**1**	**2**	**10**	**5**	**-**	**-**	**60’**	**80°C**	**18%**
14	**2**	**2**	**2**	**10**	**5**	**-**	**-**	**60’**	**80°C**	**12%**
15	-	5	2	10	5	0.1	0.02	60’	80°C	0%

[a] Cu(I) source originating from $[Cu(CH_3CN)_4]PF_6$

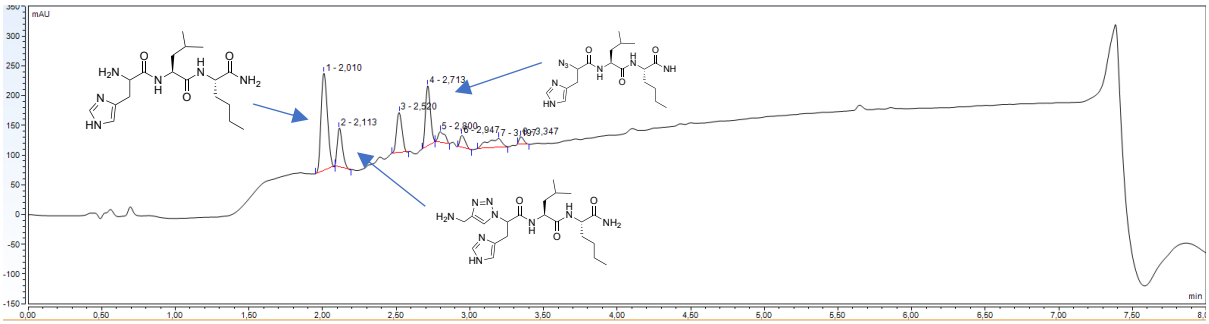

Figure 50: Analytical profile of NH_2-Glyψ[Tz]His-Leu-Nle-NH_2 (t_r = 2.113’) synthesized with conditions of reaction 13. 5 to 95 % MeCN in H_2O in 5 minutes with a 0.6 mL/min flow recorded at 220 nm. The peak at t_r = 2.713’ corresponds to the azide, the peak at t_r = 2.010’ to the amine and the other peaks show not identified side products or impurities.

4.5. Triazolopeptidomimetics

After optimization of the triazole incorporation the protocol was applied to the synthesis of different resins following the optimized 2-step procedure (diazo-transfer see chapter 4.2.2 and CuAAC see chapter 4.3.2), using different amino alkynes. A bombesin derivative was synthesized on wang resin and rink amide resin. The triazolopeptidomimetics leu-enkephalin, neurotensin and minigastrin were synthesized either on rink amide or on wang resin, leading to the NH_2 or OH C-terminus functionalized peptide respectively.

4.5.1. Bombesin derivative

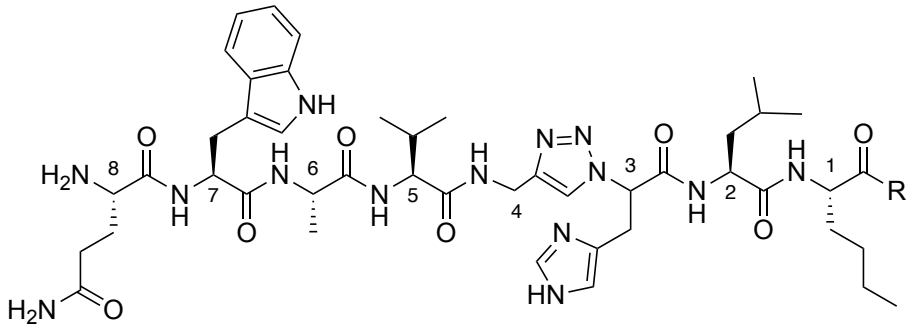

R = NH_2 (rink amide resin) or OH (wang resin)

Figure 51: Structure of H_2N-Gln-Trp-Ala-Val-Glyψ[Tz]His-Leu-Nle-NH_2 (triazolopeptidomimetic 1) and H_2N-Gln-Trp-Ala-Val-Glyψ[Tz]His-Leu-Nle-OH (triazolopeptidomimetic 2).

The backbone modified bombesin derivative was synthesized on rink amide and on wang resin following the general procedure described in chapter 3.2 in 10 hours and 11.5 hours respectively. For the triazole incorporation Fmoc-Gly-CCH (described in chapter 4.1.1) was used and inserted after amino acid 3. After cleavage and precipitation, the purity of the peptide was verified by LC-MS (Figure 52 and Figure 54). Triazolopeptidomimetic 1 was obtained with an amide function at the C-terminus with a conversion of 88%. The chromatogram in Figure 52 shows minor peaks originating from residual amounts of the azide (t_r = 7.774') and other impurities. Triazolopeptidomimetic 2 was obtained with a hydroxy function at the C-terminus with a conversion of 62%. The chromatogram in Figure 54 shows that 10% of the azide (t_r = 6.641') did not react further to the triazole. The rest of the chromatographic peaks correspond to impurities that formed during the synthesis.

The synthesis of the same sequence on two different solid supports showed the compatibility of the procedure with rink amide and wang resin. The sequence synthesized on wang resin appeared to contain more impurities and a lower conversion than the rink amide sequence. Due to the more demanding loading of the wang resin, the synthesis of the sequence took 1.5 hours longer than the synthesis on rink amide resin. This leads to a longer time in solution for the CuAAC reagents until the reaction. Also, for the bombesin sequence on wang resin the His-coupling was carried out for 20' at 50°C, deviating from the general procedure to prevent epimerization, possibly contributing to the lower conversion.

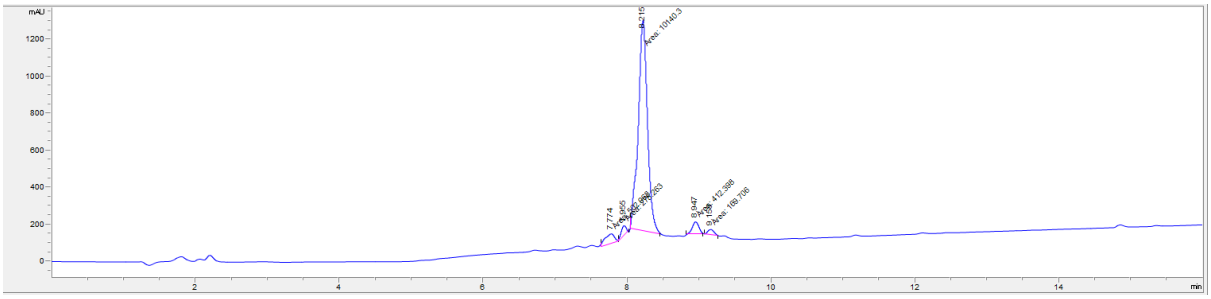

Figure 52: Analytical LC profile of triazolopeptidomimetic 1 (t_r = 8.215') with a gradient of 5 to 95% MeCN in H_2O over 15 minutes at a 0.2 mL/min flow recorded at 220 nm. The peak at t_r = 7.774' corresponds to the azide.

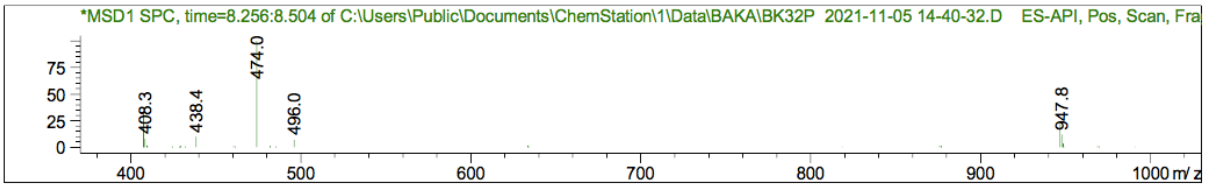

Figure 53: Mass spectrum of triazolopeptidomimetic 1 of the product signal at t_r = 8.215'. $[M+H]^+$ for $C_{45}H_{68}N_{15}O_8$ *m/z* calculated = 946.5, *m/z* found = 947.8. The spectrum also shows the double charged peak *m/z* found = 474.0.

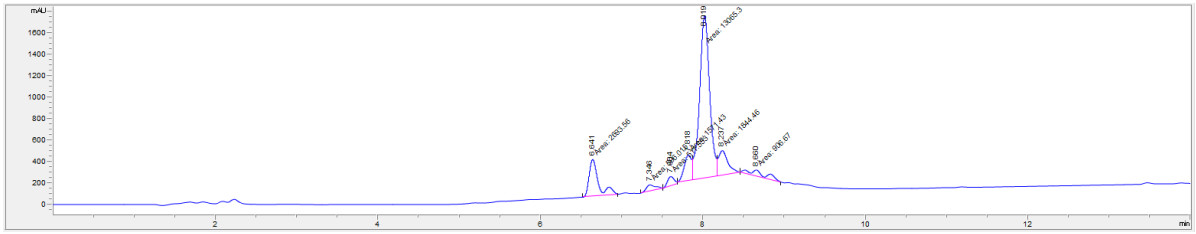

Figure 54: Analytical LC profile of triazolopeptidomimetic 2 (t_r = 8.019') with a gradient of 5 to 95% MeCN in H_2O over 13 minutes at a 0.2 mL/min flow recorded at 220 nm. The peak at t_r = 6.641' corresponds to the azide.

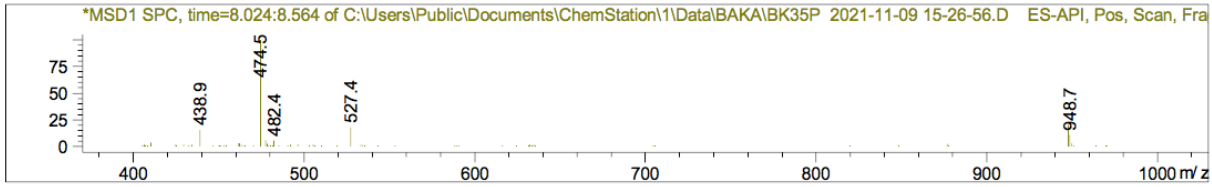

Figure 55: Mass spectrum of triazolopeptidomimetic 2 of the product signal at t_r = 8.019'. $[M+H]^+$ for $C_{45}H_{67}N_{14}O_9$ *m/z* calculated = 947.5, *m/z* found = 948.7. The spectrum also shows the double charged peak *m/z* found = 474.5.

4.5.2. Leu-enkephalin derivative

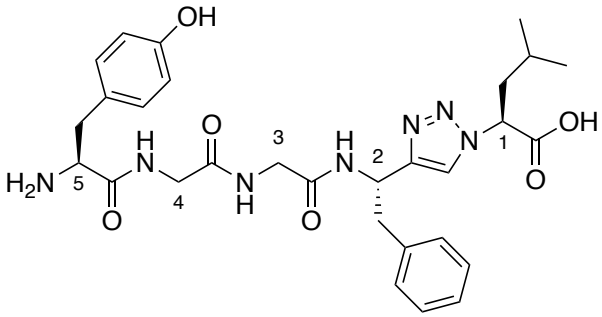

Figure 56: Structure of H_2N-Tyr-Gly-Gly-Pheψ[Tz]Leu-OH (triazolopeptidomimetic 3).

To show that the procedure is also applicable for the incorporation of amino alkynes with a sidechain the aromatic Fmoc-LPhe-CCH (described in chapter 4.1.3) was used. To see if the proximity of the triazole incorporation to the resin sterically influences the reaction, the triazole was inserted between position 1 and 2, starting from the C-terminus/resin. The backbone modified Leu-enkephalin derivative (triazolopeptidomimetic 3) was synthesized on wang resin following the general procedure described in chapter 3.2 in 8 hours, with variation that the peptide was precipitated with diethyl ether. After cleavage and precipitation, the purity of the peptide was verified by LC-MS. Triazolopeptidomimetic 3 was obtained with a hydroxy function at the C-terminus with a conversion of 90%. The chromatogram in Figure 57 also shows five small peaks originating from impurities and traces of the sequence until the glycine at position four (m/z = 417.3), indicating that the tyrosine coupling take place completely. The high conversion of 90% proves that the proximity of the triazole to the resin and the aromatic side chain of the incorporated amino alkyne do not influence the efficacy of the procedure.

Triazolopeptidomimetic 3 contains the phenylalanine residue originating from Fmoc-LPhe-CCH with an enantiomeric purity of 96%. Due to the high enantiomeric purity, only one diastereomer of the triazolopeptidomimetic could be observed, as shown in Figure 57.

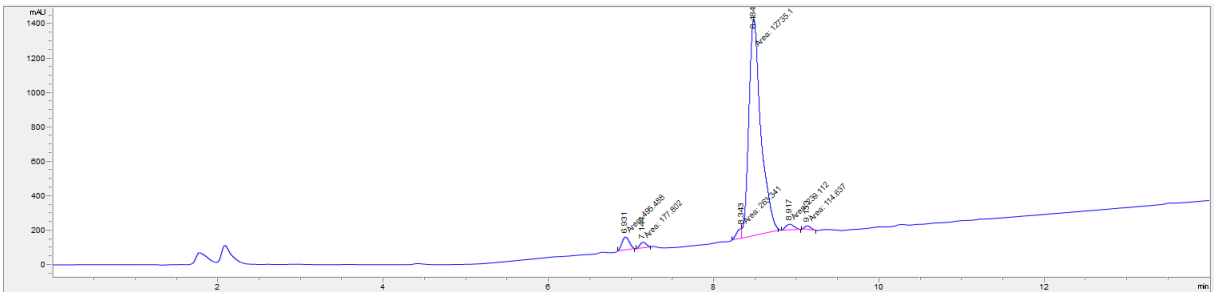

Figure 57: Analytical LC profile of triazolopeptidomimetic 3 (t_r = 8.484') with a gradient of 20 to 85% MeCN in H_2O over 14 minutes at a 0.2 mL/min flow recorded at 220 nm.

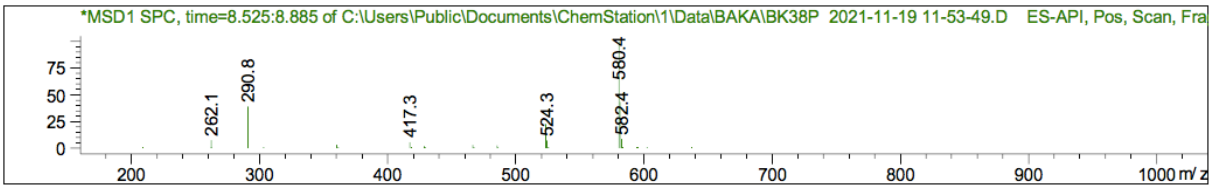

Figure 58: Mass spectrum of triazolopeptidomimetic 3 of the product signal at t_r = 8.484'. $[M+H]^+$ for $C_{29}H_{38}N_7O_6$ *m/z* calculated = 580.3, *m/z* found = 580.4. The spectrum also shows the double charged peak *m/z* found = 290.8.

4.5.3. Neurotensin derivative

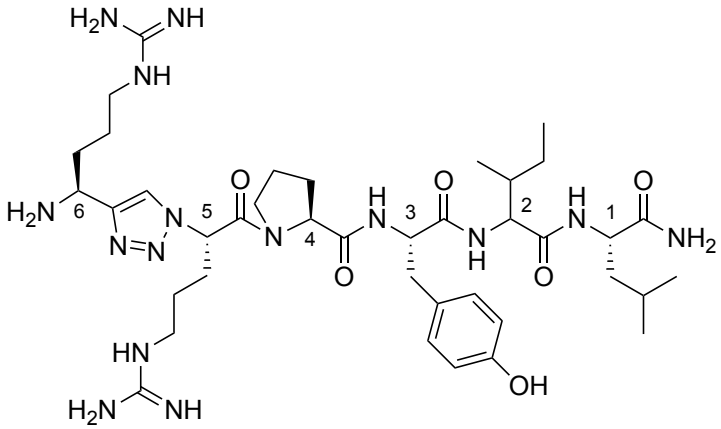

Figure 59: Structure of H_2N-Argψ[Tz]Arg-Pro-Tyr-ILe-Leu-NH_2 (triazolopeptidomimetic 4).

To show that the procedure is also applicable for amino alkynes with bulky and protected sidechains, Fmoc-Arg(Boc)$_2$-CCH (described in chapter 4.1.5) was incorporated into a neurotensin derivative.

The first trial implied the synthesis of the sequence until position 5 including the diazo-transfer. This resulted in a mixture of the sequence until the arginine in position 5 (9%), the sequence until the proline (26%) and the desired sequence until the azide-functionalized arginine with an extent of 62%. As the arginine coupling did not work sufficiently, the next approach included a double argininge coupling of 2x10 minutes at 48°C and the diazo-transfer resulting in 80% of the azide.

Another approach was carried out including a double arginine coupling for 2x5 minutes at 75°C resulting in 83% of the azide.

The whole backbone modified neurotensin derivative (triazolopeptidomimetic 4) was synthesized on rink amide resin following the general procedure described in chapter 3.2 in 8,5 hours with a scale of 0.015 mmol and a double arginine coupling (2 x 5', 75°C). After cleavage and precipitation, the purity of the peptide was verified by LC-MS. Triazolopeptidomimetic 4 was obtained with an amide function at the C-terminus with a conversion of 43% (t_r = 3.384') whereas still 30% of the azide (t_r = 14.105'), 3% of the sequence until the first arginine (t_r = 6.119') and 2% of the sequence until the proline (t_r = 10.055') were present as shown in Figure 60.

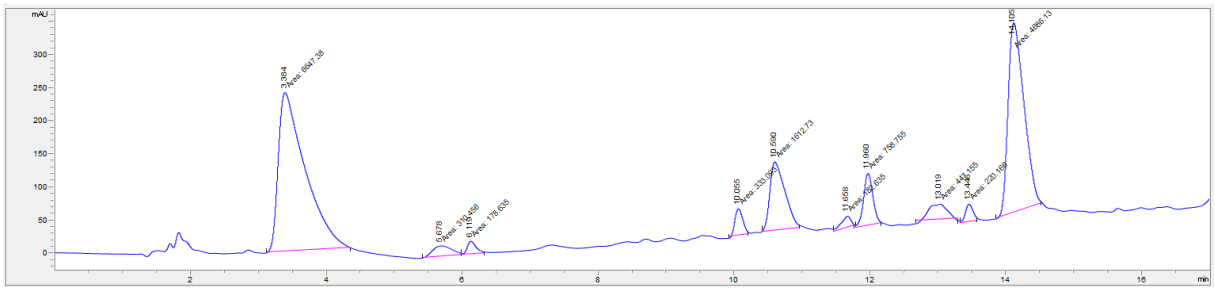

Figure 60: Analytical LC profile of triazolopeptidomimetic 4 (t_r = 3.384') with a gradient of 10 to 30% MeCN in H_2O over 13 minutes at a 0.2 mL/min flow recorded at 220 nm. The peak at t_r = 14.105' corresponds to the azide functionalized peptide (*m/z* = 685.4) , the peak at t_r = 6.119' to the sequence until the arginine at position five (*m/z* = 659.4) and the peak at t_r = 10.055' corresponds to the sequence until the proline (*m/z* = 503.3).

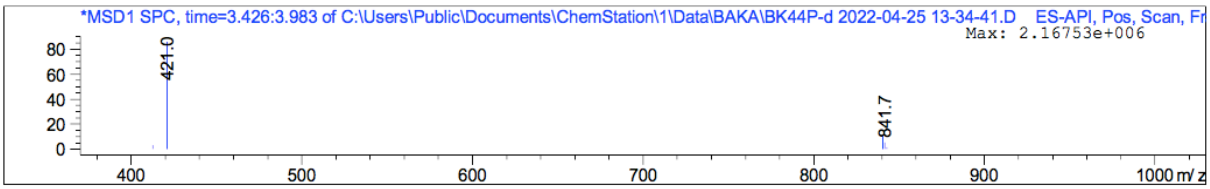

Figure 61: Mass spectrum of triazolopeptidomimetic 4 of the product signal at t_r = 3.384'. $[M+H]^+$ for $C_{39}H_{66}N_{15}O_6$ *m/z* calculated = 840.5, *m/z* found = 841.7. The spectrum also shows the double charged peak *m/z* found = 421.0.

The synthesis of the complete sequence was repeated three times in total by using arginine alkyne from a different batch, varying the equivalents (2, 4 and 5 equiv.) and paying particular attention to the complete solubility of the arginine alkyne. Still no better result could be achieved. The low conversion might result from the bulkiness of the arginine alkyne and showed that the procedure might need improvement for the sterically more demanding incorporation of bulky, protected amino alkynes. Possibly also different reaction conditions for the CuAAC are necessary when incorporating Fmoc-Arg(Boc)$_2$-CCH as the diazo-transfer did not seem to be the limiting factor of the synthesis.

Triazolopeptidomimetic 4 contains the arginine residue resulting from Fmoc-Arg(Boc)$_2$-CCH (4 equiv.) with an enantiomeric purity of 88% (L-enantiomer), resulting in two diastereomers of the peptide.

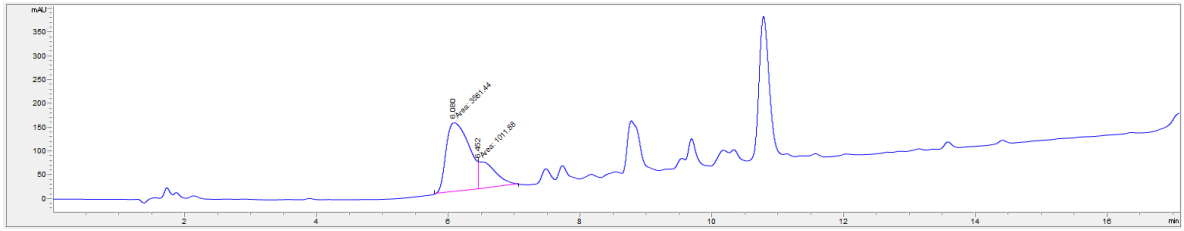

Figure 62: Analytical LC profile of triazolopeptidomimetic 4 (t_r = 6.080'/6.452') with a gradient of 10 to 50% MeCN in H_2O over 13 minutes at a 0.2 mL/min flow recorded at 220 nm.

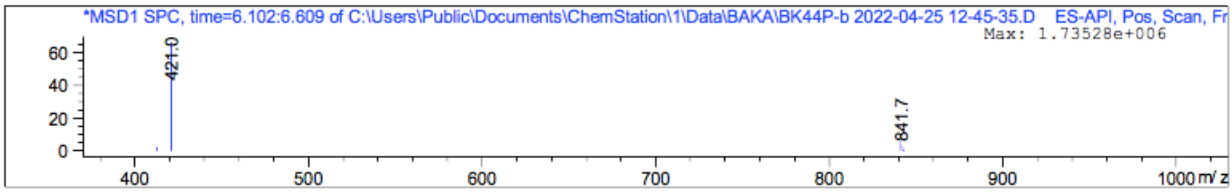

Figure 63: Mass spectrum of triazolopeptidomimetic 4 of the product signal at t_r = 6.080'. $[M+H]^+$ for $C_{39}H_{66}N_{15}O_6$ *m/z* calculated = 840.5, *m/z* found = 841.7. The spectrum also shows the double charged peak *m/z* found = 421.0.

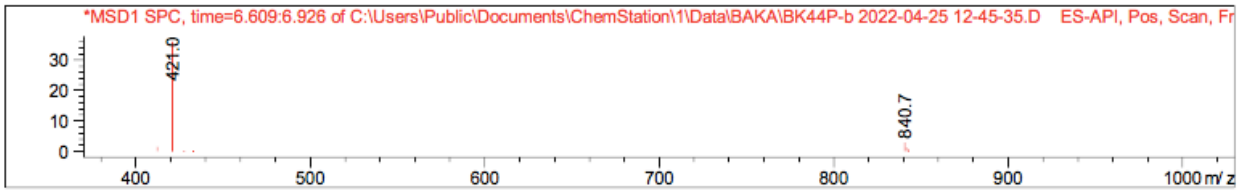

Figure 64: Mass spectrum of triazolopeptidomimetic 4 of the product signal at t_r = 6.452'. $[M+H]^+$ for $C_{39}H_{66}N_{15}O_6$ *m/z* calculated = 840.5, *m/z* found = 840.7. The spectrum also shows the double charged peak *m/z* found = 421.0.

Peak 1 (t_r = 6.080) and peak 2 (t_r = 6.452) in Figure 62 correspond to the two diastereomers of triazolopeptidomimetic 4 with a ratio of 78:21. Even with a flatter gradient over the same time (10-30% MeCN, shown in Figure 60) the two diastereomers could not be separated any better, making it hard to determine the enantiomeric ratio exactly. Nevertheless, the ratio of the enantiomers of

Fmoc-Arg(Boc)$_2$-CCH (88% L- and 12% D-enantiomer) is reflected in form of diastereomers of triazolopeptidomimetic 4 approximately, shown in Figure 62.

4.5.4. Minigastrin derivative

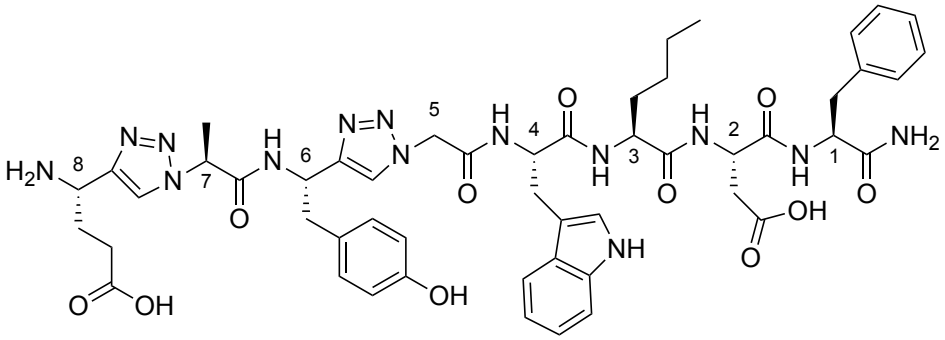

Figure 65: Structure of H_2N-Gluψ[Tz]Ala-Tyrψ[Tz]Gly-Trp-NLe-Asp-Phe-NH_2 (triazolopeptidomimetic 5).

To demonstrate the robustness of the procedure and its application with multiple triazole incorporations, a sequence consisting out of eight amino acids containing two triazoles was considered. The backbone modified minigastrin derivative (triazolopeptidomimetic 5) was synthesized on rink amide resin following the general procedure described in chapter 3.2 in 12.5 hours. For the two triazole incorporations Fmoc-Tyr(OtBu)-CCH (described in chapter 4.1.2) and Fmoc-Glu(OtBu)-CCH (described in chapter 4.1.4) were used. After cleavage and precipitation, the purity of the peptide was verified by LC-MS. Triazolopeptidomimetic 5 was obtained with an amide function at the C-terminus with a conversion of 79% (Figure 66). The synthesis showed that the protocol is also suitable for the synthesis of multiple triazole peptidomimetics and that the position where the triazoles are inserted do not affect the results.

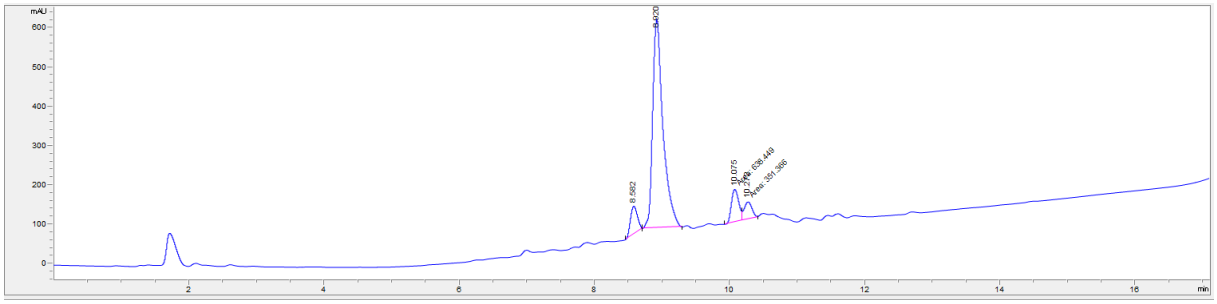

Figure 66: Analytical LC profile of triazolopeptidomimetic 5 (t_r = 8.920') with a gradient of 20 to 65% MeCN in H_2O over 14 minutes at a 0.2 mL/min flow with an at 220 nm. The other peaks at t_r = 8.582', 10.075' and 10.272' show impurities.

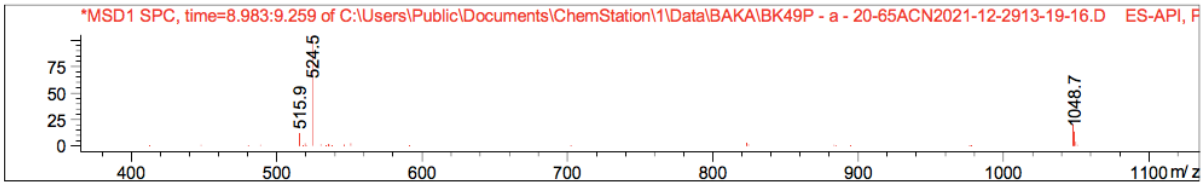

Figure 67: Mass spectrum of triazolopeptidomimetic 5 of the product signal at t_r = 8.920'. $[M+H]^+$ for $C_{51}H_{62}N_{14}O_{11}$ *m/z* calculated = 1047.5, *m/z* found = 1048.7. The spectrum also shows the double charged peak *m/z* found = 524.5.

Triazolopeptidomimetic 5 contains a tyrosine residue originating from Fmoc-Tyr(OtBu)-CCH with an enantiomeric purity of 86% (L-enantiomer) and a glutamic acid residue originating from Fmoc-Glu(OtBu)-CCH with an enantiomeric purity of 85% (L-enantiomer). This results in four different diastereomers of the peptide. The peaks in Figure 68 numbered with 1, 2, 3 and 4 correspond to a molecule with the mass $[M+H]^+$ *m/z* = 1047, which is the mass of Triazolopeptidomimetic 5. These peaks represent the four diastereomers of the peptide. Peak 1 (t_r = 10.273') and peak 4 (t_r = 11.290') show the diastereomer containing D-Tyr and L-Glu and the diastereomer containing L-Tyr and D-Glu. Peak 2 (t_r = 10.540') and peak 3 (t_r = 10.857') show the diastereomer containing the D-configuration of both amino acids and the diastereomer containing the L-configuration of both amino acids, respectively.

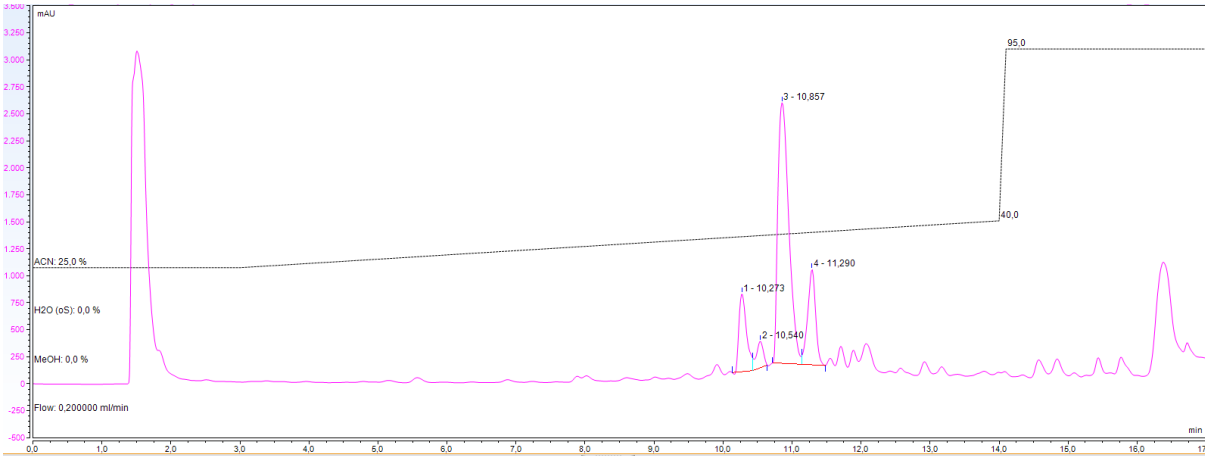

Figure 68: HPLC profile of triazolopeptidomimetic 5 with a gradient of 25 to 40% MeCN in H_2O over 14 minutes at a 0.2 mL/min flow recorded at 220 nm. Peak 1, 2, 3 and 4 correspond to triazolopeptidomimetic 5, the other peaks correspond impurities.

5. Conclusion

With this thesis an optimized, fully automated and broadly applicable protocol for the synthesis of peptides bearing 1,4-disubstituted 1,2,3-triazoles is presented. The reliability and efficacy of the developed method was demonstrated by the synthesis of four different triazolopeptidomimetics.

The adaptation of the reactions for the triazole incorporation from a manual to an automated a SPPS compatible setup was accomplished. Using water as a solvent, the stability issues regarding the diazo-transfer reagent were overcome. Its sufficient stability in water was demonstrated with a stability study and it was proven that the used amounts of water does not interfere with the swelling of the resin. The stability of the CuAAC reagents $[Cu(CH_3CN)_4]PF_6$ and TBTA was shown to be efficient enough for the synthesized triazolopeptidomimetics in this thesis. Nevertheless, the 24 hours stability study revealed that the reagents degrade over time posing possible limitations for the synthesis of longer sequences. Moreover, the experiments have shown that when triazoles are incorporated in positions further away from the resin, the CuAAC reagents are in solution for a longer time, resulting in poorer conversions of the final peptidomimetic.

It was demonstrated that the protocol is suitable for the synthesis of different sequences using a variety of amino alkynes. The method is applicable to different resins and amide and hydroxy C-terminal functionalized peptidomimetics can be obtained by using rink amide and wang resin. The procedure is appropriate for the incorporation of triazoles by amino alkynes with no side chain as well as for amino acids with bulky, protected and aromatic side chains. It was proven that the insertion of triazoles close to the resin does not affect the synthesis in terms of steric hinderance. The experiments display that the insertion of a triazole is possible at any position and that the insertion of multiple triazoles doesn't affect the reliability of the protocol. Although the process for the triazole incorporation as well as the triazolopeptidomimetic synthesis overall is fully automatized, the synthesis for the amino alkynes still needs to be carried out in advance in solution. As the amino alkynes could not be synthesized enantiomerically pure the triazolopeptidomimetics appear in form of diastereomers. This does not affect the reliability of the method as the products can be identified and assigned over the equal enantiomeric and diastereomeric ratio of the amino alkyne and the resulting peptidomimetic.

Table 4: Summary of the results for the synthesized triazolopeptidomimetics. The "time to CuAAC" shows how long the CuAAC reagents are in solution until the start of the CuAAC reaction.

peptido-mimetic	sequence	Trz position	time to CuAAC	synthesis time	resin	amino alkyne	conversion
1	H_2N-Gln-Trp-Ala-Val-Glyψ[Tz]His-Leu-Nle-NH_2	3/7	3.5 h	10 h	rink amide	Gly	88%
2	H_2N-Gln-Trp-Ala-Val-Glyψ[Tz]His-Leu-Nle-OH	3/7	5 h	11.5 h	wang	Gly	62%
3	H_2N-Tyr-Gly-Gly-Pheψ[Tz]Leu-OH	1/5	2.5 h	8.5 h	wang	Phe	90%
4	H_2N-Argψ[Tz]Arg-Pro-Tyr-ILe-Leu-NH_2	4/4	5 h	8 h	rink amide	Arg	43%
5	H_2N-Gluψ[Tz]Ala-Tyrψ[Tz]Gly-Trp-NLe-Asp-Phe-NH_2	5/8 & 7/8	5 h, 9 h	12.5 h	rink amide	Tyr, Glu	79%

Table 4 summarizes the conditions and results for the synthesized triazolopeptidomimetics within this thesis. The peptides were obtained with conversions ranging from 43% to 79%.

With this protocol peptidomimetics containing 1,4-disubstituted 1,2,3-triazoles can be synthesized with good yields and in a time saving and efficient manner. To gain other structural diverse peptidomimetics and to mimic *cis*-amide bond characteristics, the insertion of 1,5- disubstituted 1,2,3-triazoles is possible.[6] This was not reproducible in our hand and that is why the focus was set on the synthesis of peptidomimetics containing 1,4-disubstituted 1,2,3-triazoles.

The diversity of the method provides a broad range and variety for the synthesis of triazole bearing peptides in terms of sequence length, amino acid characteristics and position of the incorporated triazole. The developed method facilitates the application of efficient amide-to-triazole scans and provides more accessibility for the synthesis of triazolopeptidomimetics for peptide chemists. Limitations that come with the protocol are that loss of efficacy of the CuAAC over time and the manual in-solution synthesis of the amino alkynes.

6. References

1. Recnik, L., Kandioller, W. & Mindt, T. L. 1,4-Disubstituted 1,2,3-Triazoles as Amide Bond Surrogates for the Stabilisation of Linear Peptides with Biological Activity. *Molecules* **25**, 3576 (2020).
2. Tang, J. *et al.* Peptide-guided functionalization and macrocyclization of bioactive peptidosulfonamides by Pd(II)-catalyzed late-stage C–H activation. *Nat. Commun.* **9**, 1–8 (2018).
3. Nestor, J. The Medicinal Chemistry of Peptides. *Currend Med. Chem.* **26**, 4399–418 (2009).
4. Boöttger, R., Hoffmann, R. & Knappe, D. Differential stability of therapeutic peptides with different proteolytic cleavage sites in blood, plasma and serum. *PLoS One* **12**, 1–15 (2017).
5. Ruzza, P. Peptides and Peptidomimetics in Medicinal Chemistry. *Med. Chem. Drug Des.* (2012). doi:10.5772/38240
6. Grob, N. M., Schibli, R., Béhé, M., Valverde, I. E. & Mindt, T. L. 1,5-Disubstituted 1,2,3-Triazoles as Amide Bond Isosteres Yield Novel Tumor-Targeting Minigastrin Analogs. *ACS Med. Chem. Lett.* **12**, 585–592 (2021).
7. Grob, N. M. *et al.* Triazolo-peptidomimetics: novel radiolabeled minigastrin analogs for improved tumor targeting. *J. Med. Chem.* **63**, 4484–4495 (2020).
8. Lau, J. L. & Dunn, M. K. Therapeutic peptides: Historical perspectives, current development trends, and future directions. *Bioorganic Med. Chem.* **26**, 2700–2707 (2018).
9. Mäde, V., Els-Heindl, S. & Beck-Sickinger, A. G. Automated solid-phase peptide synthesis to obtain therapeutic peptides. *Beilstein J. Org. Chem.* **10**, 1197–1212 (2014).
10. Mitchell, A. R. Bruce Merrifield and solid-phase peptide synthesis: A historical assessment. *Biopolym. - Pept. Sci. Sect.* **90**, 175–184 (2008).
11. Merrifield, R. B. Automated Synthesis of Peptide: Solid-Phase Peptide Synthesis. *Science (80-.).* **150**, 178–185 (1965).
12. Merrifield, R. B., Stewart, J. M. & Jernberg, N. Instrument for Automated Synthesis of Peptides. *Anal. Chem.* **38**, 1905–1914 (1966).
13. Stawikowski, M. & Fields, G. B. *Introduction to Peptide Synthesis*. *Current Protocol Protein Science* (2002). doi:10.1002/0471140864.ps1801s26.Introduction
14. D'Hondt, M. *et al.* Related impurities in peptide medicines. *J. Pharm. Biomed. Anal.* **101**, 2–30 (2014).
15. Lawrenson, S., North, M., Peigneguy, F. & Routledge, A. Greener solvents for solid-phase synthesis. *Green Chem.* **19**, 952–962 (2017).
16. Lau, J. L. & Dunn, M. K. Therapeutic peptides: Historical perspectives, current development trends, and future directions. *Bioorganic Med. Chem.* **26**, 2700–2707 (2018).
17. Gentilucci, L., Tolomelli, A. & Squassabia, F. Peptides and Peptidomimetics in Medicine, Surgery and Biotechnology. *Curent Med. Chem.* **13**, 2449–2466 (2006).
18. Erak, M., Bellmann-Sickert, K., Els-Heindl, S. & Beck-Sickinger, A. G. Peptide chemistry

toolbox – Transforming natural peptides into peptide therapeutics. *Bioorganic Med. Chem.* **26**, 2759–2765 (2018).

19. Muttenthaler, M., King, G. F., Adams, D. J. & Alewood, P. F. Trends in peptide drug discovery. *Nat. Rev. Drug Discov.* **20**, 309–325 (2021).
20. Raucher, D. Tumor targeting peptides: novel therapeutic strategies in glioblastoma. *Curr. Opin. Pharmacol.* **47**, 1–11 (2020).
21. Evans, B. J., King, A. T., Katsifis, A., Matesic, L. & Jamie, J. F. Methods to enhance the metabolic stability of peptide-based PET radiopharmaceuticals. *Molecules* **25**, (2020).
22. Vonderheide, R. H., Hahn, W. C., Schultze, J. L. & Nadler, L. M. The telomerase catalytic subunit is a widely expressed tumor-associated antigen recognized by cytotoxic T lymphocytes. *Immunity* **10**, 673–679 (1999).
23. Sue Carter, C. *et al.* Is oxytocin "nature's medicine"? *Pharmacol. Rev.* **72**, 829–861 (2020).
24. Kong, G. & Hicks, R. J. Peptide Receptor Radiotherapy: Current Approaches and Future Directions. *Curr. Treat. Options Oncol.* **20**, (2019).
25. Ulapane, K. R., Kopec, B. M., Moral, M. E. G. & Siahaan, T. J. Peptides and Drug Delivery. in *Peptides and Peptide-based Biomaterials and their Biomedical Applications* 164–184 (Springer, 2017).
26. Etrych, T. *et al.* Fluorescence optical imaging in anticancer drug delivery. *J. Control. Release* **226**, 168–181 (2016).
27. Pirooznia, N. *et al.* 177Lu-labeled cyclic RGD peptide as an imaging and targeted radionuclide therapeutic agent in non-small cell lung cancer: Biological evaluation and preclinical study. *Bioorg. Chem.* **102**, 104100 (2020).
28. Chatzisideri, T., Leonidis, G. & Sarli, V. Cancer-targeted delivery systems based on peptides. *Future Med. Chem.* **10**, 2201–2226 (2018).
29. Werle, M. & Bernkop-Schnürch, A. Strategies to improve plasma half life time of peptide and protein drugs. *Amino Acids* **30**, 351–367 (2006).
30. Marastoni, M. *et al.* Synthesis and activity of new linear and cyclic peptide T derivatives. *Drug Res. (Stuttg).* **44**, 1073–1076 (1994).
31. Su, C.-M. *et al.* In Vitro Stability of Growth Hormone Releasing Factor (GRF) Analogs in Porcine Plasma. *Horm. Metab. Res.* **23**, 15–21 (1991).
32. C-terminal modifications. (2015). Available at: https://www.pepscan.com/custom-peptide-synthesis/peptide-modifications/c-terminal-modifications/.
33. N-terminal modifications. (2015). Available at: https://www.pepscan.com/custom-peptide-synthesis/peptide-modifications/n-terminal-modifications/.
34. Brinckerhoff, L. H. *et al.* Terminal modifications inhibit proteolytic degradation of an immunogenic MART-127-35 peptide: Implications for peptide vaccines. *Int. J. Cancer* **83**, 326–334 (1999).
35. Hong, S. Y., Oh, J. E. & Lee, K. H. Effect of D-amino acid substitution on the stability, the secondary structure, and the activity of membrane-active peptide. *Biochem. Pharmacol.* **58**, 1775–1780 (1999).

36. Harris, K. S. *et al.* Rapid optimization of a peptide inhibitor of malaria parasite invasion by comprehensive N-methyl scanning. *J. Biol. Chem.* **284**, 9361–9371 (2009).

37. Meyer, J. P., Gillespie, T. J., Hom, S., Hruby, V. J. & Davis, T. P. In vitro stability of some reduced peptide bond pseudopeptide analogues of dynorphin A. *Peptides* **16**, 1215–1219 (1995).

38. De Bont, D. B. A., Sliedregt-Bol, K. M., Hofmeyer, L. J. F. & Liskamp, R. M. J. Increased stability of peptidesulfonamide peptidomimetics towards protease catalyzed degradation. *Bioorganic Med. Chem.* **7**, 1043–1047 (1999).

39. Sun, S., Jia, Q. & Zhang, Z. Applications of amide isosteres in medicinal chemistry. *Bioorganic Med. Chem. Lett.* **29**, 2535–2550 (2019).

40. Kracker, O. *et al.* Design Principles for a Class of Versatile Peptidomimetics. *Chem. - Eur. J.* **24**, 953–961 (2018).

41. Tornøe, C. W., Christensen, C. & Meldal, M. Peptidotriazoles on solid phase: [1,2,3]-Triazoles by regiospecific copper(I)-catalyzed 1,3-dipolar cycloadditions of terminal alkynes to azides. *J. Org. Chem.* **67**, 3057–3064 (2002).

42. Rostovtsev, V. V., Green, L. G., Fokin, V. V. & Sharpless, K. B. A stepwise huisgen cycloaddition process: Copper(I)-catalyzed regioselective 'ligation' of azides and terminal alkynes. *Angew. Chemie - Int. Ed.* **41**, 2596–2599 (2002).

43. Castro, V., Rodríguez, H. & Albericio, F. CuAAC: An Efficient Click Chemistry Reaction on Solid Phase. *ACS Comb. Sci.* **18**, 1–14 (2016).

44. Castro, V., Blanco-Canosa, J. B., Rodriguez, H. & Albericio, F. Imidazole-1-sulfonyl azide-based diazo-transfer reaction for the preparation of azido solid supports for solid-phase synthesis. *ACS Comb. Sci.* **15**, 331–334 (2013).

45. Beckmann, H. S. G. & Wittmann, V. One-pot procedure for diazo transfer and azide-alkyne cycloaddition: Triazole linkages from amines. *Org. Lett.* **9**, 1–4 (2007).

46. Chan, T. R., Hilgraf, R., Sharpless, K. B. & Fokin, V. V. Polytriazoles as copper(I)-stabilizing ligands in catalysis. *Org. Lett.* **6**, 2853–2855 (2004).

47. Jubb, A. M. *et al.* Neuropilin-1 expression in cancer and development. *J. Pathol.* **226**, 50–60 (2012).

48. Mascarin, A., Valverde, I. E., Vomstein, S. & Mindt, T. L. 1,2,3-Triazole Stabilized Neurotensin-Based Radiopeptidomimetics for Improved Tumor Targeting. *Bioconjug. Chem.* **26**, 2143–2152 (2015).

49. Mascarin, A., Valverde, I. E. & Mindt, T. L. Radiolabeled analogs of neurotensin (8-13) containing multiple 1,2,3-triazoles as stable amide bond mimics in the backbone. *Medchemcomm* **7**, 1640–1646 (2016).

50. Valverde, I. E. *et al.* 1 , 2 , 3-Triazoles as Amide Bond Mimics : Triazole Scan Yields Protease- Resistant Peptidomimetics for Tumor Targeting Angewandte. *Angew. Chemie Int. Ed.* **52**, 8957–8960 (2013).

51. Reubi, J. C., Schaer, J.-C. & Waser, B. Cholecystokinin(CCK)-A and CCKB/Gastrin Receptors in Human Tumors. *Cancer Res.* **57**, 1377–1386 (1997).

52. Fedorczyk, B. *et al.* Triazolopeptides Inhibiting the Interaction between Neuropilin-1 and Vascular Endothelial Growth Factor-165. *Molecules* **24**, 1–19 (2019).

53. Alper, P. B., Hung, S. C. & Wong, C. H. Metal catalyzed diazo transfer for the synthesis of azides from amines. *Tetrahedron Lett.* **37**, 6029–6032 (1996).

54. Kubas, J. TETRAKIS(ACETONITRILE)COPPER(l HEXAFLUOROPHOSPHATE(1-). **28**, 68–70 (1990).

55. Kritchenkov, I. S., Shakirova, J. R. & Tunik, S. P. Efficient one-pot green synthesis of tetrakis(acetonitrile)copper(i) complex in aqueous media. *RSC Adv.* **9**, 15531–15535 (2019).

56. Movahedi, A., Moth-Poulsen, K., Eklöf, J., Nydén, M. & Kann, N. One-pot synthesis of TBTA-functionalized coordinating polymers. *React. Funct. Polym.* **82**, 1–8 (2014).